AD_____

Award Number: DAMD17-96-1-6274

TITLE: Molecular Interactions of Bcl-2 Family Members in Breast Cancer Cells

PRINCIPAL INVESTIGATOR: Gabriel Nunez, M.D.

CONTRACTING ORGANIZATION: University of Michigan
Ann Arbor, Michigan 48103-1274

REPORT DATE: August 2000

TYPE OF REPORT: Final

PREPARED FOR: U.S. Army Medical Research and Materiel Command
Fort Detrick, Maryland 21702-5012

DISTRIBUTION STATEMENT: Approved for Public Release;
Distribution Unlimited

REPORT DOCUMENTATION PAGE

Form Approved
OMB No. 074-0188

1. AGENCY USE ONLY (Leave blank)	2. REPORT DATE	3. REPORT TYPE AND DATES COVERED
	August 2000	Final (1 Sep 96 - 31 Aug 00)

4. TITLE AND SUBTITLE
Molecular Interactions of Bcl-2 Family Members in Breast Cancer Cells

5. FUNDING NUMBERS
DAMD17-96-1-6274

6. AUTHOR(S)
Gabriel Nunez, M.D.

7. PERFORMING ORGANIZATION NAME(S) AND ADDRESS(ES)
University of Michigan
Ann Arbor, Michigan 48103-1274

E-MAIL:
gabriel.nunez@umich.edu

8. PERFORMING ORGANIZATION REPORT NUMBER

9. SPONSORING / MONITORING AGENCY NAME(S) AND ADDRESS(ES)
U.S. Army Medical Research and Materiel Command
Fort Detrick, Maryland 21702-5012

10. SPONSORING / MONITORING AGENCY REPORT NUMBER

11. SUPPLEMENTARY NOTES

12a. DISTRIBUTION / AVAILABILITY STATEMENT
Approved for public release; distribution unlimited

12b. DISTRIBUTION CODE

13. ABSTRACT ***(Maximum 200 Words)***

A major genetic event that occurs in the pathogenesis of breast carcinoma involves alterations in the Bcl-2 survival pathway. We have performed studies to determine the mechanism involved in Bcl-x_S-mediated apoptosis and to characterize cellular proteins that interact with Bcl-x_S using biochemical and genetic approaches. The analysis showed that Bcl-x_S requires its BH3 and C-terminal mitochondrial anchoring domains for killing. Bcl-XS-induced killing is, at least in part, mediated through an Apaf-1-caspase-9 pathway. Bcl-x_S associates with Bcl-x_L via its BH3 domain and with Apaf-1 possibly through Bcl-x_L. We have cloned and characterized several Apaf-1 cDNAs and showed that a novel Apaf-1 isoform activates procaspase-9 in a cytochrome c and dATP-dependent manner.

14. SUBJECT TERMS
Breast Cancer

15. NUMBER OF PAGES
66

16. PRICE CODE

17. SECURITY CLASSIFICATION OF REPORT	18. SECURITY CLASSIFICATION OF THIS PAGE	19. SECURITY CLASSIFICATION OF ABSTRACT	20. LIMITATION OF ABSTRACT
Unclassified	Unclassified	Unclassified	Unlimited

Table of Contents

INTRODUCTION

Cancer is the result of multiple genetic events, including activation of oncogenes and inactivation of tumor suppressor genes. The protein products of the former are often mitogens, whereas the products of the latter suppress proliferation. It is becoming increasingly apparent that tumor suppressor genes like p53 function in part by activating an apoptotic death pathway. In addition, certain oncogenes such as bcl-2 appear to contribute to tumor development primarily by promoting abnormal cell survival via an apoptosis inhibitory signal. Thus, disruption of the apoptosis pathway appears integral to many malignancies including breast cancer. Furthermore, treatment of cancer with chemotherapy or radiation therapy is limited by the emergence of tumor cells resistant to these therapies. This resistance limits our ability to successfully treat these neoplasms.

bcl-2, the first member of an evolutionarily conserved family of apoptosis regulatory genes, was initially isolated from the t(14; 18) chromosomal translocation found in human B-cell follicular lymphomas, and was subsequently shown to repress cell death triggered by a diverse array of stimuli (1-2). Several members of the family, including Bcl-2, Bcl-x_L, Bcl-w, Mcl-1, and A1/Bfl-1, share conserved regions termed Bcl-2 homology domain 1, 2, 3, and 4 (BH1, BH2, BH3, and BH4), and function by repressing apoptosis (1-4). In contrast, structurally related proteins, including Bax, Bak, Bad, Bik/Nbk, Bid, Hrk, Bim, and Bok/Mtd, activate apoptosis (5-11). Biochemical and functional analyses have revealed that these pro-apoptotic proteins require the conserved BH3 region to interact with Bcl-2/ Bcl-x_L, and activate apoptosis in transient assays (5-11). Moreover, NMR studies have demonstrated that the BH3 domain of Bak interacts with a hydrophobic cleft formed by the conserved BH3 and BH1 regions of Bcl-x_L (12). To date, all death-promoting Bcl-2-related proteins heterodimerize with Bcl-2, Bcl-x_L, or Mcl-1, suggesting that these molecules promote cell death at least in part by interacting with and antagonizing Bcl-2, Bcl-x_L, and Mcl-1 (5-11). The biochemical process by which pro-survival Bcl-2 family members regulate cell death is poorly understood. It has been proposed that pro-survival family members regulate apoptosis by maintaining the integrity of the mitochondria (13). In addition, these Bcl-2 family proteins have been proposed to regulate apoptosis via physical interactions with central caspases through adaptor molecules, such as Apaf-1 and CED-4 (14-15).

A major genetic event that occurs in the genesis and/or progression of breast carcinoma involves alterations in the pathway of apoptosis. In breast cancer, one of the most common abnormalities is deregulated expression of Bcl-2 or Bcl-x_L proteins. Up to 90% of cancers originating from breast overexpress Bcl-2 or Bcl-x_L (16-17). We hypothesize deregulated expression of these proteins plays a critical role in the maintenance of breast cancer cells and resistance of tumor cells to therapy-induced apoptosis. To determine the role of the Bcl-2 family of proteins in maintaining cancer cell viability, we constructed a recombinant adenovirus vector that expresses Bcl-x_S, a dominant inhibitor of Bcl-2 and Bcl-x_L. Even in the absence of an exogenous apoptotic signal, this recombinant virus specifically and efficiently activates apoptosis in human carcinoma cells arising from multiple organs including breast, colon, stomach and sympathetic nervous tissue (18). Based on these results, we hypothesize that apoptotic signals are constitutively expressed in proliferating cancer cells and perhaps in normal cells, although repressed by members of the Bcl-2 family of proteins. In this proposal, we proposed studies (i)

to determine the mechanism involved in Bcl-x_S-mediated apoptosis using the *bcl-x_S* adenovirus to dissect molecular interactions of the Bcl-2 regulatory pathway; and (ii) to characterize cellular proteins that interact with Bcl-x_S using biochemical and genetic approaches.

BODY OF THE FINAL REPORT

Technical Objective #1: Further characterization of the interaction of Bcl-x_S with Bcl-2, Bcl-x_L and Bax in breast cancer cells.

Task 1.1: Determine whether Bcl-XS associates with Bcl-XL and/or Bcl-2 in vivo.

We presented evidence in the original proposal that MCF-7 breast tumor cells and primary breast carcinoma cells undergo apoptotic cell death after exposure to a *bcl-x$_S$* adenovirus vector. Our hypothesis was that inactivation of Bcl-2 or Bcl-x_L by Bcl-x_S unleashes endogenous death signals leading to execution of the apoptotic program. We proposed experiments to examine molecular interactions of the Bcl-2 family members following expression of Bcl-x_S protein, but prior to morphological/biochemical cell death, in order to define those interactions which may be created or destroyed as the apoptotic program is activated.

In the initial experiments, cancer cells that express stably FLAG-tagged Bcl-2 or Bcl-X_L were infected with the *bcl-x$_S$* or control beta-galactosidase adenovirus vector. Twenty hours later the infected cells were cultured in media containing ^{35}S-methionine-cysteine for 4-5 hrs to label newly synthesized proteins in infected cells. Cells were then lysed and protein was immunoprecipitated with anti-FLAG antibody in a buffer containing non-ionic detergents. After immunoprecipitation, the protein complexes were disrupted by heating in the presence of 1% SDS. The supernatant was then diluted and reimmunoprecipitated using anti- Bcl-X or control antibody. Using this approach, it was difficult to detect interactions between Bcl-X_S and Bcl-2 or Bcl-X_L due to the low sensitivity of the assay. To overcome this problem, we performed sequential Immunoprecipation/Western-blot analysis of the same lysates. In this type of experiment, cellular lysates were immunoprecipated with anti-FLAG and protein complexes were resolved by SDS-PAGE, transfered to nitrocellulose, and immunoblotted with anti-Bcl-X antibody. These experiments showed that Bcl-X_S interacts with Bcl-X_L but not with Bcl-2. To verify these results, we used transiently transfected cancer cells for the characterization of protein-protein interactions. Doing so has allowed us to perform immunoprecipitations of epitope tagged Bcl-Xs, which were previously impossible with the untagged *bcl-x$_S$* adenovirus. This model system is similar to that of the *bcl-x$_S$* adenovirus in that cancer cells undergo apoptosis in response to transient transfection of both untagged and HA-epitope tagged Bcl-Xs. To determine if Bcl-Xs associates with Bcl-XL or Bcl-2, sequential Immunoprecipitation/Western–blot analysis was done on lysates of cells transfected with Bcl-Xs-HA and Bcl-XL-Flag or Bcl-2-Flag. Lysates were immunoprecipitated with either anti-Flag or anti-HA antibodies. Washed protein complexes were resolved by SDS-PAGE, transferred to nitrocellulose and immunoblotted with the reciprocal antibody. These experiments showed that Bcl-Xs clearly interacts with Bcl-XL-Flag but weakly or not at all with Bcl-2 Flag (Figure 1)

In additional experiments, we have performed extensive mutagenesis of the Bcl-Xs protein to determine the regions of Bcl-Xs required for its interaction with Bcl-X_L and those involved in breast cancer cell killing. We have expressed the Bcl-Xs mutants in cells *in vivo* (Figure 2A), and have analyzed these mutants for their ability to kill a variety of cancer cells in the transient transfection assay. Results of these studies have mapped the domain required for killing as the BH3 domain (amino acids 86-98) and the hydrophobic C-terminal domain (amino acids 144-170)

that is required for targeting to the outer mitochondria (Figure 2B) Interestingly, the broad range caspase inhibitor, viral p35, is able to completely inhibit Bcl-xs killing, suggesting that Bcl-xs kills through a caspase dependent mechanism.

We performed interaction analysis of Bcl-XL with Bcl-XS mutants to determine whether the killing activity of Bcl-XS correlates with its ability to bind Bcl-XL. In these experiments, Flag-tagged Bcl-x_L and various HA-tagged Bcl-x_S mutant constructs were transfected into 293T cancer cells and Bcl-x_L complexes were immunoprecipitated with anti-Flag antibody. In Figure 3A, we showed that the BH3 domain of Bcl-x_S (residues 116-132) is required for binding to Bcl-x_L. Bcl-x_S (with deletion of residues 116-132) was expressed as detected by immunoblotting of total NP-40 lysates (panel B of Figure 3). Furthermore, these results were specific in that other Bcl-x_S mutants in which other regions of the molecule were deleted still bound to Bcl-x_L (Figure 3A).

Task 1.2: Determine whether Bcl-XS disrupts the interaction of Bcl-XL with Bax and Bak

We determined next if Bcl-X_S expression could alter the interaction of Bcl-X_L with BAX in transiently transfected cancer cells. In these experiments, FLAG-tagged Bcl-X_L/Bax complexes were immunoprecipitated with anti-FLAG in the presence or absence of Bcl-X_S, and the amount of bound endogenous BAX was determined by immunoblotting with anti-BAX antibody. The results showed that Bcl-X_S is unable to displace BAX from Bcl-X_L, even in cells that undergo Bcl-xs mediated cell death (Figure 4) We could not determine if Bcl-X_S could alter Bcl-XL binding to BAK, because the cancer cell lines we tested did not express detectable levels of endogenous BAK.

Task 1.3: Determine whether Bcl-XS functions by association with other proteins that regulate apoptosis

Recent experiments with nematode CED-9, CED-4 and CED-3 have suggested that Bcl-2 and Bcl-x_L regulate apoptosis by interacting with and inhibiting caspases (death proteases) through Apaf-1, a mammalian homologue of the *C. Elegans* CED-4 protein (19-21). These observations suggested that Bcl-XS might antagonize Bcl-XL by interfering with the ability of Bcl-XL to inactivate the caspase regulator Apaf-1. We performed experiments to test whether Bcl-XL could associate with Apaf-1 procaspase-9, a central death protease that associates with Apaf-1. The analysis showed that Bcl-x_L and caspase-9 co-immunoprecipitated *in vivo*. Detailed of these experiments is provided in a manuscript by Hu *et al.* Proc. Natl. Acad. Sci. USA, 1998 (See Appendix). These observations suggested that Bcl-x_S might antagonize Bcl-x_L by interfering with the ability of Bcl-x_L to inactivate the caspase regulator Apaf-1. To assess whether Bcl-x_S can promote apoptosis via the Apaf-1/caspase-9 pathway, we expressed Bcl-x_S in the presence or absence of caspases inhibitors including baculovirus p35 and cell-permeable modified peptide BOC-fmk and more importantly with a dominant interfering mutant of caspase-9. In figure 5, it is shown that normal mouse embryo fibroblasts (MEFs), Bcl-x_S killing is inhibited by Bcl-2 and Bcl-x_L, but also by p35 and BOC-fmk, and more importantly by dominant negative caspase-9.

To further verify these results, we used MEFs derived from mutant mice in which the Apaf-1 or caspase-9 genes have been ablated by homologous recombination (24-45). Bcl-x_S killed wild-type (WT) MEFs, as detected by a great reduction of cells that expressed a reporter LacZ gene

(blue cells), but not Apaf-1 -/- or caspase-9 -/- deficient MEFs (Figure 6A, 6B and 6C). These results further indicate that Bcl-x_S can kill cells via an Apaf-1/caspase-9 pathway of apoptosis.

These observations suggest that Bcl-2/Bcl-x_L control apoptosis at least in part through physical association with Apaf-1, and that Bcl-XS might promote apoptosis by interfering with the ability of Bcl-XL to associate with Apaf-1. We tested first whether Bcl-x_S, was capable of interacting with Apaf-1. The analysis showed that Bcl-XS co-immunoprecipitated with Apaf-1 (Figure 7). This result indicates that regions outside the BH1-2 domains that are present in Bcl-XS may mediate contact with Apaf-1. These preliminary results suggest that Bcl-XS promotes apoptosis by competing with Bcl-XL for Apaf-1 binding. Alternatively, the cellular interaction we have observed between Apaf-1 and Bcl-XS might be indirect and mediated by binding of Bcl-XS to endogenous Bcl-XL or another adaptor protein. To assess the former, we determined whether the binding of Bcl-x_S to Apaf-1 was enhanced by Bcl-x_L expression. In these experiments, HA-tagged Bcl-x_S and Myc-tagged Apaf-1 mutant constructs were transfected into 293T cancer cells in the presence or absence of Flag-tagged Bcl-x_L. Immunoprecipitation of Bcl-x_S complexes with anti-HA antibody revealed that the binding of Bcl-x_S to Apaf-1 was enhanced by Bcl-x_L, as determined by immunoblotting for Apaf-1 with anti-Myc antibody (Figure 7). This results cannot be explained by increased expression of Bcl-x_S protein as assessed by immunoblotting with anti-HA antibody (Figure 7, middle panel).

The studies with Bcl-XL has been performed with Apaf-1S (see Figure 8A). However, we were unable to demonstrate cytochrome c binding (see below) to the Apaf-1S isoform originally described by Zou *et al.* (22) and also cloned by us from HeLa cDNA (Figure 8). We also noticed that endogenous 293T Apaf-1 protein appeared to migrate somewhat slower than transfected Apaf-1S (see below in Figure 8E), and in our hands we were unable to demonstrate cytochrome c/dATP-dependent *in vitro* activation of procaspase-9 by the Apaf-1S isoform (see below). We, therefore, used RT-PCR to clone other potential full length Apaf-1 cDNAs from 293T cells. Two full length Apaf-1 cDNAs were cloned from 293T cells and were identical to the Apaf-1S isoform, except that they contained an 11 amino acid insert (GKDSVSGITSY) at position 98 between the CARD and ATPase domain and a 43 amino acid WDR inserted between the fifth and sixth existing WDRs of Apaf-1S (Figure 8). The presence of the N-terminal insert is consistent with the utilization of an alternative exon donor site in exon 3 and a single acceptor site in exon 4 (Genbank accession numbers AF098871 and AF098873, respectively). The presence of the additional C-terminal WDR is consistent with the utilization of an additional exon 17a (Genbank accession numbers AF117658 and AF117659). Recently, Zou *et al.* (26) have also reported the cloning of this Apaf-1 cDNA from HeLa cells. For consistency and clarity, we have termed this isoform Apaf-1XL. This was done to distinguish it from two other alternative human Apaf-1 cDNA splice variants (Figs. 8B,C, D) that are also longer than the originally identified Apaf-1S (Figure 8A). We constructed these two alternative Apaf-1 cDNAs using the Apaf-1S and Apaf-1XL cDNAs as described in Experimental Procedures. For clarity, we have termed them Apaf-1LC (Long C-terminus: containing the additional WDR, but lacking the N-terminal insert) and Apaf-1LN (Long N-terminus: containing the N-terminal insert, but lacking the additional WDR) (Figure 8A). Detailed description of these results is provided in an attached manuscript by Benedict *et al.* J. Biol. Chem., 2000 (Appendix).

All of the human Apaf-1 cDNAs described have been isolated from tumor cell lines. To determine if multiple Apaf-1 cDNAs are present in normal human tissues, we performed full length Apaf-1 PCR analysis on cDNAs generated from normal human tissue RNAs (Figure 8B). This analysis demonstrated the existence of at least two Apaf-1 cDNA forms. The larger form co-migrated with the cloned Apaf-1XL fragment, while the smaller form migrated slightly above that of Apaf-1S (Figure 8B). Restriction mapping of each of these gel purified full length Apaf-1 PCR products confirmed their identities as Apaf-1 cDNAs. Because of limited gel resolution, minor amounts of other Apaf-1 cDNAs may have been present but not detectable. To better examine the relative amounts of the different Apaf-1 forms, we performed PCR analysis of the human tissue cDNAs using two sets of primers that flank the two different insertions. Primers N1 and N2 flank the N-terminal 11 amino acid insertion, while primers C1 and C2 flank the additional WDR (Figure 8A). PCR analysis using primers N1 and N2 showed that in all tissues the great majority of the products (> 80%) contained the 11 amino acid N-terminal insertion, as determined by comparison with control reactions containing various ratios of Apaf-1XL and Apaf-1S DNAs (Figure 8C). PCR analysis using primers C1 and C2 showed that in all tissues both types of products are represented, although the relative amounts of the two types varied among the tissues (Figure 8D). A compilation of the PCR results from Figures 1C and 1D suggests that the major full length Apaf-1 cDNAs observed in most of these tissues appears to be Apaf-1XL (containing both N-terminal and C-terminal insertions). At the level of mRNA expression, tissues such as bone marrow, colon and spleen appear to have roughly equal amounts of Apaf-1XL and Apaf-1LN (containing just the N-terminal insertion), while tissues such as brain, kidney, stomach, and skeletal muscle express more Apaf-1XL.

To determine whether multiple Apaf-1 isoforms are also expressed at the protein level, we examined multiple cell lines by immunoblotting using a polyclonal anti-Apaf-1 antibody. Lysates of 293T cells transiently transfected with the different Apaf-1 forms (described in Figure 5A) were run as controls. The major immunoreactive band in each of the cell lines co-migrated with the Apaf-1XL form (Figure 8E), which is consistent with the data from the mRNA analysis of human tissues identifying Apaf-1XL as the major form expressed (Figures 8B, C, D). As in the tissue mRNAs, multiple Apaf-1 protein isoforms were also expressed in these cell lines (Figure 8E). These other bands appear to co-migrate with the Apaf-1LN and Apaf-1S forms, however, exact identification would require either protein sequencing or isoform-specific antibodies. Similar results were obtained when lysates from normal breast tissue and two breast cancer cell lines were immunoblotted with anti-Apaf-1 antibody (data not shown). Immunoblotting of these lysates with another polyclonal anti-Apaf-1 antibody (Cayman Chemical Company) confirmed these results.

Purified Apaf-1 has been reported to activate procaspase-9 in a cytochrome c and dATP-dependent fashion (23). To determine if the newly identified Apaf-1 cDNAs also share this activity, and to determine the role of the N-terminal and C-terminal insertions, the four full length Myc-tagged Apaf-1 constructs (Figure 9) and the originally described untagged Apaf-1S were expressed in 293T cells. Cytosolic extracts of these cells were prepared and anti-Apaf-1 immunoblotting confirmed comparable expression of each of the transfected Apaf-1 forms (Figure 9). Ten ugs of the fresh cytosolic extracts were also analyzed for their ability to activate procaspase-9 *in vitro*. Extracts were diluted so that endogenous Apaf-1 activity could not be detected. As shown in Fig. 9, only Apaf-1XL and Apaf-1LC containing the extra WDR, but not those isoforms lacking it, were able to activate procaspase-9 in a cytochrome c and dATP-dependent fashion as indicated by the appearance of the intermediate p35 proteolytic fragments. These same results were obtained using one or thirty μgs of

cytosolic extracts (data not shown). Due to the presence of low levels of dATP or ATP in the cytosolic extracts, we confirmed the requirement for ATP by the addition of the non-hydrolyzable ATP analogue, ATP-γ-S, which almost completely inhibited the cytochrome-c/dATP-dependent activation of procaspase-9 (Figure 9). Although the original untagged Apaf-1S was previously reported to activate procaspase-9 in a cytochrome c/dATP-dependent fashion (23), we were unable to detect such activity under our assay conditions (Figure 9).

The apparent requirement of the extra WDR for cytochrome c/dATP-dependent activation of procaspase-9 prompted us to examine the ability of the different Apaf-1 forms to bind cytochrome c. As shown in Fig. 10A, following anti-Myc antibody immunoprecipitation in the presence or absence of cytochrome c, dATP or ATP-γ-S and immunoblotting with mouse anti-cyt c antibody, only the Apaf-1 constructs Apaf-1XL and Apaf-1LC, containing the extra WDR, bound to cytochrome c. This cytochrome c binding also required ATP/dATP, as binding was greatly inhibited by the addition of the non-hydrolyzable ATP analogue, ATP-γ-S (Figure 10A). The N-terminal 11 amino acid insert was not required for cytochrome c binding, as the form Apaf-1LC, lacking the N-terminal insert, bound cytochrome c (Fig. 10A). Cytochrome c binding to the C-terminal deletion mutant, C+ (Apaf-1XL 479-1248), containing the extra WDR was not detected, suggesting that this region, although necessary (Figure 10A), is not sufficient to mediate cytochrome c binding (Figure 10B). Cytochrome c also failed to bind to either the N+ (Apaf-1XL 1-570) or N- (Apaf-1S 1-559) deletion mutants (Figure 10B). This data is consistent with a model in which the C-terminal WDR region with the additional WDR contains a binding site for cytochrome c that may be unmasked only following a conformational change driven by ATP hydrolysis in the N-terminus.

We and others have previously shown that Apaf-1 can self-associate to form homo-oligomers (27-29). As our previous studies utilized Apaf-1 protein in NP-40 cellular extracts, we first used NP-40 extracts to compare the four different full length Apaf-1 constructs for their ability to form homo-oligomers. Myc- and HA-tagged isoforms were expressed in 293T cells, lysed in NP-40 buffer, immunoprecipitated with anti-Myc antibody and immunoblotted with anti-HA or anti-Myc antibodies. As shown in Fig. 11A, all four Apaf-1 isoforms were able to self-associate. Anti-HA immunoblotting confirmed similar expression of the HA-Apaf-1 isoforms in the NP-40 extracts. Since these studies were performed in the presence of detergent, we repeated these self-association experiments under more physiological conditions. Cytosolic extracts of Myc- and HA-Apaf-1 isoforms made without detergent were mixed in the presence or absence of cytochrome c, dATP, or ATP-γ-S. Under these conditions, only Apaf-1XL and Apaf-1LC, both containing the extra WDR, underwent cytochrome c/dATP-dependent self-association (Figure 11B). Because Apaf-1LC lacks the N-terminal 11 amino acid insert, this region is clearly not required for cytochrome c/dATP-dependent self-association. Anti-HA immunoblotting confirmed similar expression of the HA-Apaf-1 isoforms. This data is consistent with a model in which cytochrome c binds the Apaf-1 C-terminus with the extra WDR, thus relieving the inhibition of the N-terminus, and allowing Apaf-1 self-association. The requirement of the extra WDR for Apaf-1 Self-association is also consistent with our observation that it is required for procaspase-9 activation. Not surprisingly, the two constructs, Apaf-1XL and Apaf-1LC, with the extra WDRs, were capable of forming cytochrome c/dATP-dependent hetero-oligomers (Figure 11B). However, hetero-oligomers between the two major cDNAs detected in human tissues, Apaf-1XL (with the extra WDR) and Apaf-1LN (lacking the extra WDR), were not observed (data

not shown). In addition, we verified the ability of Apaf-1XL but not Apaf-1LN to form oligomers in a dATP/cytochrome c-dependent fashion by gel filtration analysis (Benedict et al. Appendix).

We and others have previously demonstrated the binding between the originally described Apaf-1S and procaspase-9 (14-15, 23). We, therefore, compared the four full length Apaf-1 isoforms for their ability to associate with procaspase-9 in the presence of NP-40. Each Myc-tagged Apaf-1 construct and HA-procaspase-9 (C287S) were expressed in 293T cells, lysed in NP-40 buffer, immunoprecipitated with anti-Myc antibody and immunoblotted with anti-HA or anti-Myc antibodies. As shown in Fig. 12A, all Apaf-1 isoforms tested bound to procaspase-9. Anti-HA immunoblotting confirmed similar expression of procaspase-9 in each extract. However, when binding was analyzed in cytosolic extracts lacking detergent, in the presence or absence of cytochrome c, dATP or ATP-γ-S, only Apaf-1XL and Apaf-1LC containing the extra WDR bound to procaspase-9 in a cytochrome c and dATP-dependent fashion (Figure 12B). Because Apaf-1LC lacks the N-terminal 11 amino acid insert, this region is clearly not required for cytochrome c/dATP-dependent procaspase-9 binding. The requirement of the extra WDR for procaspase-9 binding is in complete agreement with our observation that this region is also required for procaspase-9 activation. Previous data from our laboratory suggests that the C-terminal WDRs of Apaf-1 can bind and inhibit the ability of the N-terminus to self-associate and to activate procaspase-9 *in vitro* (27). Taken together, the data presented herein suggest a model in which cytochrome c, in the presence of ATP/dATP, binds to the C-termini of only those Apaf-1 isoforms containing the extra WDR, thus relieving the inhibition of the N-terminus, and allowing Apaf-1 self-association, procaspase-9 binding, and the activation of procaspase-9. A biochemical model of caspase-9 activation by Apaf-1 using the newly identified Apaf-1XL has been recently reported by us (30).

Technical Objective #2: Further characterization and purification of p15, a cellular protein that interacts with Bcl-x_S.

A mechanism that might explain the apoptosis-promoting activity of Bcl-x_S is through binding to an upstream activator or a downstream effector of Bcl-2/Bcl-x_L mediated survival. In preliminary results, we provided evidence in the original application that Bcl-x_S interacts with a cellular protein, p15, in cancer cells infected with the *bcl-x_S* adenovirus. The significance of the Bcl-x_S-p15 interaction was unclear. p15 could represent a death effector which is activated by the expression of Bcl-x_S. Alternatively, p15 could be a cellular protein required for survival whose activity is inhibited by the Bcl-x_S interaction. Clearly, biochemical characterization of p15 and isolation of the p15 cDNA was needed to further assess the role of p15 in Bcl-x_S-mediated apoptosis.

Task 2.1: Biochemical Purification and N-Terminal Microsequencing of p15

We purified p15 by virtue of its association not only with Bcl-xs, but also with Bcl-2. Stably transfected Shep-1 neuroblastoma cells expressing Bcl-2 Flag were used as a source of the Bcl-2-associated p15 protein. We purified p15 isolated from preparative gels and submitted the material for microsequencing. The N-terminal sequence we obtained from the p15 material was: M/K-R-D-P-V-A-R-T-S. Except for the first amino acid, this sequence corresponds to amino acids of human Bcl-2 that are part of its flexible loop region (27). Two potential caspase cleavage sites occur within the loop at positions 34 and 64. However, the Bcl-2 fragment we sequenced failed to corresponded to either caspase cleavage site. It is most likely the result of non-specific protealysis of the exposed loop region, and is therefore a degradation product of Bcl-2. The original p15 protein identified as a Bcl-xs binding protein is clearly different from the p15 we observed as a Bcl-2 associated band. However, we have been unable to detect any 15 kDa protein associating with Bcl-xs-HA in variety of cancer lines tested. As the original p15 was detected in adenovirus bcl-xs infected cells, it is possible that the p15 was an adenoviral gene product. Given these results we are no longer pursuing the characterization of the protein band termed p15.

Task 2.2: Genetic Screen for Bcl-x-Binding Proteins using the Two-Hybrid Yeast Assay

To search for Bcl-x-interacting proteins, we screened placenta and brain cDNA libraries using Gal4-Bcl-x_L and Gal4-Bcl-x_S as "baits" in the yeast two-hybrid assay. In the first screen using the GAL4-Bcl-x_L bait, fifty six positive clones were identified that interacted with Gal4-Bcl-x_L. Forty one cDNAs encoded Bad, a Bcl-2 family member recently isolated by binding to Bcl-2. Ten cDNAs encoded Bcl-2 which is known to bind Bcl-X_L in the two-hybrid system. The nucleotide sequences of four cDNAs were novel in that they did not reveal significant homology to any known gene or translated products in the databases. Three of these novel cDNAs encoded the same gene which we have named *harakiri*. The same gene was identified as an interacting partner of Bcl-2 (28). *Harakiri* functions as a regulator of Bcl-2 and Bcl-X_L and apoptotic cell death in mammalian cells. The *hrk* product (HRK) does not exhibit significant homology to Bcl-2 or Bcl-X_L and lacks the conserved BH1 and BH2 domains that are shared by Bcl-2 family members. Significantly, HRK physically interacts with anti-apoptosis proteins Bcl-2 and Bcl-X_L but not with death-promoting Bcl-2 members such as Bax and Bak. Expression of HRK induces rapid onset of cell death in mammalian cells including breast cancer cells. Importantly, the death-promoting activity of HRK is repressed by Bcl-2 and Bcl-X_L, suggesting that HRK is a common target of the anti-apoptosis proteins Bcl-2 and Bcl-X_L. Details of these results have

been recently published (Inohara *et al.* The EMBO J. 1997, Appendix). Because analysis of HRK is beyond the statements of work, we are not pursuing the analysis of HRK with funds provided by this grant.

KEY RESEARCH ACCOMPLISHMENTS

- Identification and cloning of harakiri, a proapoptotic BH3-containing protein that associates with Bcl-2 and Bcl-XL
- Bcl-XS requires BH3 and hydrophobic C-terminal domain for apoptosis and associates with Bcl-XL through its BH3 domain
- Bcl-XS associates with Bcl-XL but weakly or not at all with Bcl-2

- Bcl-XS killing is mediated, at least in part, through the Apaf-1-caspase-9 pathway of apoptosis
- Bcl-XS binds Apaf-1 which appears to mediated through Bcl-XL
- Identification and cloning of novel Apaf-1 cDNAs including functional Apaf-1 cDNA
- Expression and functional characterization of Apaf-1 isoforms

REPORTABLE OUTCOMES

Manuscripts:

- Inohara N, Ding D, Chen S, Nuñez G. harakiri, a novel regulator of cell death, encodes a protein that activates apoptosis and interacts selectively with survival-promoting proteins Bcl-2 and Bcl-xL. *EMBO J.* 16:1686-1694 (1997).

- Hu Y, Benedict M, Wu D, Inohara N, Nuñez G. Bcl-x_L interacts with Apaf-1 and inhibits Apaf-1-dependent Caspase-9 activation. *Proc Natl Acad Sci USA.* 95:4386-4391 (1998).

-Hu Y., Benedict M.A., Ding L., and Nuñez G. Role of Cytochrome c and dATP/ATP Hydrolysis in Apaf-1-Mediated Caspase-9 Activation and Apoptosis. *EMBO J.* 18: 3586-3595 (1999).

-Benedict M.A., Hu Y., Inohara N., and Nuñez G. Expression and functional analysis of Apaf-1 Isoforms: Extra WD-40 repeat is required for cytochrome c binding and regulated activation of procaspase-*9. J Biol Chem.* 275:8461-8468 (2000)

Grants:

-RO1 CA75136 grant from National Institutes of Health entitled "HRK, a novel apoptosis regulatory gene" 01/01/98-12/3/02 (PI: Gabriel Nunez)

Graduate Thesis

- DOD grant supported work to fullfill the requirements for Ph. D of a graduate student, Mary Benedict (thesis defense scheduled for Fall 2000).

CONCLUSIONS

The studies supported by the grant have provided information regarding the mechanism by which the Bcl-X_S kills tumor cells. Bcl-XS physically associated with Bcl-XL but weakly or not at all with and Bcl-2 in cancer and normal cells. Mutational analysis has revealed that the BH3 domain and the C-terminal hydrophobic domain of Bcl-XS are critical for induction of apoptosis. The binding of Bcl-XS to Bcl-XL was mediated by the BH3 region of Bcl-XS. Apoptosis by Bcl-XS involved activation of Apaf-1 and caspase-9. These results suggest that Bcl-XS promote apoptosis by antagonizing Bcl-X_L through Apaf-1. Several isoforms of Apaf-1 were identified. One form, Apaf-1XL, was the predominant protein found in human tissues including the breast. Apaf-1XL bound cytochrome c and activated caspase-9 in an ATP/cytochrome c-dependent manner.

A recombinant adenovirus expressing Bcl-XS in currently being evaluated for ex-vivo killing of cancer cells contaminating the bone marrow of breast cancer patients, as the virus spares hematopoietic stem cells. The work presented is relevant to the mechanism by which Bcl-XS kills cancer cells.

REFERENCES

1. Vaux DL, Cory S, Adams JM. Bcl-2 gene promotes haemopoietic cell survival and cooperates with c-myc to immortalize pre-B cells. *Nature*. 335:440-442 (1988).
2. Nuñez G, London L, Hockenbery D, Alexander M, McKearn JP, Korsmeyer SJ. Deregulated Bcl-2 gene expression selectively prolongs survival of growth factor-deprived hemopoietic cell lines. *J Immunol*. 144:3602-3610 (1990).
3. Boise LH, González-Garcia M, Postema CE, Ding L, Lindsten T, Turka LA, Mao X, Nuñez G, Thompson CB. *bcl-x*, a *bcl-2* related gene that functions as a dominant regulator of apoptotic cell death. *Cell*. 74:597-608 (1993).
4. Zha H, Aime-Sempe C, Sato T, Reed JC. Proapoptotic protein Bax heterodimerizes with Bcl-2 and homodimerizes with Bax via a novel domain (BH3) distinct from BH1 and BH2. *J Biol Chem*. 271:7440-7444 (1996).
5. Oltvai ZN, Milliman, CL, Korsmeyer SJ. Bcl-2 heterodimerizes *in vivo* with a conserved homolog, Bax, that accelerates programmed cell death. *Cell*. 74:609-619 (1993).
6. Yang E, Zha J, Jockel J, Boise LH, Thompson CB, Korsmeyer SJ. Bad, a heterodimeric partner for Bcl-x_L and Bcl-2, displaces Bax and promotes cell death. *Cell*. 80:285-291 (1995).
7. Han J, Sabbatini P, White E. Induction of apoptosis by human Nbk/Bik, a BH3-containing protein that interacts with E1B 19K. *Mol Cell Biol*. 16:5857-5864 (1996).
8. Wang K, Yin XM, Chao DT, Milliman CL, Korsmeyer SJ. BID: a novel BH3 domain-only death agonist. *Genes Dev*. 10:2859-2869 (1996).
9. Inohara N, Ding D, Chen S, Nuñez G. *harakiri*, a novel regulator of cell death, encodes a protein that activates apoptosis and interacts selectively with survival-promoting proteins Bcl-2 and Bcl-x_L. *EMBO J*. 16:1686-1694 (1997).
10. Inohara N, Ekhterae D, Garcia I, Carrio R, Merino J, Merry A, Chen S, Nuñez G. Mtd, a novel Bcl-2 family member activates apoptosis in the absence of heterodimerization with Bcl-2 and Bcl-x_L. *J Biol Chem*. 273(15):8705-8710 (1998).
11. Chittenden T, Flemington C, Houghton AB, Ebb RG, Gallo GJ, Elangovan B, Chinnadurai G, Lutz RJ. A conserved domain in Bak, distinct from BH1 and BH2, mediates cell death and protein binding functions. *EMBO J*. 14(22):5589-5596 (1995).
12. Sattler M, Liang H, Nettesheim D, Meadows RP, Harlan JE, Eberstadt M, Yoon HS, Shuker SB, Chang BS, Minn AJ, Thompson CB, Fesik SW. Structure of Bcl-xL-Bak peptide complex: recognition between regulators of apoptosis. *Science*. 275:983-986 (1997).
13. Vander Heider MG, Chandel NS, Williamson EK, Schumacker PT, Thompson CB. Bcl-xL regulates the membrane potential and volume homeostasis of mitochondria. *Cell*. 91(5):627-637 (1997).
14. Pan G, O'Rourke K, Dixit VM. Caspase-9, Bcl-x_L, and Apaf-1 form a ternary complex. *J Biol Chem*. 273:5841-5845 (1998).
15. Hu Y, Benedict M, Wu D, Inohara N, Nuñez G. Bcl-x_L interacts with Apaf-1 and inhibits Apaf-1-dependent Caspase-9 activation. *Proc Natl Acad Sci USA*. 95:4386-4391 (1998).
16. Silvestrini R, Veneroni S, Daidone MG, Benini E, Boracchi P, Mezzetti M, Di Fronzo G, Rilke F, Veronesi U. The Bcl-2 protein: a pronostic indicator strongly related to p53 protein in lymph node-negative breast cancer patients. *J Natl Cancer Inst*. 86:499-504 (1994).

17. Olopade OI, Adeyanju MO, Safa AR, Hagos F, Mick R, Thompson CB, Recant WM. Overexpression of Bcl-x protein in primary breast cancer is assoicated with high tumor grade and nodal metastases. *Cancer J.* 230-237, 1997.
18. Clarke MF, Apel IJ, Benedict MA, Eipers PJ, Sumantran V, González-García M, Doedens M., Fukunaga N, Davidson B, Dick JE, Minn AJ, Boise LH, Thompson CB, Wicha M, Núñez G. A recombinant *bcl-x$_S$* adenovirus selectively induces apoptosis in cancer cells, but not normal bone marrow cells. *Proc Natl Acad Sci USA.* 92:11024-11028 (1995).
19. Wu D, Wallen HD, Nuñez G. Interaction and regulation of subcellular localization of CED-4 by CED-9. *Science.* 275:1126-1128 (1997).
20. Chinnaiyan AM, Chaudhary D, O'Rourke K, Koonin EV, Dixit VM. Interaction of CED-4 with CED-3 and CED-9: a molecular framework for cell death. *Nature.* 388:728-729 (1997).
21. Spector MS, Desnoyers S, Hoeppner DJ, Hengartner MO. Interaction between the *C. elegans* cell-death regulators CED-9 and CED-4. *Nature.* 385:653-656 (1997).
22. Zou H, Henzel WJ, Liu X, Lutschg A, Wang X. Apaf-1, a human protein homologous to *C. elegans*, CED-4, participates in cytochrome c-dependent activation of caspase-3. *Cell.* 90:405-413 (1997).
23. Li, P., Nijhawan, D., Budihardjo, I., Srinivasula, S.M., Ahmad, M., Alnemri, E.S. and Wang, X. Cytochrome c and dATP-dependent formation of Apaf-1/caspase-9 complex initiates an apoptotic protease cascade. *Cell,* 91: 479-489 (1997)
24. Hakem, R., Hakem, A., Duncan, G.S., Henderson, J.T., Woo, M., Soengas, M.S., Elia, A., de Pompa, J.L., Kagi, D., Khoo, W., Potter, J., Yoshida, R., Kaufman, S.A., Lowe, S.W., Penninger, J.M. and Mak, T.W. Differential requirement for caspase 9 in apoptotic pathways in vivo. *Cell,* 94: 339-352 (1998)
25. Yoshida, H., Kong, Y.Y., Yoshida, R., Elia, A.J., Hakem, A., Hakem, R., Penninger, J.M. and Mak, T.W. Apaf1 is required for mitochondrial pathways of apoptosis and brain development. *Cell,* 94: 739-750 (1998)
26. Zou, H., Li, Y., Liu, X. and Wang, X. An APAF-1.Cytochrome c multimeric complex is a functional apoptosome that activates procaspase-9. *J. Biol. Chem.*, 274:11549-11556 (1999)
27. Hu, Y., Ding, L., Spencer, D.M. and Núñez, G. WD-40 repeat region regulates Apaf-1 self-association and procaspase-9 activation. *J. Biol. Chem.,* 273: 33489-33494 (1998)
28. Srinivasula, S.M., Ahmad, M., Fernandes-Alnemri, T. and Alnemri, E.S. Autoactivation of procaspase-9 by Apaf-1-mediated oligomerization. *Mol Cell,* 1: 949-957 (1998)
29. Hu Y., Benedict MA, Ding L., and Núñez G. Role of Cytochrome c and dATP/ATP Hydrolysis in Apaf-1-Mediated Caspase-9 Activation and Apoptosis. *EMBO J.* 18: 3586-3595 (1999).

Figure 1

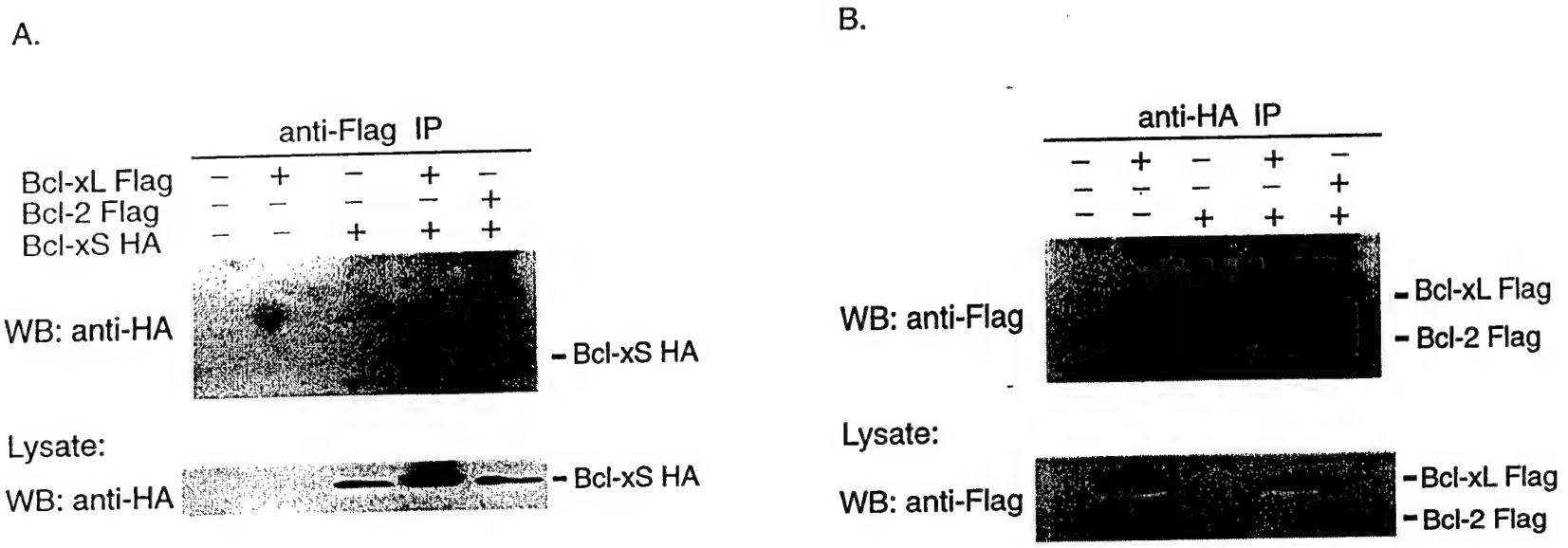

Figure 1 Bcl-xs-HA associates with both Bcl-XL-Flag and Bcl-2-Flag in cancer cells

Cancer cells were transiently transfected with Bcl-xs-HA and Bcl-xL-Flag or Bcl-2-Flag. Anti-Flag (A) or Anti-HA (B) complexes were immunoprecipitated and immunoblotted with the reciprocal antibody. The lower panels are immunoblots of transfected cell lysates.

Figure 2

A.

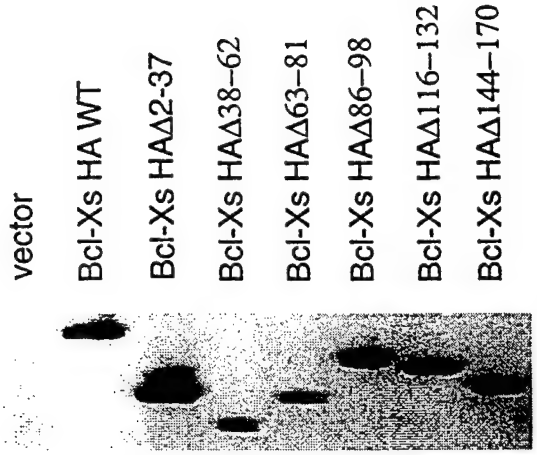

B.

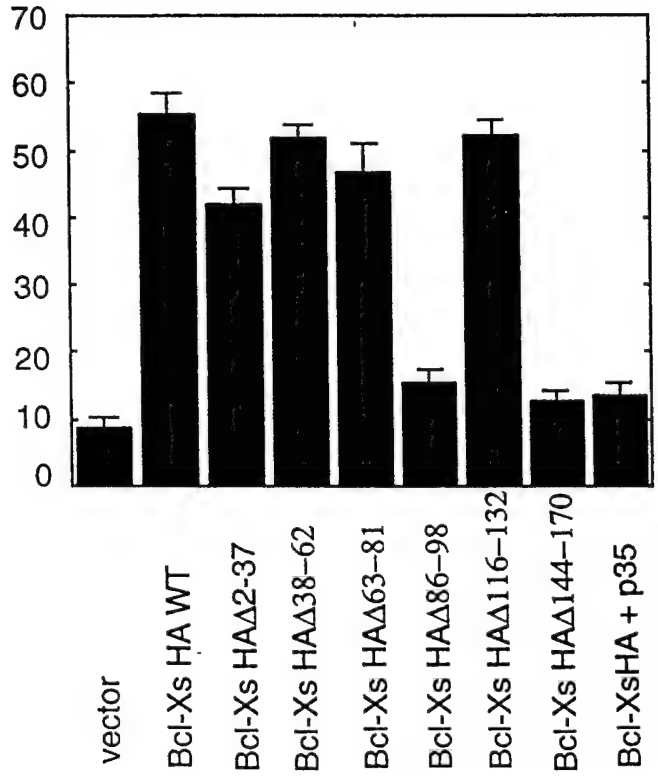

Figure 2 Deletion Analysis of Bcl-xS

A. Anti-HA Western Blot of HA-Bcl-xs mutants transiently expressed in cancer cells.
B. Transient transfection assay to measure Bcl-xs killing of cancer cells. Plasmids were co-transfected with pCMV Bgal; 18 hrs. post-transfection, cells were stained with X-gal and % blue cells with apoptotic morphology was measured.

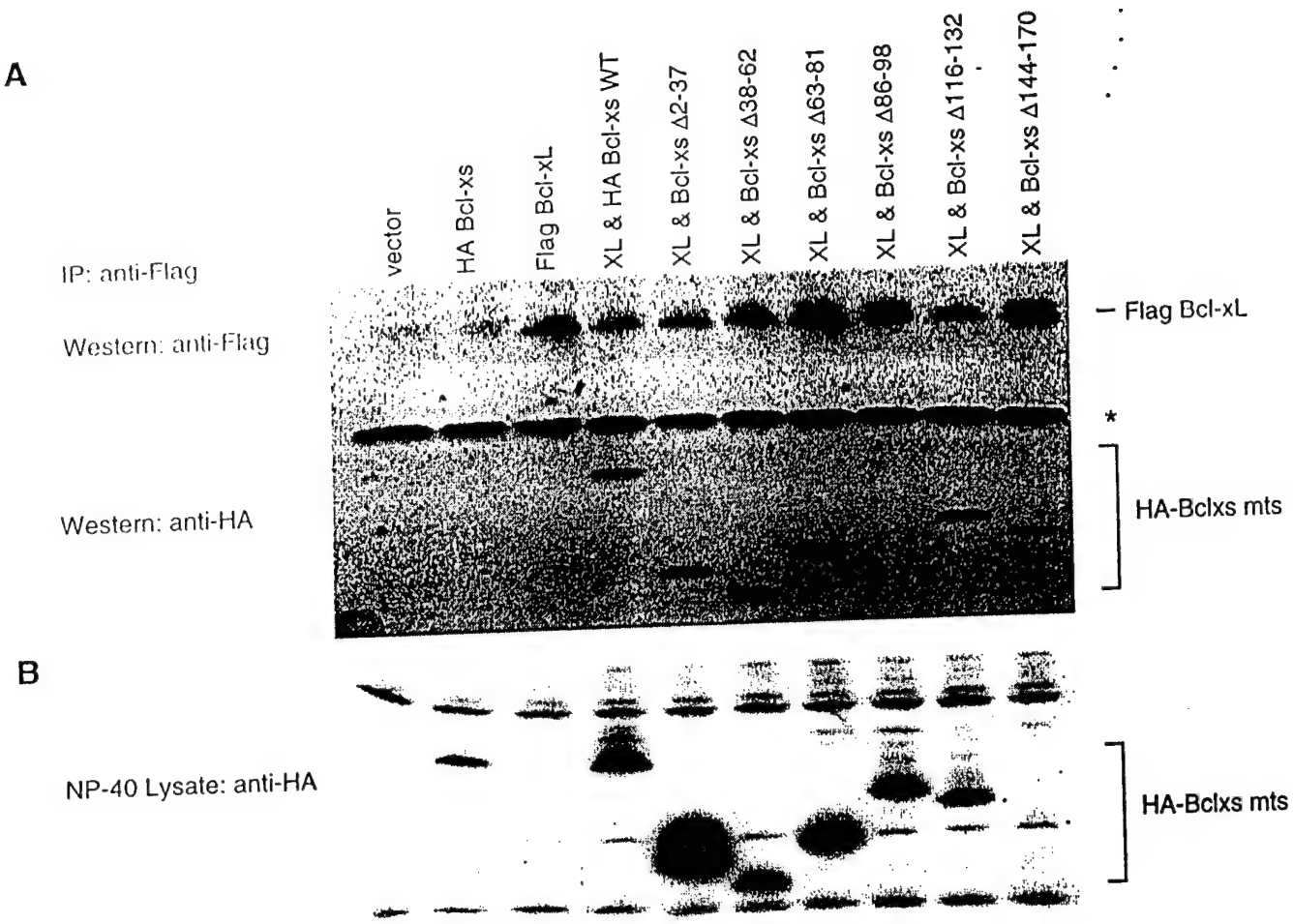

BH3 domain of Bcl-xs is required for binding to Bcl-xL

Cancer cells were transiently co-transfected with plasmids encoding Bcl-xL and Bcl-xs or Bcl-xs deletion mutants as indicated. Bcl-xS/ Bcl-xL complexes were immunoprecipitated with anti-Flag and immunoblotted with anti-HA and anti-Flag. Panel A shows immunoprecipitated Bcl-xL and bound Bcl-xS deletion mutants. * indicates non-specific IgG bands. Panel B shows an anti-HA immunoblot of NP-40 lysates used for the above immunoprecipitations, and demonstrates the expression of the Bcl-xs mutants. Note: Although deletion mutant Δ144-170 is expressed (see [illegible] it is not visible on this exposure.

Figure 4

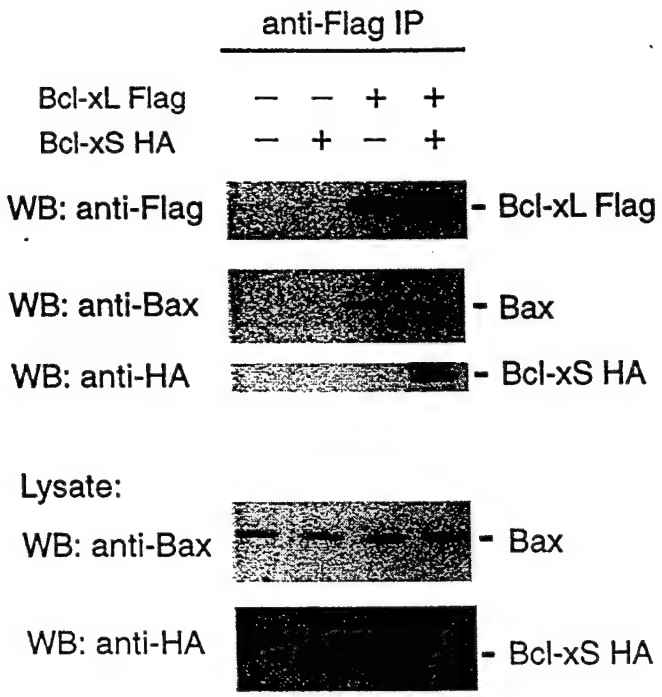

Figure Bcl-xs fails to disrupt Bax/Bcl-XL complexes

Cancer cells were transiently transfected with Bcl-xs-HA and/or Bcl-xL-Flag. Endogenous Bax/Bcl-xL complexes were immunoprecipitated with anti-Flag and immunoblotted with either anti-Bax, anti-HA or anti-Flag. The lower panels are anti-Bax and anti-HA immunoblots of transfected cell lysates.

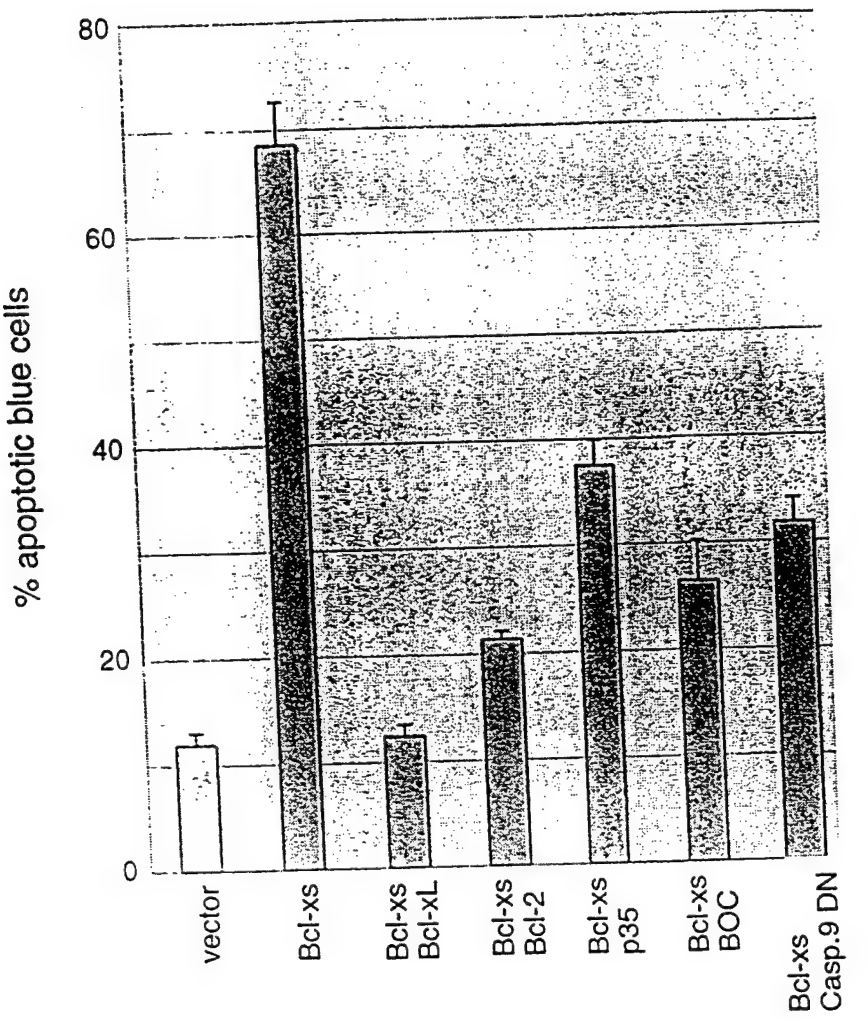

Bcl-xs killing is inhibited by Bcl-XL, Bcl-2 and a panel of caspase inhibitors.

Murine embryo fibroblasts were co-transfected in triplicate with Bgal, Bcl-xs and the indicated plasmids. In some experiments, transfected cells were incubated with the pan-caspase inhibitor, BOC-fmk. 16 hrs post-transfection, the number of blue cells with and without apoptotic morphology were counted. Data is expressed as % apoptotic blue cells of total number of blue cells per well, (average +/- SEM).

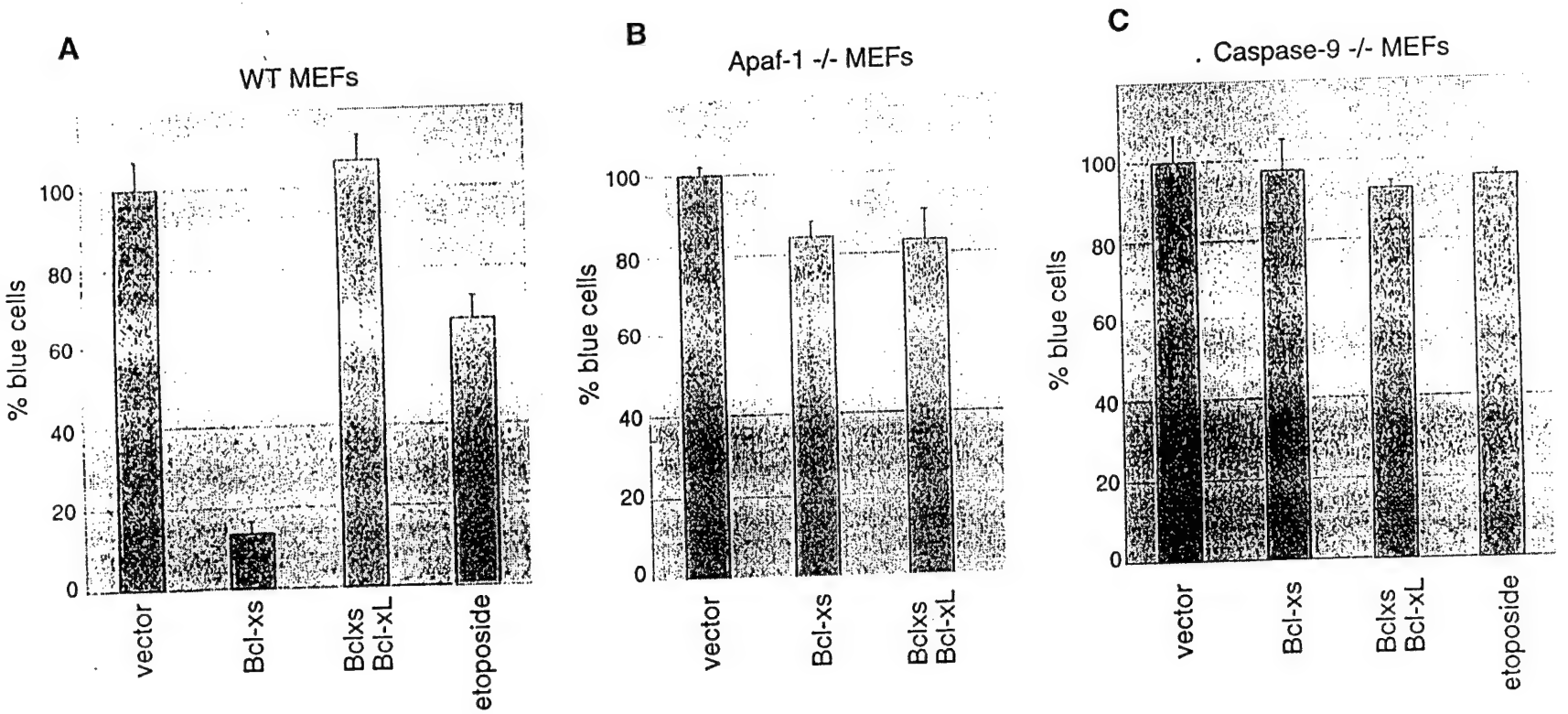

Bcl-xs killing requires both Apaf-1 and Caspase-9

Murine embry fibroblasts from wildtype (A), Apaf-1 knockout (B), and Caspase-9 knockout (C) mice were transiently co-transfected in triplicate with plasmids encoding Bgal and the empty vector, Bcl-xs, or Bcl-xs/Bcl-xL. Some vector/Bgal transfected cells were also treated with etoposide to confirm the phenotype of the knockout fibroblasts. 36 hrs post-transfection, cells were stained with X-gal, and the number of blue cells/well were counted. Data is expressed as % blue cells relative to the vector control (100%), (average +/- SEM).

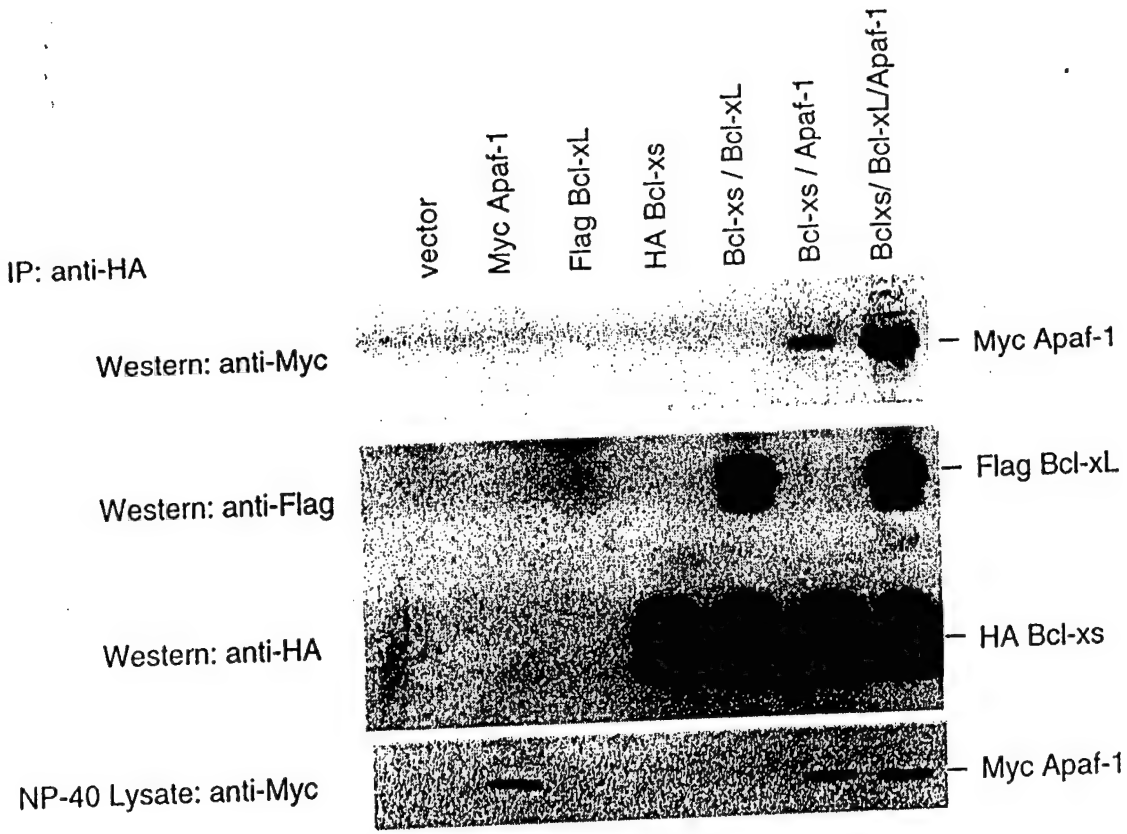

Bcl-Xs/Apaf-1 binding is increased by co-expression with Bcl-xL

Cancer cells were transiently transfected with plasmids expressing HA Bcl-xs, Flag Bcl-xL and Myc Apaf-1. Bcl-xs complexes were immunoprecipitated with anti-HA antibody and immunoblotted with anti-Flag, anti-HA, and anti-Myc. Upper panel shows Apaf-1 co-precipitated with Bcl-xs. Middle pannel shows immunoprecipitated Bcl-xs and bound Bcl-xL. Lower panel shows equal levels of Apaf-1 in the NP-40 lysates used for immunoprecipitations.

Figure 9

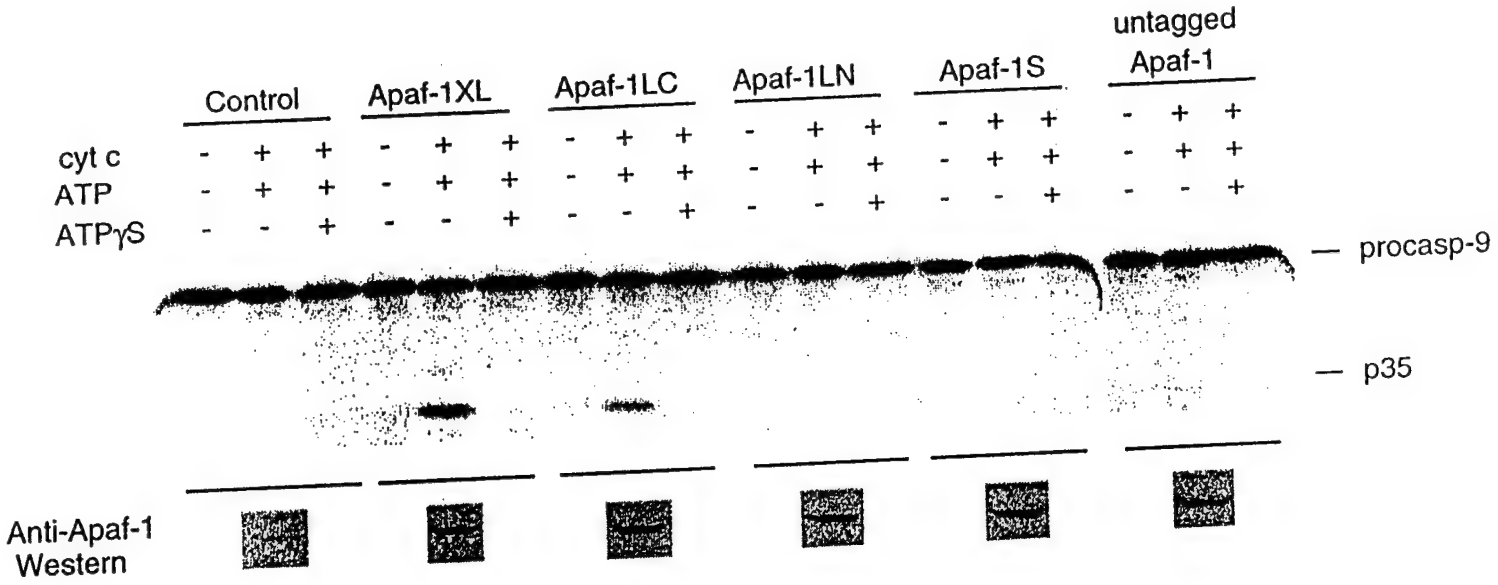
Control
Apaf-1XL
Apaf-1LC
Apaf-1LN
Apaf-1S
untagged Apaf-1
cyt c
ATP
ATPγS
procasp-9
p35
Anti-Apaf-1 Western

Figure 10

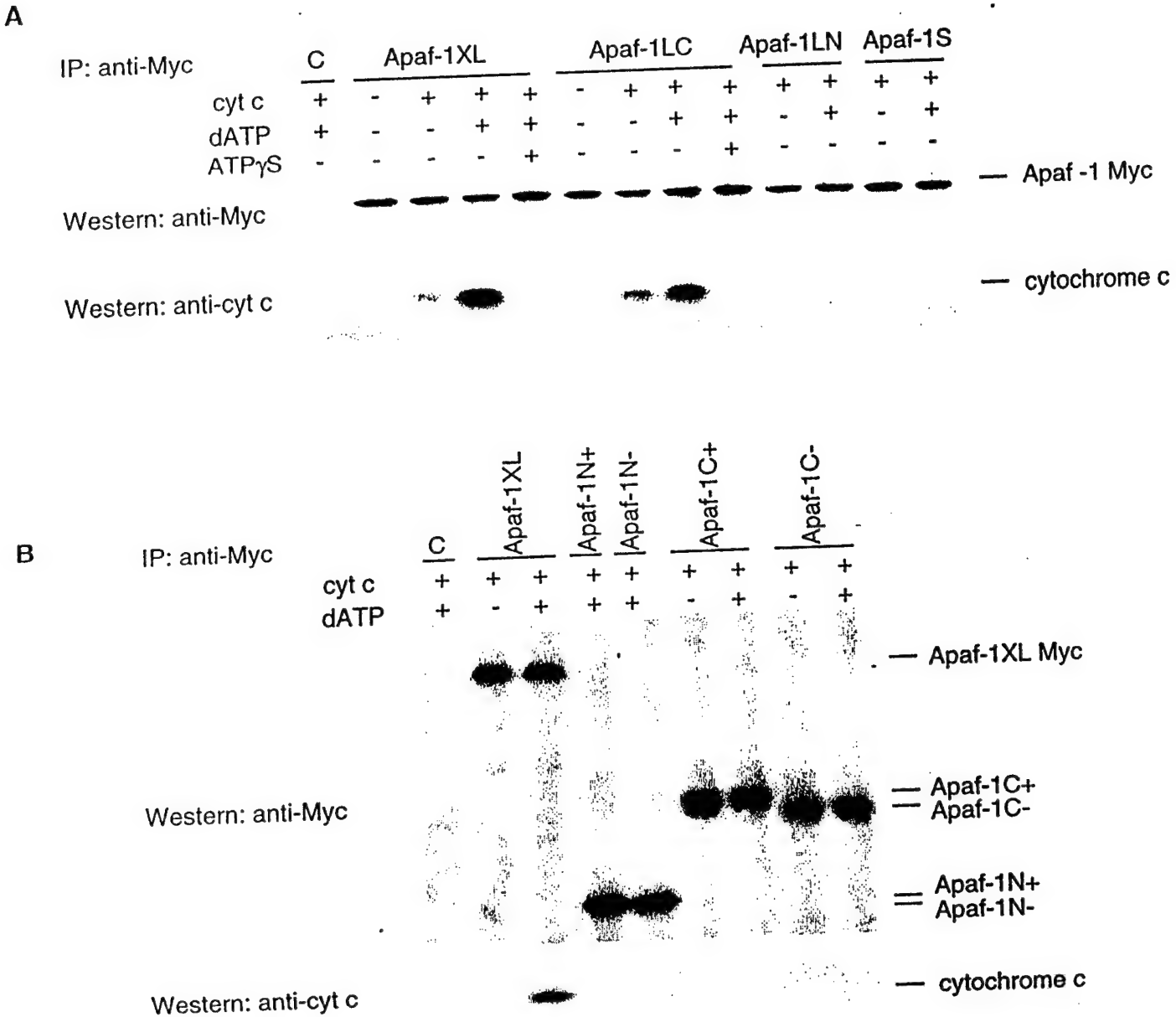
A
IP: anti-Myc
C
Apaf-1XL
Apaf-1LC
Apaf-1LN
Apaf-1S
cyt c
dATP
ATPγS
Apaf -1 Myc
Western: anti-Myc
cytochrome c
Western: anti-cyt c
B
IP: anti-Myc
C
Apaf-1XL
Apaf-1N+
Apaf-1N-
Apaf-1C+
Apaf-1C-
cyt c
dATP
Apaf-1XL Myc
Western: anti-Myc
Apaf-1C+
Apaf-1C-
Apaf-1N+
Apaf-1N-
cytochrome c
Western: anti-cyt c

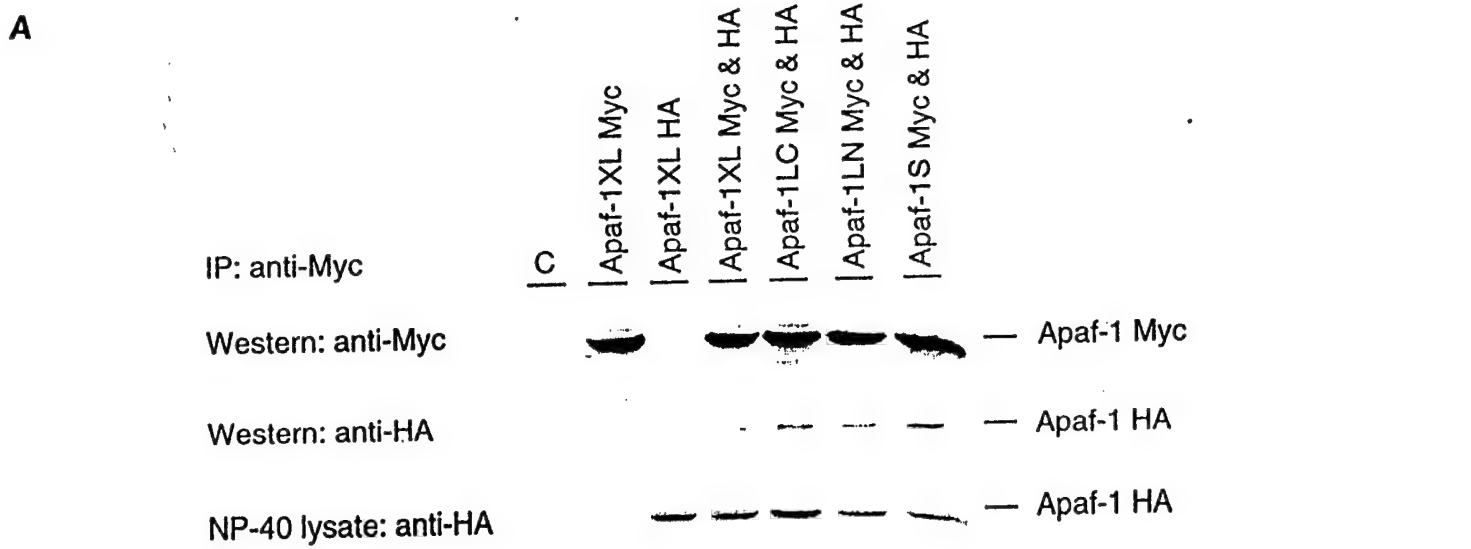
A
C
Apaf-1XL Myc
Apaf-1XL HA
Apaf-1XL Myc & HA
Apaf-1LC Myc & HA
Apaf-1LN Myc & HA
Apaf-1S Myc & HA
IP: anti-Myc
Western: anti-Myc
Apaf-1 Myc
Western: anti-HA
Apaf-1 HA
NP-40 lysate: anti-HA
Apaf-1 HA

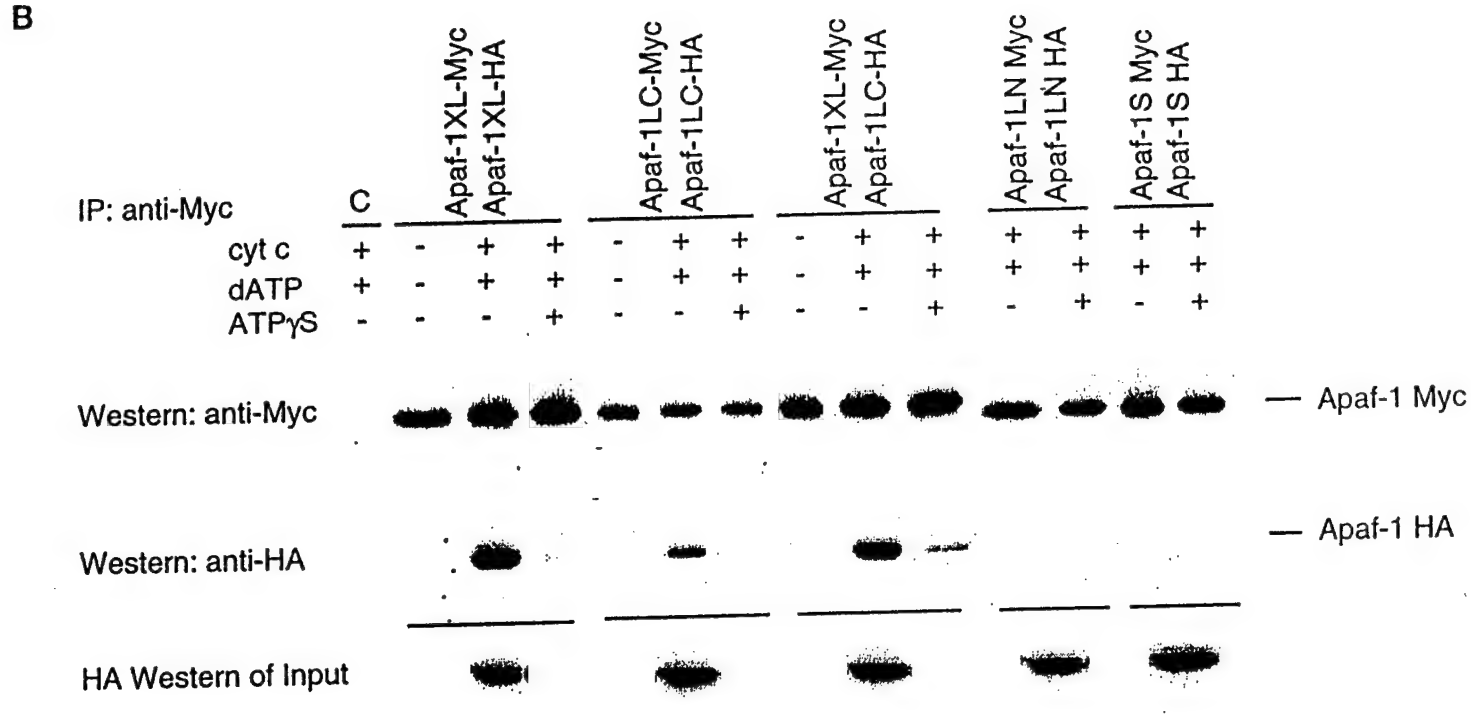
B
IP: anti-Myc
C
Apaf-1XL-Myc
Apaf-1XL-HA
Apaf-1LC-Myc
Apaf-1LC-HA
Apaf-1XL-Myc
Apaf-1LC-HA
Apaf-1LN Myc
Apaf-1LN HA
Apaf-1S Myc
Apaf-1S HA
cyt c
dATP
ATPγS
Western: anti-Myc
Apaf-1 Myc
Western: anti-HA
Apaf-1 HA
HA Western of Input

A

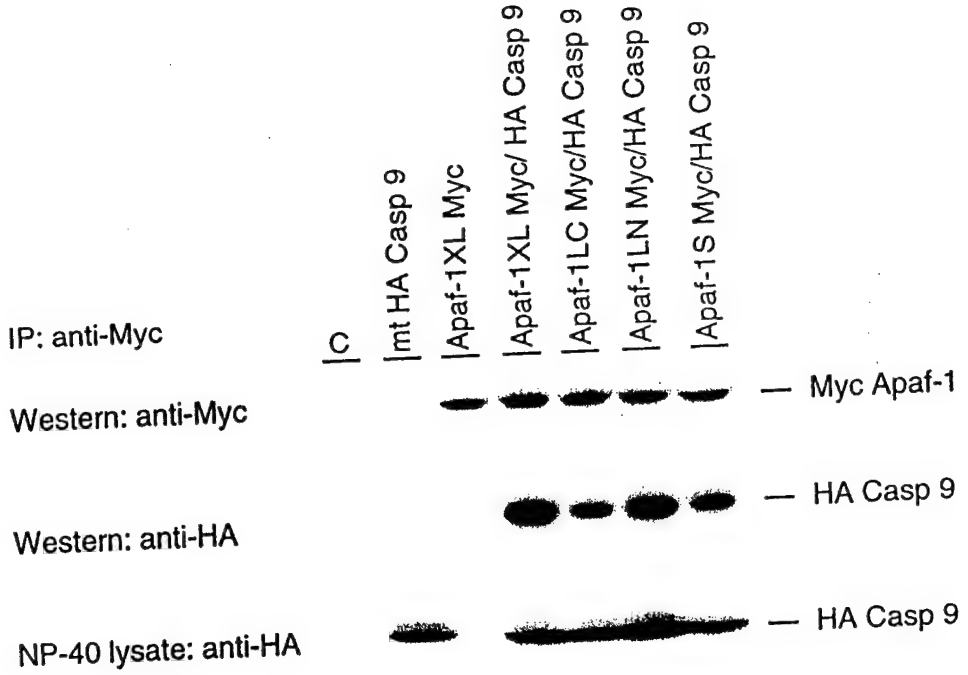
IP: anti-Myc
C
mt HA Casp 9
Apaf-1XL Myc
Apaf-1XL Myc/ HA Casp 9
Apaf-1LC Myc/HA Casp 9
Apaf-1LN Myc/HA Casp 9
Apaf-1S Myc/HA Casp 9
Western: anti-Myc
Myc Apaf-1
Western: anti-HA
HA Casp 9
NP-40 lysate: anti-HA
HA Casp 9

B

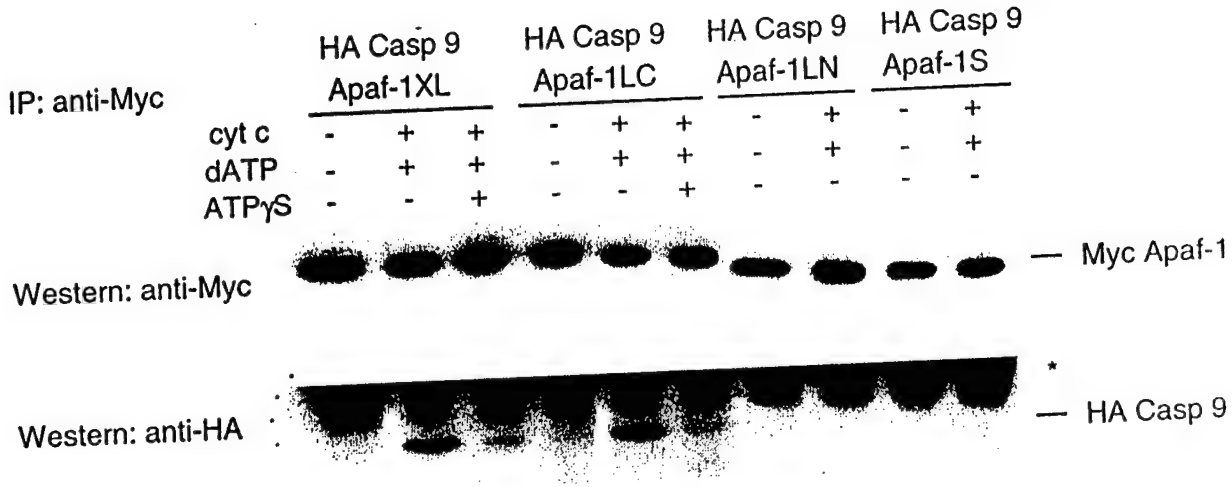
IP: anti-Myc
HA Casp 9 Apaf-1XL
HA Casp 9 Apaf-1LC
HA Casp 9 Apaf-1LN
HA Casp 9 Apaf-1S
cyt c
dATP
ATPγS
Western: anti-Myc
Myc Apaf-1
Western: anti-HA
HA Casp 9

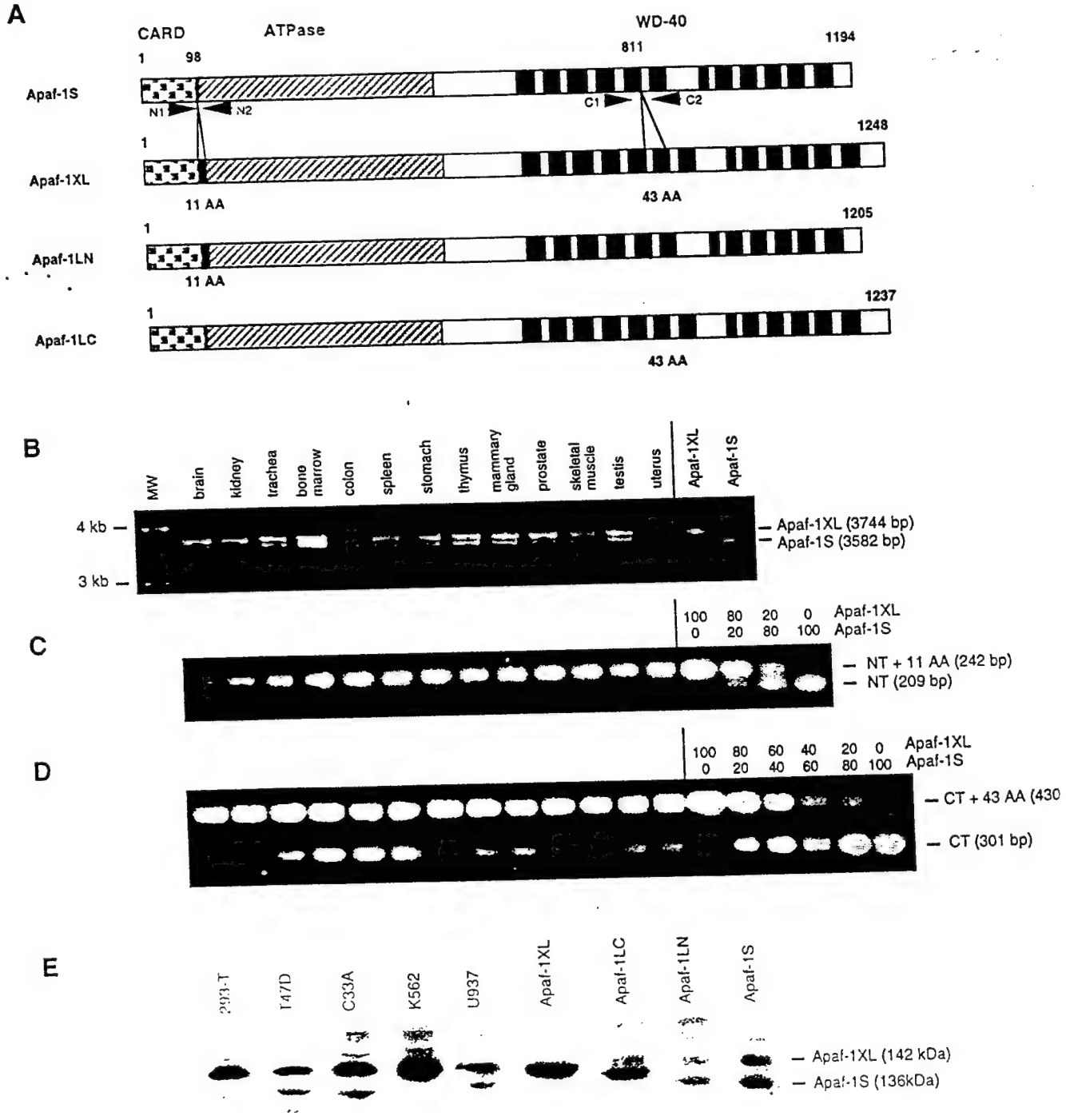
A
CARD
ATPase
WD-40
1
98
811
1194
Apaf-1S
N1
N2
C1
C2
1248
Apaf-1XL
11 AA
43 AA
1205
Apaf-1LN
11 AA
1237
Apaf-1LC
43 AA
B
MW
brain
kidney
trachea
bone marrow
colon
spleen
stomach
thymus
mammary gland
prostate
skeletal muscle
testis
uterus
Apaf-1XL
Apaf-1S
4 kb
3 kb
Apaf-1XL (3744 bp)
Apaf-1S (3582 bp)
C
100 80 20 0 Apaf-1XL
0 20 80 100 Apaf-1S
NT + 11 AA (242 bp)
NT (209 bp)
D
100 80 60 40 20 0 Apaf-1XL
0 20 40 60 80 100 Apaf-1S
CT + 43 AA (430
CT (301 bp)
E
293-T
T47D
C33A
K562
U937
Apaf-1XL
Apaf-1LC
Apaf-1LN
Apaf-1S
Apaf-1XL (142 kDa)
Apaf-1S (136kDa)

Legends for Figures 5-8

Fig. 8. **Expression of Apaf-1 isoforms.** A, schematic representation of Apaf-1 isoforms examined in this study. The caspase recruitment domain (CARD)[1], ATPase domain, and WDRs are shown, as are the presence or absence of the 11 amino acid N-terminal insert following the CARD and the 43 amino acid C-terminal insert between the fifth and sixth WDRs. N1/N2 and C1/C2 represent the primers used to amplify the regions flanking the N-terminal and C-terminal inserts, respectively. The deletion mutant Apaf-1S (1-559) has been termed "N-", while the deletion mutant Apaf-1XL (1-570) has been termed "N+". "C-" refers to the deletion mutant Apaf-1S (468-1194), while "C+" refers to the deletion mutant Apaf-1XL (479-1248). B, RT-PCR analysis of the expression of full length Apaf-1 forms in human tissue RNAs. Primers used were identical to those used to amplify full length Apaf-1 cDNAs (see Experimental Procedures). The last two lanes are positive control reactions using either 10 pg of gel purified Apaf-1XL or Apaf-1S inserts as templates. C, RT-PCR analysis of the same human tissue RNAs as above, using primers N1 and N2. The last four lanes are positive control reactions in which the templates were 10 pg of Apf-1 XL and Apaf-1S, mixed at the indicated ratios. D, RT-PCR analysis of the human tissue RNAs using primers C1 and C2. The last six lanes are positive controls, with Apaf-XL and Apaf-1S mixed at the indicated ratios. E, Anti-Apaf-1 immunoblot analysis of 200 μg of cell lysate from various tumor cell lines. The last four lanes are positive control lysates from 293T cells transiently transfected with the indicated Apaf-1 plasmid. In addition to the transfected Apaf-1 isoforms, an endogenous Apaf-1 protein is observed in 293T cells.

Fig. 9. **Cytochrome c-dependent *in vitro* activation of procaspase-9 requires the additional WD-40 repeat.** Ten μg cytosolic extracts of 293T cells transiently transfected with either the vector control or the indicated Myc-tagged or untagged Apaf-1 isoforms were incubated with *in vitro* translated [^{35}S] methionine-labeled procaspase-9, with or without 1 mM dATP, 8 μg/ml cytochrome c, or 5 mM ATP-γ-S at 30 °C for 30 min. Anti-Apaf-1 (X. Wang) immunoblot analysis of the cytosolic extracts used to measure *in vitro* procaspase-9 activation, is shown in the lower panel. Endogenous Apaf-1 protein, although present, is not detected in this exposure.

Fig. 10. **The additional WD-40 repeat of Apaf-1 is necessary but not sufficient for the binding of cytochrome c.** Cytosolic extracts from 293T cells transiently transfected with either vector control or the indicated Myc-tagged Apaf-1 plasmids were incubated with or without 8 μg/ml cytochrome c, 1 mM dATP and 5 mM ATP-γ-S in the presence of monoclonal anti-Myc antibody and protein A/G-agarose beads. After incubation for 2 h at 4°C, immunoprecipitation was performed as described in Experimental Procedures. Cytochrome c associated with Apaf-1 proteins was detected by immunoblotting. A, Immunoprecipitated full length Myc-tagged Apaf-1 proteins are shown in the upper panel. Cytochrome c bound to Apaf-1 proteins is shown in the lower panel. B, Immunoprecipitated Myc-Apaf-1XL and Myc-tagged Apaf-1 deletion mutants are shown in the upper panel. Bound cytochrome c is shown in the lower panel.

Fig. 11. **Cytochrome c/dATP-dependent Apaf-1 Self-association requires the additional WD-40 repeat.** A, In NP-40 extracts, all Apaf-1 isoforms can self-associate. NP-40 extracts of 293T cells transiently transfected with the indicated Myc- or HA-tagged Apaf-1

plasmids were immunoprecipitated with rabbit anti-Myc antibody and immune complexes were immunoblotted with either mouse anti-Myc or mouse anti-HA. Immunoprecipitated Myc-Apaf-1 proteins are shown in the upper panel, and self-associated HA-Apaf-1 proteins are shown in the middle panel. The lower panel depicts an anti-HA immunoblot of the NP-40 extracts to confirm equivalent expression of the HA-Apaf-1 isoforms used. B, In cytosolic extracts, cytochrome c/dATP-dependent Apaf-1 Self-association requires the additional WD-40 repeat. 293T cells were transiently transfected with the indicated Myc- or HA-tagged Apaf-1 plasmid. Cytosolic extracts of the indicated plasmids were combined with or without 8 μg/ml cytochrome c, 1 mM dATP and 5 mM ATP-γ-S, in the presence of polyclonal anti-Myc antibody and protein A/G-agarose beads. Immunoprecipitation and anti- Myc or -HA immunoblotting was performed as described above. Immunoprecipitated Myc-Apaf-1 isoforms are shown in the upper panel, and associated HA-Apaf-1 isoforms are shown in the middle panel. The lower panel depicts an anti-HA immunoblot of the cytosolic extracts to confirm equivalent expression of the HA-Apaf-1 isoforms used.

Fig. 12. **Cytochrome c-dependent binding of Apaf-1 to procaspase-9 requires the extra WD-40 repeat.** A, In NP-40 extracts, all Apaf-1 isoforms can bind to procaspase-9. NP-40 extracts of 293T cells transiently co-transfected with the indicated Myc- Apaf-1 plasmids and HA-mt procaspase-9(C287S) were immunoprecipitated with rabbit anti-Myc antibody and immune complexes were immunoblotted with either mouse anti-Myc or mouse anti-HA. Immunoprecipitated Myc Apaf-1 isoforms are shown in the upper panel, and associated HA-mt procaspase-9 is shown in the middle panel. The lower panel depicts an anti-HA immunoblot of the NP-40 extracts to confirm similar expression of HA-mt procaspase-9 in each extract. B, In cytosolic extracts, cytochrome c/dATP-dependent binding of Apaf-1 to procaspase-9 requires the additional WDR. 293T cells were transiently transfected with the indicated Myc-Apaf-1 plasmid or HA-mt procaspase-9. Cytosolic extracts of the indicated plasmids were combined with or without 8 μg/ml cytochrome c, 1 mM dATP and 5 mM ATP-γ-S, in the presence of polyclonal anti-Myc antibody and protein A/G-agarose beads. Immunoprecipitation and anti- Myc or -HA immunoblotting was performed as described above. Immunoprecipitated Myc-Apaf-1 isoforms are shown in the upper panel and associated HA-mt procaspase-9 is shown in the bottom panel. The asterisk denotes non-specific IgG heavy chain bands.

The EMBO Journal Vol.16 No.7 pp.1686–1694, 1997

harakiri, a novel regulator of cell death, encodes a protein that activates apoptosis and interacts selectively with survival-promoting proteins Bcl-2 and Bcl-X_L

Naohiro Inohara, Liyun Ding, Shu Chen and Gabriel Núñez[1]

Department of Pathology and Comprehensive Cancer Center, The University of Michigan Medical School, Ann Arbor, MI 48109, USA

[1]Corresponding author

Programmed cell death is essential in organ development and tissue homeostasis and its deregulation is associated with the development of several diseases in mice and humans. The precise mechanisms that control cell death have not been elucidated fully, but it is well established that this form of cellular demise is regulated by a genetic program which is activated in the dying cell. Here we report the identification, cloning and characterization of *harakiri*, a novel gene that regulates apoptosis. The product of *harakiri*, Hrk, physically interacts with the death-repressor proteins Bcl-2 and Bcl-X_L, but not with death-promoting homologs, Bax or Bak. Hrk lacks conserved BH1 and BH2 regions and significant homology to Bcl-2 family members or any other protein, except for a stretch of eight amino acids that exhibits high homology with BH3 regions. Expression of Hrk induces cell death which is inhibited by Bcl-2 and Bcl-X_L. Deletion of 16 amino acids including the conserved BH3 region abolished the ability of Hrk to interact with Bcl-2 and Bcl-X_L in mammalian cells. Moreover, the killing activity of this mutant form of Hrk (Hrk ΔBH3) was eliminated or dramatically reduced, suggesting that Hrk activates cell death at least in part by interacting with and inhibiting the protection afforded by Bcl-2 and Bcl-X_L. Because Hrk lacks conserved BH1 and BH2 domains that define Bcl-2 family members, we propose that Hrk and Bik/Nbk, another BH3-containing protein that activates apoptosis, represent a novel class of proteins that regulate apoptosis by interacting selectively with survival-promoting Bcl-2 and Bcl-X_L.

Keywords: apoptosis/Bcl-2 family/Hrk/programmed cell death

Introduction

Apoptosis, a morphologically distinguished form of programmed cell death, is critical not only during development and tissue homeostasis but also in the pathogenesis of a variety of diseases including cancer, autoimmune disease, viral infection and neurodegenerative disorders (Thompson, 1995). The precise mechanisms that regulate apoptosis have not been elucidated; however, it appears that this form of cell death is controlled by a genetic program which is activated in the dying cell (Thompson, 1995; White, 1996). Several regulatory components of the apoptotic pathway have been identified in various living organisms including man (Thompson, 1995; White, 1996). *bcl-2*, the first member of an evolutionarily conserved family of apoptosis regulatory genes, was isolated initially from the t(14;18) chromosomal translocation found in human B-cell follicular lymphomas and subsequently was shown to repress cell death triggered by a diverse array of stimuli (Vaux *et al.*, 1988; Núñez *et al.*, 1990; Strasser *et al.*, 1991). Several members of the family including Bcl-2, Bcl-X_L, Mcl-1, A1, Bcl-w and Ced-9 share conserved regions termed Bcl-2 homology domain 1, 2, 3 and 4 (BH1, BH2, BH3 and BH4) and function by repressing apoptosis (for review, see White, 1996). In contrast, other members of the family, such as Bax and Bak, share BH1, BH2 and BH3 domains and regulate apoptosis by promoting cell death at least in part through physical interactions with death-repressing Bcl-2 family members (Oltvai and Korsmeyer, 1994; Sato *et al.*, 1994).

Two members of the family, Bcl-2 and Bcl-X_L, are expressed in many embryonic and adult tissues, and their importance has been revealed by analysis of mutant mice deficient in Bcl-2 or Bcl-X_L. Null mutations of *bcl-x* are embryonic lethal with the occurrence of profound cell death, whereas mice deficient in *bcl-2* die early after birth (Veis *et al.*, 1993; Motoyama *et al.*, 1995). However, the biochemical process by which Bcl-2 and Bcl-X_L repress cell death and the mechanisms that regulate their functions are poorly understood. The susceptibility of a cell to apoptotic signals appears to be regulated in part by the relative levels and competing dimerizations of different Bcl-2 family members (Oltvai and Korsmeyer, 1994). In addition to Bcl-2 family members, Bcl-2 is known to interact with several cellular proteins that include R-Ras, Nip proteins and BAG-1 which appear to be part of signal transduction pathways (Boyd *et al.*, 1994; Fernandez-Sarabia and Bischoff, 1994; Takayama *et al.*, 1995; Wang *et al.*, 1996). However, the biochemical significance of these Bcl-2 interactions is unclear and poorly understood.

Here we report the identification, cloning and characterization of *harakiri*, a novel apoptosis regulatory gene. The product of *harakiri*, Hrk, physically interacts with the death-repressor proteins Bcl-2 and Bcl-X_L, but not with death-promoting Bax or Bak. Hrk lacks conserved BH1 and BH2 regions and significant homology to Bcl-2 family members or any other protein, except for a stretch of eight amino acids that exhibits high homology with BH3 regions. Hrk structurally resembles Bik/Nbk, another BH3-containing protein which was identified recently as an interacting partner of the adenovirus E1B 19K protein and Bcl-2 (Boyd *et al.*, 1995; Han *et al.*, 1996b). Beyond the conserved BH3 region, however, Bik/Nbk and Hrk do not share any significant amino acid homology. Expression of Hrk induced cell death which was repressed by Bcl-2 and

Bcl-X_L. Deletion of the conserved BH3 region in Hrk abolished its ability to interact with Bcl-2 and Bcl-X_L, and dramatically diminished its killing activity when compared with wild-type Hrk. Because Hrk lacks conserved BH1 and BH2 domains that define Bcl-2 family members, we propose that Bik/Nbk and Hrk represent a novel class of proteins that regulate apoptosis at least in part by interacting selectively with survival-promoting Bcl-2 and Bcl-X_L.

Results

Two-hybrid screening for proteins that bind to Bcl-2 reveals a novel protein that interacts with anti-apoptosis proteins Bcl-2 and Bcl-X_L but not with death-promoting proteins Bax and Bak

To search for Bcl-2-interacting proteins, we screened a HeLa cDNA library using GAL4–Bcl-2 as a 'bait' in the yeast two-hybrid assay. In a screen of 3×10^6 library clones, 30 positive clones were identified that interacted with the GAL4–Bcl-2 bait. Plasmids recovered from the original yeast strain were used in a co-transformation assay with the original GAL4–Bcl-2 bait or control heterologous baits to discard false-positive clones. Twenty one cDNAs (designated BP1–21) were found to contain inserts of different sizes (from 1.3 to 0.7 kb) that interacted with the GAL4–Bcl-2 bait but not with control baits. These cDNA clones were characterized by restriction enzyme mapping and nucleotide sequence analysis. As expected, multiple clones encoded proteins which are known to associate with Bcl-2 in mammalian cells. Seven cDNAs encoded Bad, three encoded Bax and two encoded Bik/Nbk (Oltvai *et al.*, 1993; Boyd *et al.*, 1995; Yang *et al.*, 1995; Han *et al.*, 1996b). Four cDNAs encoded a Ras-related protein (Yamagata *et al.*, 1994). The two-hybrid screen also yielded five cDNA clones with novel nucleotide sequences. Restriction enzyme and sequence analysis revealed that four of the novel positive clones contained identical inserts of 712 bp fused to the GAL4 DNA-binding domain. One of these four cDNA clones was characterized further. We have named this novel gene '*harakiri*' and the product that it encodes Hrk, after the Japanese suicide ritual (see below).

To characterize the specificity of the Hrk interactions further, we determined the ability of Hrk to interact with Bax, Bak and Bcl-X_S, three Bcl-2-related proteins that promote cell death. In the yeast two-hybrid system, Hrk interacted with Bcl-2 and Bcl-X_L but not with Bax, Bak or Bcl-X_S (Figure 1). These results indicate that Hrk selectively interacts with Bcl-2 family members such as Bcl-2 and Bcl-X_L which are functionally related in that they are capable of inhibiting apoptosis. Importantly, Hrk failed to associate with Bcl-X_S, an alternative form of Bcl-X, that lacks an internal region of 62 amino acids that is required for Bcl-X_L protective function (Boise *et al.*, 1993).

Hrk interacts with Bcl-2 and Bcl-X_L in mammalian cells

To confirm that Hrk associates with Bcl-2 and Bcl-X_L in mammalian cells, a 293T human kidney cell line was transiently co-transfected with expression plasmids producing a Flag-tagged Hrk protein and Bcl-2, Bcl-X_L or control plasmid. In these initial experiments, the entire *harakiri* sequence that was fused to the GAL4 DNA-binding domain was cloned into expression plasmids to produce Flag-Hrk. Immunoprecipitates were prepared using hamster anti-Bcl-2 monoclonal antibody and subjected to SDS–PAGE and immunoblotting using anti-Flag or Bcl-2 antibody. Immunoblotting with anti-Bcl-2 antibody revealed that Flag-Hrk was co-immunoprecipitated with Bcl-2 (Figure 2A). Control immunoblotting with anti-Bcl-2 antibody confirmed that Bcl-2 was immunoprecipitated in lysates of cells transfected with the *bcl-2* plasmid (Figure 2A). The Hrk–Bcl-2 interaction was specific in that it required co-expression of both Bcl-2 and Flag-Hrk, and was not detected when the lysate was immunoprecipitated with control antibody (Figure 2A). To verify the interaction, we performed reciprocal experiments using anti-Flag antibody to immunoprecipitate Flag-Hrk, followed by Western blot with anti-Bcl-2 antibody. In agreement with the reverse experiment, Bcl-2 co-immunoprecipitated specifically with Flag-Hrk (Figure 2B).

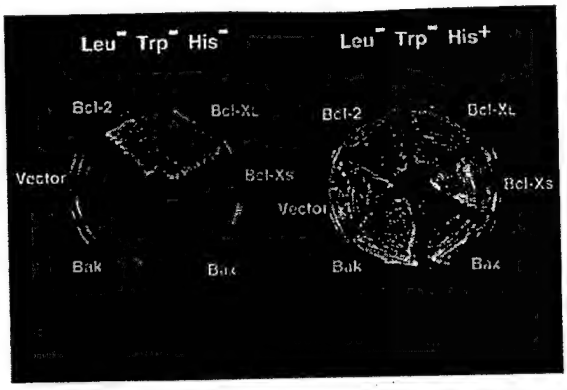

Fig. 1. Specificity of the interaction between Hrk and Bcl-2 family members in yeast. A plasmid expressing Hrk fused to the GAL4 DNA-binding domain was co-transfected with plasmids expressing Bcl-2 family members fused to the GAL4 transcriptional activation domain (AD). Growth of yeast in the absence of leucine, tryptophan and histidine is indicative of protein–protein interaction. Growth in the absence of leucine and tryptophan is shown as a control.

To determine if Hrk associates with Bcl-X_L in mammalian cells, we performed immunoprecipitation experiments similar to those performed to assess the Hrk–Bcl-2 interaction. After transfection of 293T cells with expression plasmids producing a Flag-tagged Hrk protein and Bcl-X_L or control plasmid, immunoprecipitates were prepared using anti-Bcl-X antibody and subjected to SDS–PAGE immunoblotting using anti-Flag antibody. Importantly, Flag-Hrk was co-immunoprecipitated specifically with Bcl-X_L (Figure 2C). To confirm the interaction, we performed reciprocal experiments using anti-Flag antibody to immunoprecipitate Flag-Hrk, followed by Western blot with anti-Bcl-X antibody. In agreement with the reverse experiment, Bcl-X_L co-immunoprecipitated specifically with Flag-Hrk (Figure 2D). We also tested if Hrk interacts with Bax in 293T cells and found that Flag-Hrk failed to co-immunoprecipitate with Bax, confirming our results in the yeast assay (data not shown).

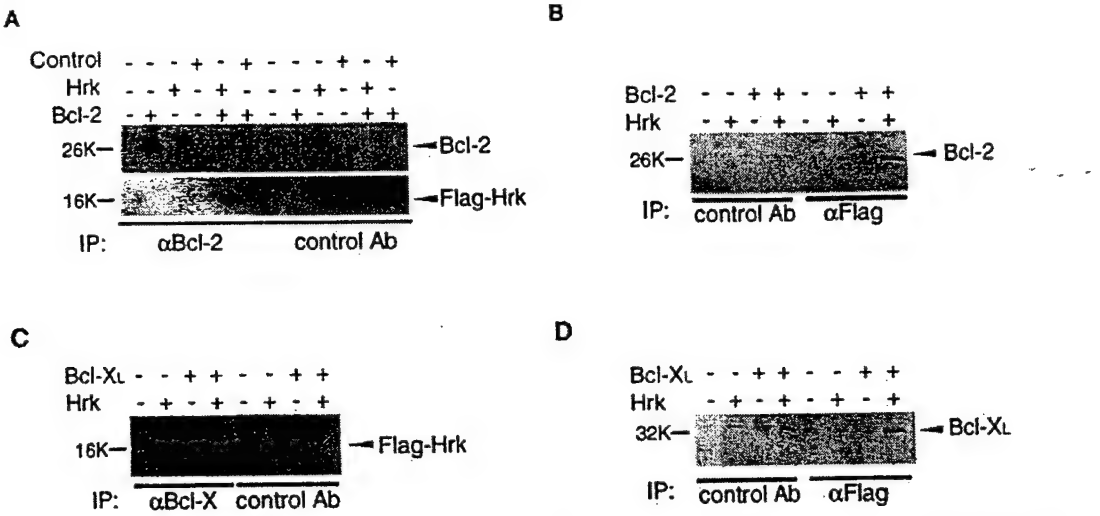

Fig. 2. Hrk interacts with Bcl-2 and Bcl-X_L in mammalian cells. 293T cells (5×10^6 per 100 mm plate) were transiently transfected with 10 μg of the indicated plasmids, pSFFV-Flag-tagged BP25 (control), pSFFV-Flag-Hrk16K (Hrk), pSFFV-hBcl-2 (Bcl-2), pSFFV-HA-hBcl-X_L (Bcl-X_L) or pSFFV-HA-mBax (Bax). In the case of transfection with a single plasmid, cells were co-transfected with 10 μg of empty pSFFV-neo vector and the total amount of plasmid DNA was always 20 μg. **(A)** Lysates were immunoprecipitated with anti-Bcl-2 or control antibody. Immunoprecipitates were immunoblotted with anti-Bcl-2 or anti-Flag antibody. **(B)** Anti-Flag or control antibody immunoprecipitates were immunoblotted with anti-Bcl-2 antibody. **(C)** Anti-Bcl-X or control antibody immunoprecipitates were immunoblotted with anti-Flag antibody. **(D)** Anti-Flag or control antibody immunoprecipitates were immunoblotted with anti-Bcl-X antibody. Notice that pSFFV-Flag-Hrk16K produces 16 kDa protein. as the entire *harakiri* cDNA including its 5′ untranslated region was fused in-frame with the Flag sequence and the amino-terminus of Hrk.

harakiri encodes a novel protein with a conserved BH3 region but lacking BH1 or BH2 domains

To confirm the sequence obtained by the two-hybrid assay, a 9-week embryo human cDNA library was screened by hybridization with a labeled *harakiri* probe. Forty positive cDNA clones were identified and characterized by restriction mapping, PCR analysis and sequencing. Analysis of the longest cDNAs revealed inserts of 716 bp essentially identical in sequence to that observed previously fused to the GAL4 DNA-binding domain. A single nucleotide difference C→T at position 334 of the *harakiri* cDNA was noted between the coding sequences obtained from the HeLa and embryo cDNA libraries (Figure 3A). This nucleotide difference did not change the amino acid sequence of Hrk, reflecting perhaps a gene polymorphism. Northern blot analysis of mouse and human tissues using a labeled *harakiri* probe identified a major mRNA species of ~0.7 kb in certain tissues (see below). Taken together, these results suggest that the isolated cDNA clones are full-length. The cDNAs encode an open reading frame of 91 amino acids (Figure 3A). In the 3′ untranslated region, an ATTTA sequence motif for RNA destabilization (Shaw and Kamen, 1986) and a poly(A) tail were identified. Initial DNA searches using the NCBI BLAST program revealed that the nucleotide sequence was novel in that they did not reveal significant homology to any known gene or translated products in the databases. However, close inspection of the Hrk protein revealed a stretch of eight amino acids, Hrk 37–44, with high homology to a BH3 motif. This conserved region is shared by Bcl-2 family members (Chittenden *et al.*, 1995b; Zha *et al.*, 1996). The BH3 region of Hrk was contained within a predicted α-helix which has been described recently in the crystal structure of Bcl-X_L (Muchmore *et al.*, 1996), and predicted to be present in other Bcl-2 family members (Figure 3C). A region of 28 hydrophobic residues that may serve as a membrane-spanning domain was identified at the COOH-terminus of the Hrk coding region (Figure 3A).

harakiri displays a highly restricted expression in human tissues

To characterize *harakiri* further, its expression pattern was examined by Northern blot analysis using a *harakiri* probe of various RNA samples isolated from human adult tissues. A major 0.7 kb transcript was detected in all lymphoid tissues tested but was expressed predominantly in bone marrow and spleen (Figure 4). Further analysis showed that *harakiri* mRNA was also expressed in pancreas and at very low or undetectable levels in kidney, liver, lung and brain (data not shown).

The Flag-Hrk protein is a non-nuclear intracellular protein

In order to begin to assess the subcellular localization of Hrk, we transiently transfected a Flag-*harakiri* construct into 293 cells and determined the intracellular localization of the Flag-Hrk protein by laser scanning confocal microscopy. Analysis of labeled cells with anti-Flag monoclonal antibody revealed that Flag-Hrk displays a labeling pattern which was granular and extranuclear, consistent with a localization confined to membranes of intracellular organelles (Figure 5A). The labeling pattern of Hrk was similar to that previously reported for Bcl-2 and Bcl-X_L, suggesting that Hrk, Bcl-2 and Bcl-X_L localize to similar intracellular compartments in mammalian cells (Krajewski *et al.*, 1993; González-García *et al.*, 1994). The specificity of the labeling was determined by assessing the staining

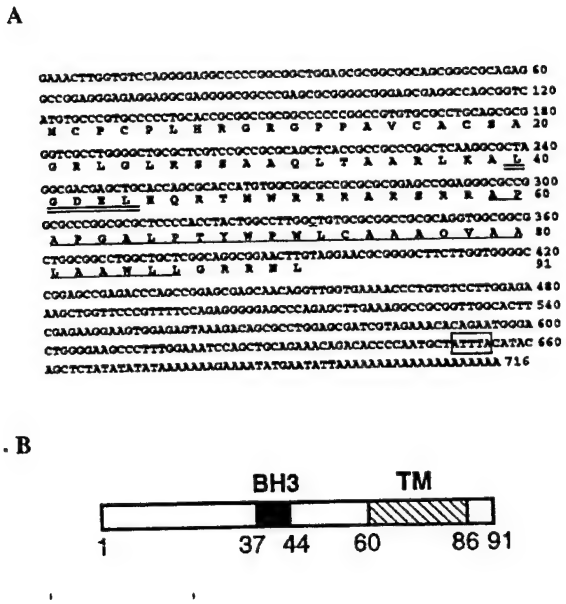

Fig. 3. *harakiri* encodes a novel BH3-containing protein. (A) The nucleotide sequence of human *harakiri* cDNA. The sequence from the longest cDNA clone isolated from a 9-week embryo is shown. The coding region is indicated with its amino acid sequence. A conserved BH3 region and a putative transmembrane domain are indicated by double and single underlining in the amino acid sequence, respectively. An ATTTA sequence motif for RNA destabilization identified in the 3′ untranslated region is boxed. A putative nucleotide polymorphism was observed, C→T at position 334 of the cDNA, and is shown by underlining in the nucleotide sequence. (B) Schematic structure of Hrk. (C) Comparison of the BH3 domains between Hrk and Bcl-2 family members. Identical and conserved hydrophobic residues are indicated by bold letters and stars, respectively. References for hBax, hBcl-2, hBcl-X, Bik/Nbk, Bak and Mcl-1 proteins are given in the Introduction.

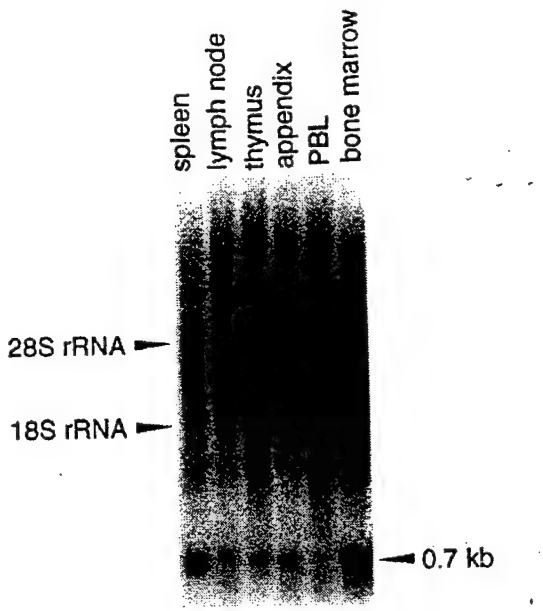

Fig. 4. Expression of *harakiri* mRNA by Northern blot analysis. A filter loaded with 2 μg of poly(A) RNA from various tissues of the immune system was hybridized with the entire *harakiri* cDNA probe labeled with ^{32}P, washed with 0.2× SSC at 65°C for 1 h. The filter was exposed to X-ray film for 12 h. 28S rRNA, 18S rRNA and the major transcript of 0.7 kb are indicated by arrowheads. PBL, peripheral blood leukocytes.

pattern obtained after transfection with a control Flag-tagged GATA-1 expression plasmid. Staining of the GATA-1 protein with anti-Flag antibody revealed a nuclear labeling pattern, as expected for a nuclear transcriptional factor (Figure 5B).

Expression of Hrk induces rapid cell death which is repressed by Bcl-2 and Bcl-X_L

The effect of *harakiri* on cell survival was examined initially in 293T cells using a transient transfection assay. Transfection of a *harakiri* expression plasmid into 293T cells resulted in a dramatic loss of cell viability at 36 h post-transfection (Figure 6B and F). This was specific in that transfection of 293T cells with empty vector, *bcl-2* or *bcl-x_L* expression plasmids did not have any effect on cell survival (Figure 6A, C, E and G). Significantly, co-expression of Bcl-2 or Bcl-X_L inhibited the death-promoting activity of Hrk (Figure 6D and H). To verify these results further, we performed additional experiments in which Hrk plasmids were transfected into 293, HeLa and FL5.12 progenitor B cells. Transient transfection of 293 and HeLa cells with Hrk plasmids induced cell death with kinetics similar to those observed with 293T cells (data not shown). To date, we have been unable to generate any stable FL5.12 cell lines that express transfected Hrk in the absence of exogenous Bcl-2 or Bcl-X_L, suggesting that Hrk expression is also lethal to these cells (data not shown).

Hrk requires a region of 16 amino acids containing BH3 to interact with Bcl-2 and Bcl-X_L

To determine the ability of Hrk to associate with Bcl-2 or Bcl-X_L through BH3, we engineered a mutant form of Hrk lacking BH3. A deletion mutant was designed to eliminate residues 34–49 of Hrk, a predicted α-helix, to minimize secondary effects on folding of the Hrk protein. The deleted residues contained the most conserved amino acids of the BH3 homology region of Hrk (Figures 3C and 7A). Expression plasmids producing wild-type or mutant Flag-tagged Hrk and Bcl-2 or Bcl-X_L were transiently co-transfected into 293T cells. Immunoprecipitates were prepared using anti-Flag to recognize wild-type and mutant Flag-Hrk and subjected to SDS–PAGE and immunoblotting using anti-Bcl-2 and anti-Bcl-X antibodies. Deletion of residues 34–49 (Hrk mutant ΔBH3) completely eliminated the ability of Hrk to interact with

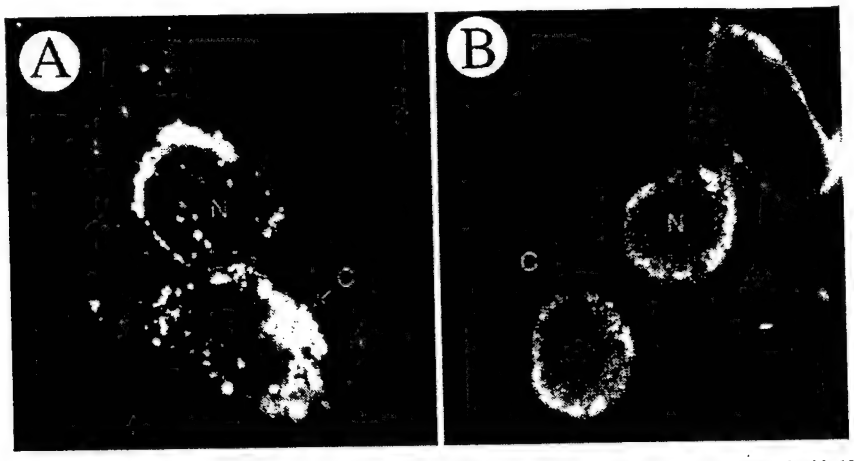

Fig. 5. Flag-Hrk protein is a non-nuclear intracellular protein. 293 cells (5×10^6 cells per 100 mm plate) were transfected with 10 μg of pSFFV-Flag-Hrk16K (**A**) or Flag-GATA-1 (**B**) as a control. Shown are confocal images after labeling with anti-Flag and secondary fluorescein-conjugated antibody. Samples were prepared at 18 h after transfection. Nuclei and cytoplasm are indicated by N and C, respectively. Notice that cells transfected with pSFFV-Flag-Hrk16K round up. Scattered bright particles probably represent cellular fragments from dying neighboring cells.

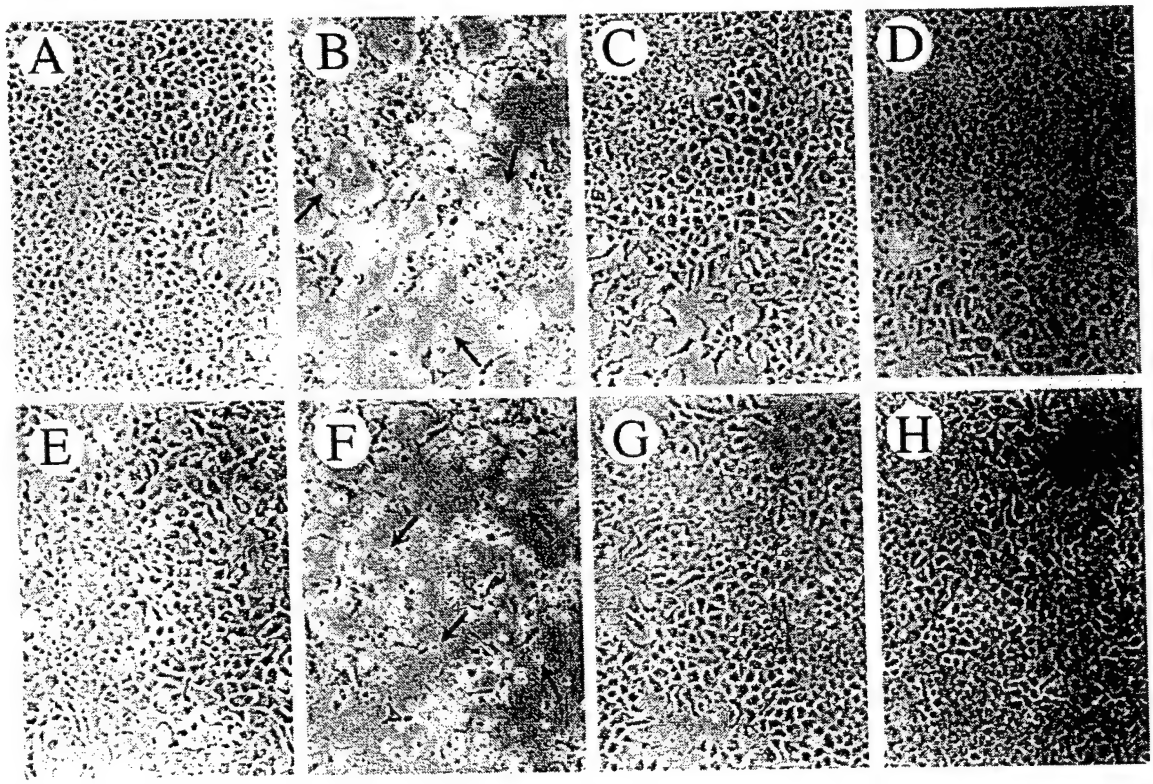

Fig. 6. Expression of Hrk induces cell death which is repressed by Bcl-2 or Bcl- X_L. 293T cells (5×10^6 per 100 mm plate) were co-transfected with 20 μg of pSFFV-neo (**A** and **E**), 10 μg of pSFFV-Flag-Hrk16K plus 10 μg of pSFFV-neo (**B** and **F**), 10 μg of pSFFV-hBcl-2 plus 10 μg of pSFFV-neo (**C**), 10 μg of pSFFV-Flag-Hrk16K plus 10 μg of pSFFV-hBcl-2 (**D**), 10 μg of pSFFV-HA-hBcl-X_L and 10 μg of pSFFV-neo (**G**), 10 μg of pSFFV-Flag-Hrk16K plus 10 μg of pSFFV-HA-hBcl-X_L (**H**) as described in Figure 2. Photographs represent cells at 36 h after transfection. Notice that cultures transfected with Flag-*harakiri* show a paucity of attached live cells and shrunken dead cells (arrows) which are blocked by co-transfection with *bcl-2* or *bcl-*x_L.

Bcl-2 and Bcl-X_L (Figure 7B). To confirm these results, we performed reciprocal experiments using anti-Bcl-2 antibody, followed by Western blot with anti-Flag antibody. In agreement with the reverse experiment, wild-type Hrk but not mutant Hrk co-immunoprecipitated specifically with Bcl-2 (Figure 7C). Analysis of total lysates from the

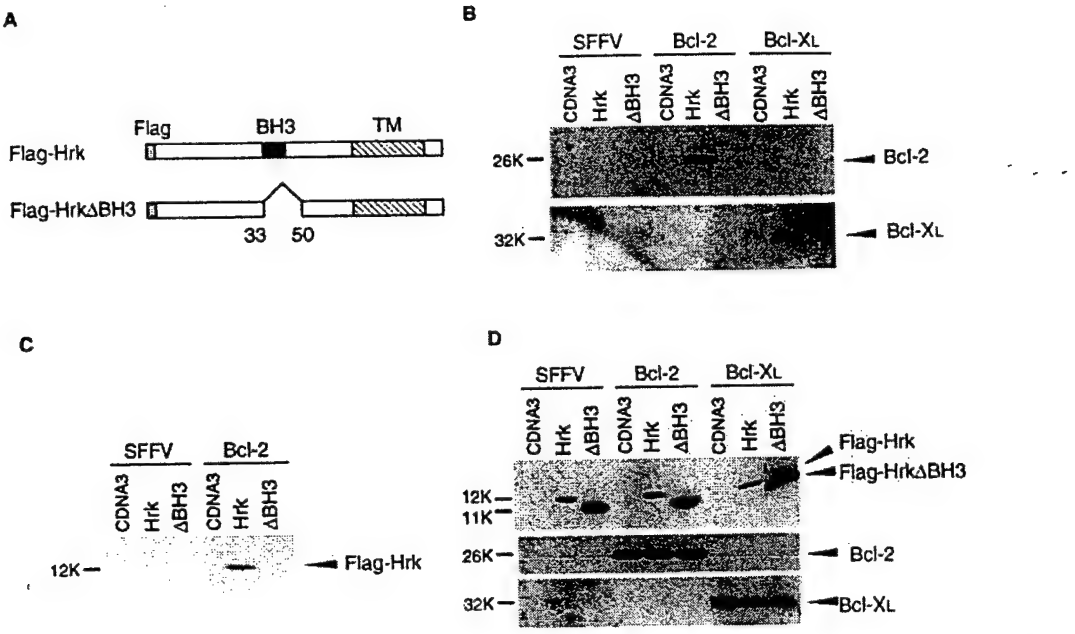

Fig. 7. Hrk requires a region of 16 amino acids containing BH3 to interact with Bcl-2 and Bcl- X_L. (A) Schematic structure of wild-type (Flag-Hrk) and mutant (Flag-Hrk ΔBH3) proteins. (B) 293T cells (5×10^6 per 100 mm plate) were co-transfected with 2 μg of pCDNA3 (CDNA3), pCDNA3-Flag-Hrk (Hrk) or pCDNA3-Flag-Hrk ΔBH3 (Flag-Hrk ΔBH3) and 10 μg of pSFFV-neo (SFFV), pSFFV-hBcl-2 (Bcl-2) or pSFFV-HA-hBcl-X_L (Bcl-X_L) as described in Figure 1. Anti-Flag immunoprecipitates were immunoblotted by anti-Bcl-2 (upper) and anti-Bcl-X antibody (lower). (C) Anti-Bcl-2 immunoprecipitates were immunoblotted with anti-Flag antibody. (D) Twenty μg of total lysate were immunoblotted with anti-Flag, anti-Bcl-2 or anti-Bcl-X antibody.

same cellular extracts by immunoblotting confirmed that 293T cells transfected with the corresponding plasmids expressed Bcl-2, Bcl-X_L, wild-type and mutant Hrk proteins (Figure 7D).

The BH3 domain of Hrk is required for the induction of cell death

To determine if the BH3 domain of Hrk is necessary to induce cell death, we compared the killing activity of wild-type and mutant Hrk proteins by a transient transfection assay in 293T cells. The cells were co-transfected with a reporter plasmid expressing GFP (green fluorescence protein), in combination with either an expression plasmid encoding Hrk proteins or control plasmids. The cell killing activity of wild-type and mutant Hrk was measured by a reduction in the number of cells that express the reporter GFP protein relative to that obtained by transfection with a control expression plasmid. The results of these experiments showed that deletion of residues 34–49 of Hrk (Hrk mutant ΔBH3) dramatically reduced the ability of Hrk to kill 293T cells, when compared with the activity exhibited by wild-type Hrk (Figure 8A). Furthermore, expression of Bcl-2 or Bcl-X_L inhibited the killing activity of wild-type Hrk, confirming the results presented in Figure 6. The loss of viability and the morphology of the cells observed after transfection with Hrk plasmids in Figure 6 suggested that Hrk may induce apoptotic cell death. To determine if the cell death activated by transient Hrk expression was caused by apoptosis, the nuclei of 293T cells were stained with acridine arange and ethidium bromide. Cells transfected with wild-type Hrk but not with mutant Hrk ΔBH3 nor control plasmid displayed nuclear fragmentation, a cytological change associated with apoptosis (Figure 8B).

Discussion

We have identified *harakiri*, a novel regulator of apoptosis that exhibits death-inducing activity in mammalian cells. Hrk interacts with Bcl-2 and Bcl-X_L, two death-repressing Bcl-2 family members that play essential roles in maintaining cell survival in embryonic and adult tissues (Veis *et al.*, 1993; Motoyama *et al.*, 1995). Hrk shares homology with Bcl-2 in the BH3 domain but, unlike most other Bcl-2 family members, it lacks conserved BH1 and BH2 regions. The BH3 region appears to represent a critical domain for interaction with Bcl-2 family members and regulation of apoptosis. For example, BH3 is required for death-promoting Bax and Bak to associate with Bcl-2 and Bcl-X_L (Chittenden *et al.*, 1995a; Han *et al.*, 1996a; Simonian *et al.*, 1996; Zha *et al.*, 1996). Moreover, deletion of BH3 prevented the killing activity of Bak and expression of a 30 amino acid region of Bak containing BH3 linked to a membrane anchor sequence was sufficient for cell killing activity in transient assays (Chittenden *et al.*, 1995b). In our studies, a 16 amino acid region of Hrk encompassing BH3 was required for Hrk to interact with Bcl-2 and Bcl-X_L, and its deletion eliminated or greatly reduced the killing activity of Hrk. In addition, these studies demonstrate that a region of 62 residues containing the BH1 and BH2 regions in Bcl-X_L is essential for its binding to Hrk since Bcl-X_S, an alternative form of

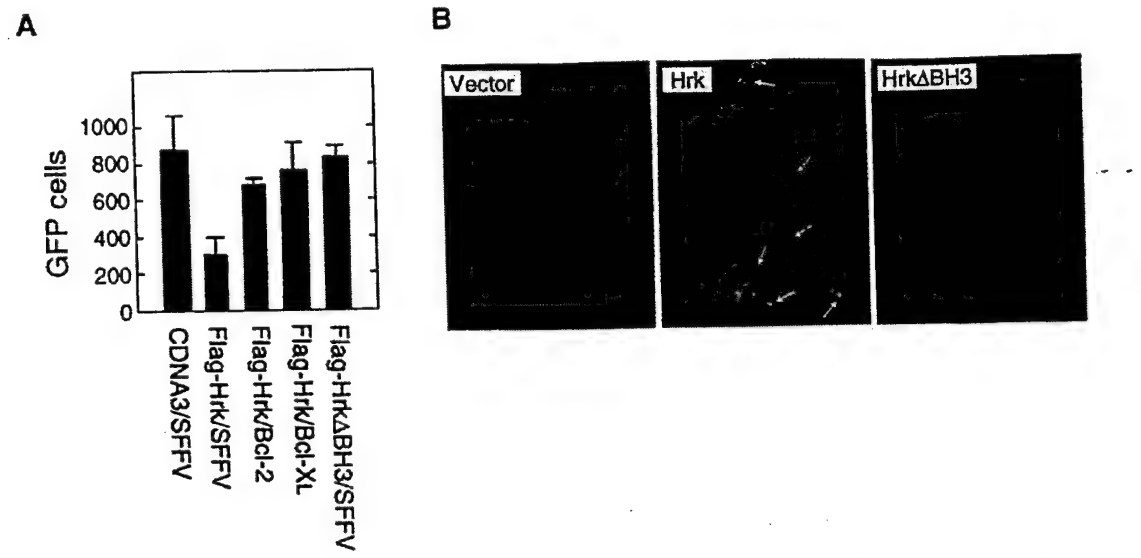

Fig. 8. The BH3 domain of Hrk is required for the induction of cell death. (A) 293T cells (1.7×10^6 per 35 mm plate) were transfected with 0.3 μg of pRK7.GFP and 0.8 μg of pCDNA3 (control), 0.8 μg of pCDNA3-Flag-Hrk (Hrk) or 0.8 μg of pCDNA3-Flag-Hrk ΔBH3 (ΔBH3) in the presence or absence of 6.7 μg of pSFFV-neo, pSFFV-hBcl-2 (Bcl-2) or pSFFV-HA-hBcl-X_L (Bcl-X_L) in triplicate. The number of live cells expressing GFP was determined at 48 h after transfection by analysis of 5×10^3 cells as described in Materials and methods. The results are shown as the mean of triplicate values ± SD. (B) 293T cells transfected with 0.8 μg of pCDNA3 (vector), pCDNA3-Flag-Hrk (Hrk) and pCDNA3-Flag-Hrk ΔBH3 (Hrk ΔBH3) were stained at 18 h after transfection with acridine orange and ethidium bromide to stain nuclei. Notice that nuclei of cells transfected with pCDNA3-Flag-Hrk were condensed and some of them are fragmented (arrows). In the experiment shown, ~20% of the transfected cells exhibited apoptotic changes in the nuclei.

Bcl-X lacking these conserved domains, failed to associate with Hrk.

Susceptibility of a cell to apoptotic signals appears to be regulated in part by the relative levels and competing dimerizations of death-suppressing and death-promoting Bcl-2 family members (Oltvai and Korsmeyer, 1994; Sato *et al.*, 1994). How could Hrk activate cell death? Two non-exclusive models could be proposed to explain the role of Hrk in cell death. Hrk could be an effector molecule with intrinsic death-inducing activity, and death-suppressing Bcl-2 and Bcl-X_L may serve as dominant inhibitors. In support of this model, overexpresssion of Bcl-2 or Bcl-X_L inhibited the killing activity of Hrk. Alternatively, Hrk could promote cell death by inhibiting the protective activity of Bcl-2 and Bcl-X_L and perhaps other functional homologs. Inactivation of Bcl-2 and Bcl-X_L would require the interaction of these survival proteins with Hrk and be mediated by the formation of Bcl-2–Hrk and/or Bcl-X_L–Hrk complexes. The analysis of the Hrk ΔBH3 mutant strongly supports the latter model in that a region of 16 residues containing the BH3 domain required for Hrk to interact with Bcl-2/Bcl-X_L was also necessary for Hrk killing activity. However, these studies cannot rule out that Hrk could also act as a death effector molecule as it is formally possible that the 16 amino acid deletion in Hrk directly or indirectly also affects an intrinsic death-inducing activity. Similarly, deletion mutant analysis of Bak has shown that elimination of BH3 greatly diminished the killing activity of Bak (Chittenden *et al.*, 1995b). Thus definitive evidence for the second model will require additional mutational studies and analysis of cells deficient in Hrk.

Oncogenic signals such as deregulated c-Myc or adenovirus E1A can promote or induce apoptosis in cell lines (Askew *et al.*, 1991; White *et al.*, 1991; Evan *et al.*, 1992). Thus, it is conceivable that in tumor cells, apoptotic signals are constitutively expressed, although repressed by Bcl-2 and/or Bcl-X_L. Consistent with this is the observation that expression of Bcl-X_S, a functional inhibitor of Bcl-2 and Bcl-X_L (Boise *et al.*, 1993), activates apoptosis in a wide variety of cancer cells (Clarke *et al.*, 1995). Thus, physical inactivation of Bcl-2 and Bcl-X_L by Hrk could similarly unleash endogenous death signals leading to execution of the apoptotic program. This hypothesis is consistent with recent observations in mutant mice lacking Bcl-2 and Bcl-X (Veis *et al.*, 1993; Motoyama *et al.*, 1995). Mice deficient in Bcl-X developed massive apoptosis of neural and hematopoietic tissues and died at E12–13 of embryonic development (Motoyama *et al.*, 1995), whereas newly born Bcl-2-deficient mice exhibited fulminant apoptosis of lymphoid tissues (Veis *et al.*, 1993). Thus, in addition to cancer cells, expression of Bcl-X or Bcl-2 appears necessary to counter death signals that arise during normal development. The precise mechanism of death triggered by Hrk needs to be determined, but we hypothesize that it involves the activation of interleukin 1-β converting enzyme-like proteases, a step which appears to be downstream of Bcl-2 and Bcl-X_L in the death pathway (Chinnaiyan *et al.*, 1996).

harakiri is the second member of a class of cell death regulatory genes that also include *bik/nbk*. Unlike 'classical' *bcl-2* family members, the proteins that they encode lack conserved BH1, BH2 or BH4 regions but share the BH3 domain. Our studies indicate that the BH3

domain of Hrk is critical for its interaction with Bcl-2 and Bcl-X_L. Although Hrk and Bik/Nbk share both a BH3 domain and a hydrophobic region at the COOH-terminus predicted to mediate attachment to intracellular membranes, these proteins are distinct and do not share additional amino acid homology. Thus, it is possible that there are subtle differences in the function of Hrk and Bik/Nbk. In this respect, it has been shown that Bcl-X_S interacts with Bik/Nbk (Boyd *et al.*, 1995), but our analysis revealed that Bcl-X_S fails to associate with Hrk. In addition, Hrk and Bik/Nbk differ in their pattern of expression in tissues (Boyd *et al.*, 1995), which suggests that they play distinct roles in the regulation of apoptosis *in vivo*. Future studies need to address a role for *harakiri* in the regulation of physiological cell death during tissue development and homeostasis.

Materials and methods

Screening for Bcl-2-interacting proteins by the yeast two-hybrid system

A HeLa cDNA library fused to the GAL4 activation domain of the pGAD-GH vector (Hannon *et al.*, 1993) was screened for proteins that interact with human Bcl-2, using the HF7c yeast reporter strain (Feilotter *et al.*, 1994). Briefly, the pGAD library plasmid was transformed into HF7c yeast cells harboring the pGBT-9-bcl-2 bait plasmid by standard transfection procedures. Transformed HF7 cells were plated on medium lacking tryptophan, leucine and histidine. A total of 3×10^6 library clones were screened for growth in selection medium and assayed for β-galactosidase activity. Positive clones were picked and yeast plasmid DNA from individual clones was used to transform *Escherichia coli* HB101 ($leuB^-$) cells. Library plasmids were recovered selectively from bacterial colonies by growth in media lacking leucine. False-positive clones were eliminated by testing for interaction with empty vector pGBT-8 and irrelevant 'baits'. cDNA inserts in the plasmid were characterized by restriction enzyme mapping and nucleotide sequence analysis using an automated DNA sequencer (Applied Biosystems Model 373A).

Plasmid construction

Plasmids expressing hBcl-X_L or hBcl-X_S (Boise *et al.*, 1993), mBax (Oltvai *et al.*, 1993) and hBak (Farrow *et al.*, 1995) in pGBT-9 were constructed by PCR amplification of plasmid cDNA to incorporate restriction sites, followed by ligation of the amplified DNA fragments in-frame with the GAL4 DNA-binding domain of pGBT-9. The authenticity of the GAL4 fusion plasmids was confirmed by dideoxy sequencing. The mammalian expression plasmids SFFV-Flag-hBcl-2, SFFV-Flag-hBcl-x_L and SFFV-Flag-mBax have been described (Merino *et al.*, 1995; Simonian *et al.*, 1996). Three different constructs were generated to express *harakiri* sequences. In an initial construction, a Flag epitope sequence was attached to nucleotide 7 of the 5′ untranslated region of the *harakiri* cDNA to generate Flag-Hrk16K by PCR using pGAD-GH-*harakiri* plasmid as a template (see Figure 3A). The Flag sequence in Hrk16K was in-frame with the amino-terminus of Hrk, resulting in a fusion protein with a predicted size of 16 kDa. In a second construction, a Flag-Hrk insert was constructed by introducing a Flag epitope tag at the amino-terminus of Hrk by PCR. A deletion of amino acids 34–49 that includes the BH3 domain of Hrk was generated by a two-step PCR mutagenesis method as described (Simonian *et al.*, 1996). A Flag epitope tag was attached to the amino-terminus of mutated Hrk protein to generate Flag-Hrk ΔBH3. A Flag epitope tag was attached to the amino-terminus of a control cDNA clone BP25 (N.Inohara, L.Ding and G.Núñez, unpublished data) by PCR. The Flag-tagged inserts were ligated into the *Eco*RI cloning site of pSFFV-neo or the *Bam*HI and *Xho*I sites of pCDNA3 (Invitrogen, San Diego, CA). Orientation of the inserts was determined by restriction mapping. The authenticity of all Flag-tagged constructs was confirmed by dideoxy sequencing. An expression plasmid that produces a Flag-tagged GATA-1 protein was obtained from Dr Vishva Dixit (Department of Pathology, University of Michigan).

Screening of human cDNA library by hybridization with labeled probe

A 9-week human embryo λgt11 cDNA library (Swaroop and Xu, 1993) was screened by hybridization with a ^{32}P-labeled cDNA containing the entire coding region of *harakiri*. Approximately 1×10^6 cDNA clones were screened by standard procedures, and positive phage clones were purified by sequential plating and hybridization. DNA inserts were characterized by PCR amplification of phage DNA from purified plaques, restriction enzyme mapping of phage DNA inserts and dideoxy sequencing.

Transfection, immunoprecipitation and Western blot analysis

Human embryonic kidney 293T and 293 cells were obtained from Dr Vishva Dixit (Department of Pathology, University of Michigan). Culture dishes containing cells were transfected with the indicated amount (see figure legends) of plasmid DNA by the calcium phosphate method. The expression of Flag-Bcl-X_L, Flag-Bcl-2, Flag-Hrk, Flag-Hrk ΔBH3 and Bax was determined in total lysates by Western blot analysis as previously described (Merino *et al.*, 1995; Simonian *et al.*, 1996). For immunoprecipitations, 1×10^7 cells were lysed in NP-40 isotonic lysis buffer (Oltvai *et al.*, 1993) at 38 h after transfection and the lysates were rotated with 10 μg/ml of anti-Flag M2 monoclonal antibody (Scientific Imaging Systems, Rochester, NY), hamster anti-Bcl-2 monoclonal antibody (Hockenbery *et al.*, 1991), rabbit anti-Bcl-X (Boise *et al.*, 1995) or control Ig overnight at 4°C. Then 5% (v/v) of protein A–Sepharose 4B (Zymed Laboratories Inc., San Francisco, CA) was added for an additional hour of incubation by rotation. Immune complexes were centrifuged and washed with excess cold NP-40 isotonic lysis buffer at least four times, separated on a 15% SDS–polyacrylamide gel and immunoblotted with anti-Bcl-2, anti-Flag, rabbit anti-Bcl-X or control Ig.

Northern blot analysis

A 716 bp *harakiri* cDNA was radiolabeled by the random priming method using a commercial kit (Boehringer Mannheim, Indianapolis, IN) and applied for analysis of human multiple tissue blots (Clontech Laboratories, Palo Alto, CA) according to the manufacturer's instructions.

Laser scanning confocal microscopy and fluorescence staining of nuclear DNA

293 cells were transfected with pCDNA3-Flag-Hrk, pCDNA3-Flag-GATA-1, or empty vector as described above. Twenty four hours after transfection, cells were incubated with anti-Flag monoclonal antibody or control mouse Ig for 1 h at 23°C and the labeling visualized with fluorescein-conjugated goat anti-mouse IgG. After washing, the cells were mounted in Slowfade (Molecular Probes, Eugene, OR) and examined using a BioRad MRC 600 scanning confocal microscope equipped with an argon–xenon laser (González-García *et al.*, 1994). Staining of nuclei with acridine orange and ethidium bromide was performed as described previously (Duke and Cohen, 1994).

Cell death assays

293T, 293 and HeLa cells were co-transfected by a calcium phosphate method with pRK7.GFP, a reporter plasmid expressing GFP (a gift of Roger Y.Tsien), in combination with an expression plasmid encoding Hrk, Bcl-2, Bcl-X_L or control plasmid. The number of plasmids transfected is indicated in the figure legends. Killing activity was determined at 48 h after transfection and based on the analysis of 5×10^3 cells by FACScan flow cytometry (Becton Dicknson, Mountain View, CA). In the assay, the cell killing activity was manifested by a reduction in the number of cells that express GFP relative to that obtained by transfection with the control expression plasmid.

Accession number

The accession number for the nucleotide sequence of *harakiri* cDNA reported in this paper is U76376.

Acknowledgements

We would like to thank Maria Jose Fernandez-Sarabia and Eileen White for providing the HeLa cDNA library in pGAD-GH, Maria Jose Fernandez-Sarabia for human *bcl-2* in the pGBT vector, Stuart Farrow for *bak* plasmid, David Beach for the HF7c reporter yeast strain, Roger Y.Tsien for RK7.GFP plasmid, Michael Clarke, Masao Seto and Max Wicha for stimulating discussions, Mary A.Benedict for expert advice

on apoptosis assays and analysis of protein interactions, and Mary Benedict, Phillip L.Simonian, Daryoush Ekhterae, Maribel González-García, Yuanming Hu, Herschel Wallen and Dayang Wu for a critical review of the manuscript. This work was supported in part by grant DAMD17-96-1-6019 from the US Army Medical Research Command. G.N. is the recipient of a Research Career Development Award CA-64421 from the National Institutes of Health.

References

Askew,D., Ashmun,R., Simmons,B. and Cleveland,J. (1991) Constitutive c-*myc* expression in an IL-3-dependent myeloid cell line suppresses cell cycle arrest and accelerates apoptosis. *Oncogene*, **6**, 1915–1922.

Boise,L.H., González-García,M., Postema,C.E., Ding,L., Lindsten,T., Turka,L.A., Mao,X., Núñez,G. and Thompson,C.B. (1993) *bcl-x*, a *bcl-2* related gene that functions as a dominant regulator of apoptotic cell death. *Cell*, **74**, 597–608.

Boise,L.H., Minn,A.J., Noel,P.J., June,C.H., Accavitti,M.A., Lindsten,T. and Thompson,C.B. (1995) CD28 costimulation can promote T cell survival by enhancing the expression of Bcl-X_L. *Immunity*, **3**, 87–98.

Boyd,J.M., Malstrom,S., Subramanian,T., Venkatesh,L.K., Schaeper,U., Elangovan,B., D'Sa-Eipper,C. and Chinnadural,G. (1994) Adenovirus E1B and 19 kDa and Bcl-2 proteins interact with a common set of cellular proteins. *Cell*, **79**, 341–351.

Boyd,J.M. *et al.* (1995) Bik, a novel death-inducing protein shares a distinct sequence motif with Bcl-2 family proteins and interacts with viral and cellular survival-promoting proteins. *Oncogene*, **11**, 1921–1928.

Chinnaiyan,A.M., Orth,K., O'Rourke,K., Duan,H., Poirier,G.G. and Dixit,V.M. (1996) Molecular ordering of the cell death pathway: Bcl-2 and Bcl-X_L function upstream of the CED-3-like apoptotic proteases. *J. Biol. Chem.*, **271**, 4573–4576.

Chittenden,T., Harrington,E.A., O'Connor,R., Flemington,C., Lutz,R.J., Evan,G.I. and Guild,B.C. (1995a) Induction of apoptosis by the Bcl-2 homologue Bak. *Nature*, **374**, 733–736.

Chittenden,T., Flemington,C., Houghton,A.B., Ebb,G.E., Gallo,G.J., Elangovan,B., Chinnadurai,G. and Lutz,R.J. (1995b) A conserved domain in Bak, distinct from BH1 and BH2, mediates cell death and protein binding functions. *EMBO J.*, **14**, 5589–5596.

Clarke,M.F. *et al.* (1995) A recombinant *bcl-x_s* adenovirus selectively induces apoptosis in cancer cells, but not normal bone marrow cells. *Proc. Natl Acad. Sci. USA*, **92**, 11024–11028.

Duke,R.C. and Cohen,J.J. (1994) Morphological and biochemical assays of apoptosis. In Coligan,J.E., Kruisbeek,A.M., Margulies,D.H., Shevach,E.M. and Strober,W. (eds), *Current Protocols in Immunology*. Current Protocols, NY, pp. 3.17.1–3.17.3.

Evan,G.I., Wyllie,A.H., Gilbert,C.S., Littlewood,T.D., Land,H., Brooks,M., Waters,C.M., Penn,L.Z. and Hancock,D.C. (1992) Induction of apoptosis in fibroblasts by c-myc protein. *Cell*, **69**, 119–128.

Farrow,S.N., White,J.H., Martinou,I., Raven,T., Pun,K.T., Grinham,C.J., Martinou,J.C. and Brown,R. (1995) Cloning of a *bcl-2* homologue by interaction with adenovirus E1B 19K. *Nature*, **374**, 731–733.

Feilotter,H.E., Hannon,G.J., Ruddell,C.J. and Beach,D. (1994) Construction of an improved host strain for two hybrid screening. *Nucleic Acids Res.*, **22**, 1502–1503.

Fernandez-Sarabia,M.J. and Bischoff,J.R. (1993) Bcl-2 associates with the ras-related protein R-ras p23. *Nature*, **366**, 274–275.

González-García,M., Pérez-Ballestero,R., Ding,L., Duan,L., Boise,L.H., Thompson,C.B. and Núñez,G. (1994) *bcl-x_L* is the major *bcl-x* mRNA form expressed during murine development and its product localizes to mitochondria. *Development*, **120**, 3033–3042.

Han,J., Sabbatini,P., Perez,D., Rao,L., Modha,D. and White,E. (1996a) The E1B 19K protein blocks apoptosis by interacting with and inhibiting the p53-inducible and death-promoting Bax protein. *Genes Dev.*, **10**, 461–477.

Han,J., Sabbatini,P. and White,E. (1996b) Induction of apoptosis by human Nbk/Bik, a BH3-containing protein that interacts with E1B 19K. *Mol. Cell. Biol.*, **16**, 5857–5864.

Hannon,G.J., Demetrick,D. and Beach,D. (1993) Isolation of the Rb-related p130 through its interaction with CDK2 and cyclins. *Genes Dev.*, **7**, 2378–2391.

Hockenbery,D., Núñez,G., Milliman,C., Scheiber,R.D. and Korsmeyer,S.J. (1991) Bcl-2 is an inner mitochondrial membrane protein that blocks programmed cell death. *Nature*, **348**, 334–336.

Krajewski,S., Tanaka,S., Takeyama,S., Schibler,M.J., Fenton,W. and Reed,J.C. (1993) Investigation of the subcellular distribution of the *bcl-2* oncoprotein: residence in the nuclear envelope, endoplasmic reticulum, and outer mitochondrial membranes. *Cancer Res.*, **53**, 4701–4714.

Merino,R., Grillot,D.A., Simonian,P.L., Muthukkumar,S., Fanslow,W.C., Bondada,S. and Núñez,G. (1995) Modulation of anti-IgM-induced B cell apoptosis by Bcl-X_L and CD40 in WEHI-231 cells: dissociation from cell cycle arrest and dependence of the antibody–IgM receptor interaction. *J. Immunol.*, **155**, 3830–3838.

Motoyama,N. *et al.* (1995) Massive cell death of immature hematopoietic cells and neurons in Bcl-x-deficient mice. *Science*, **267**, 1506–1510.

Muchmore,S.W. *et al.* (1996) X-ray and NMR structure of human Bcl-xL, an inhibitor of programmed cell death. *Nature*, **381**, 335–341.

Núñez,G., London,L., Hockenbery,D., Alexander,M., McKearn,J.P. and Korsmeyer,S.J. (1990) Deregulated Bcl-2 gene expression selectively prolongs survival of growth factor-deprived hemopoietic cell lines. *J. Immunol.*, **144**, 3602–3610.

Oltvai,Z.N. and Korsmeyer,S.J. (1994) Checkpoints of dueling dimers foil death wishes. *Cell*, **79**, 189–192.

Oltvai,Z.N., Milliman,C.L. and Korsmeyer,S.J. (1993) Bcl-2 heterodimerizes *in vivo* with a conserved homolog, Bax, that accelerates programmed cell death. *Cell*, **74**, 609–619.

Sato,T. *et al.* (1994) Interactions among members of the Bcl-2 family analyzed with a yeast two-hybrid system. *Proc. Natl Acad. Sci. USA*, **91**, 9283–9242.

Shaw,G. and Kamen,R. (1986) A conserved AU sequence from the 3′ untranslated region of GM-CSF mRNA mediates selective mRNA degradation. *Cell*, **46**, 659–667.

Simonian,P.L., Grillot,D.A.M., Merino,R. and Núñez,G. (1996) Bax can antagonize Bcl-X_L during etoposide and cisplatin-induced cell death independently of its heterodimerization with Bcl-X_L. *J. Biol. Chem.*, **271**, 22764–22772.

Swaroop,A. and Xu,J. (1993). cDNA libraries from human tissues and cell lines. *Cytogenet. Cell Genet.*, **64**, 292–294.

Takayama,S., Sato,T., Krajewski,S., Kochel,K., Irie,S., Millan,J.A. and Reed,J.C. (1995) Cloning and functional analysis of BAG-1: a novel Bcl-2-binding protein with anti-cell death activity. *Cell*, **80**, 279–284.

Thompson,C.B. (1995) Apoptosis in the pathogenesis and treatment of disease. *Science*, **267**, 1456–1462.

Vaux,D.L., Cory,S. and Adams,J.M. (1988) Bcl-2 gene promotes haemopoietic cell survival and cooperates with c-myc to immortalize pre-B cells. *Nature*, **335**, 440–442.

Veis,D.J., Sorenson,C.M., Shutter,J.R. and Korsmeyer,S.J. (1993) Bcl-2-deficient mice demonstrate fulminant lymphoid apoptosis, polycystic disease, and hypopigmented hair. *Cell*, **75**, 229–240.

Wang,H.G., Takayama,S., Rapp,U.R. and Reed,J.C. (1996) Bcl-2 interacting protein, BAG-1, binds to and activates the kinase Raf-1. *Proc. Natl Acad. Sci. USA*, **93**, 7063–7068.

White,E. (1996) Life, death and the pursuit of apoptosis. *Genes Dev.*, **10**, 1–15.

White,E., Cipriani,R., Sabbatini,P. and Denton,A. (1991) Adenovirus E1B 19-kilodalton protein overcomes the cytotoxicity of E1A proteins. *J. Virol.*, **65**, 2968–2978.

Yamagata,K., Sanders,L.K., Kaufmann,W.E., Yee,Y., Barnes,C.A., Nathans,D. and Worley,P.F. (1994) RheB, a growth factor- and synaptic activity-regulated gene, encodes a novel Ras-related protein. *J. Biol. Chem.*, **269**, 16333–16339.

Yang,E., Zha,J., Jockel,J., Boise,L.H., Thompson,C.B. and Korsmeyer,S.J. (1995) Bacl, a heterodimeric partner for Bcl-xL and Bcl-2, displaces Bax and promotes cell death. *Cell*, **80**, 285–291.

Zha,H., Aimé-Sempé,C., Sato,T. and Reed,J.C. (1996) Proapoptotic protein Bax heterodimerizes with Bcl-2 and homodimerizes with Bax via a novel domain (BH3) distinct from BH1 and BH2. *J. Biol. Chem.*, **271**, 7440–7444.

Received on November 5, 1996; revised on December 6, 1996

Proc. Natl. Acad. Sci. USA
Vol. 95, pp. 4386–4391, April 1998
Cell Biology

Bcl-X_L interacts with Apaf-1 and inhibits Apaf-1-dependent caspase-9 activation

(apoptosis/cell death)

YUANMING HU, MARY A. BENEDICT, DAYANG WU, NAOHIRO INOHARA, AND GABRIEL NÚÑEZ*

Departments of Pathology and Comprehensive Cancer Center, 1500 East Medical Center Drive, University of Michigan Medical School, Ann Arbor, MI 48109

Edited by H. Robert Horvitz, Massachusetts Institute of Technology, Cambridge, MA, and approved February 17, 1998 (received for review December 8, 1997)

ABSTRACT **Recent studies indicate that *Caenorhabditis elegans* CED-4 interacts with and promotes the activation of the death protease CED-3, and that this activation is inhibited by CED-9. Here we show that a mammalian homolog of CED-4, Apaf-1, can associate with several death proteases, including caspase-4, caspase-8, caspase-9, and nematode CED-3 in mammalian cells. The interaction with caspase-9 was mediated by the N-terminal CED-4-like domain of Apaf-1. Expression of Apaf-1 enhanced the killing activity of caspase-9 that required the CED-4-like domain of Apaf-1. Furthermore, Apaf-1 promoted the processing and activation of caspase-9 *in vivo*. Bcl-X_L, an antiapoptotic member of the Bcl-2 family, was shown to physically interact with Apaf-1 and caspase-9 in mammalian cells. The association of Apaf-1 with Bcl-X_L was mediated through both its CED-4-like domain and the C-terminal domain containing WD-40 repeats. Expression of Bcl-X_L inhibited the association of Apaf-1 with caspase-9 in mammalian cells. Significantly, recombinant Bcl-X_L purified from *Escherichia coli* or insect cells inhibited Apaf-1-dependent processing of caspase-9. Furthermore, Bcl-X_L failed to inhibit caspase-9 processing mediated by a constitutively active Apaf-1 mutant, suggesting that Bcl-X_L regulates caspase-9 through Apaf-1. These experiments demonstrate that Bcl-X_L associates with caspase-9 and Apaf-1, and show that Bcl-X_L inhibits the maturation of caspase-9 mediated by Apaf-1, a process that is evolutionarily conserved from nematodes to humans.**

Programmed cell death or apoptosis, a morphologically distinguished form of cell death, is critical for development and tissue homeostasis in multicellular organisms (1, 2). The apoptotic mechanism is evolutionarily conserved and controlled by a genetic program (1–3). Genetic studies in the nematode *Caenorhabditis elegans* have identified three genes that play critical roles in the induction and execution of programmed cell death (3). Two nematode genes, *ced-3* and *ced-4*, are required for the execution of the cell death program. The *ced-3* product is homologous to the mammalian interleukin 1β-converting enzyme (4). The *ced-9* gene functions upstream of *ced-3* and *ced-4* and protects cells that normally survive programmed cell death during worm development (5, 6). Biochemical analyses of CED-3, CED-4, and CED-9 have provided insight into the mechanism by which programmed cell death is regulated in the nematode. CED-4 interacts with CED-3 and CED-9 forming a multimeric protein complex (7–9). Furthermore, CED-4 promotes the activation of the death protease CED-3, and this activation is inhibited by CED-9 (10–12).

Several of the apoptosis regulatory genes identified in *C. elegans* have mammalian counterparts. A family of cysteine proteases (designated caspases) related to the *C. elegans* CED-3 appears to represent the effector arm of the apoptotic program (13). Each caspase contains conserved residues important for specific proteolytic activity cleaving after aspartic acid residues (13). Several caspases including caspase-4, -8, and -9 structurally resemble CED-3 in that they contain long prodomains and appear to act upstream in the caspase cascade (13, 14). Activation of downstream caspases through several stimuli leads to cleavage of target proteins and execution of the apoptotic program (13). Bcl-2 and Bcl-X_L, two members of the Bcl-2 family, function as apoptosis inhibitors and are considered homologs of the nematode CED-9 (15). Several studies have shown that these apoptosis inhibitors regulate the activation of caspases (16, 17). However, the precise mechanism by which Bcl-2 and Bcl-X_L control caspase activation and apoptosis remains controversial.

Recent studies have identified and partially characterized Apaf-1, a mammalian homolog of *C. elegans* CED-4 (18). The N-terminal region of Apaf-1 shares amino acid homology with CED-4 and the prodomains of CED-3 and several CED-3-like proteases with long prodomains. The region of homology shared between Apaf-1 and the prodomains of CED-3-like proteases has been termed caspase recruitment domain (19). The C-terminal region of Apaf-1 lacks homology with CED-4 and is composed of 12 WD repeats (18). In the presence of dATP and cytochrome *c*, a molecule that is released from mitochondria during apoptosis, Apaf-1 binds to caspase-9 and induces the activation of caspase-3, a downstream death protease (20).

In the current studies, we have sought to assess the interaction of the antiapoptotic Bcl-X_L protein with Apaf-1 and CED-3-like caspases to determine if the regulation of the death mechanism is evolutionarily conserved in nematodes and mammals. The analyses indicate that Apaf-1 interacts with several caspases containing long prodomains including caspase-4, -8, -9, and CED-3. Furthermore, Bcl-X_L physically associates with Apaf-1 and caspase-9 and inhibits Apaf-1-mediated maturation of caspase-9.

MATERIALS AND METHODS

Plasmid Construction. An expression plasmid containing the Apaf-1 cDNA (18) was obtained from X. Wang (University of Texas Southwestern Medical Center, Dallas). Apaf-1, mutant N-Apaf-1, and C-Apaf-1 were amplified by PCR using the Apaf-1 cDNA as a template and cloned into the expression vector pcDNA3-Myc to produce C-terminal tagged Apaf-1

The publication costs of this article were defrayed in part by page charge payment. This article must therefore be hereby marked "*advertisement*" in accordance with 18 U.S.C. §1734 solely to indicate this fact.

This paper was submitted directly (Track II) to the *Proceedings* office.

Abbreviations: HA, hemagglutinin; PARP, poly(ADP-ribose) polymerase.

*To whom reprint requests should be addressed. e-mail: gabriel.nunez@umich.edu.

proteins. The human caspase-3, caspase-4, wild type, and mutant (C287S) caspase-9 cDNAs were cloned into the *Bam*HI and *Xho*I sites of a pcDNA3-hemagglutinin (HA) or -Flag vectors to produce C-terminal tagged proteins. The plasmids pcDNA-3-Flag-Bcl-X_L, pcDNA3-β-galactosidase, pcDNA3-Ced-3-HA (C360S), pcDNA3-caspase-8-HA and pcDNA3-caspase-8-AU1 mutant (C377S) were described previously (10, 21, 22). The pcDNA-p35 plasmid was a gift from V. Dixit (Genentech, South San Francisco, CA).

Transfection, Immunoprecipitation, and Western Blot Analysis. Human embryonic kidney 293T cells ($2–5 \times 10^6$) were transfected with 5 μg each of the indicated plasmid DNA by the calcium phosphate method. Protein immunoprecipitation and Western blot analysis with relevant antibodies were performed as described (7). Rabbit anti-caspase-9 antibody was a gift of X. Wang, and anti-poly(ADP-ribose) polymerase (PARP) antibody was purchased from Enzyme Systems Products (Livermore, CA). The proteins were detected by using an enhanced chemiluminescence system (Amersham).

Apoptosis Assay. 293T cells (1×10^5) were seeded in each well of 12-well plates. After 12 hr, cells were transiently transfected with 0.25 μg of the reporter pcDNA3-β-galactosidase plasmid plus various combinations of the following plasmids: 0.1 μg caspase-9, 0.4 μg each of Apaf-1-Myc (WT), N-Apaf-1 (N), C-Apaf-1 (C), untagged Apaf-1 (UT), or 1 μg pcDNA3-p35. pcDNA3 was used to adjust total plasmid DNA to an equal amount. Percentage of apoptotic cells was determined 18 hr after transfection in triplicate cultures as described (10).

Preparation of Recombinant Bcl-X_L Protein. The human Bcl-X_L cDNA was excised from pSFFV-Bcl-X_L (21) and cloned into the pET30a(+) plasmid (Novagen). Bcl-X_L was purified from cultures of *Escherichia coli* BL21(DE3) expressing $(His)_6$-Bcl-X_L by Ni^{2+}-resin column chromatography. The purity of the Bcl-X_L preparation was at least 95% as determined by Coomassie blue staining. Recombinant Glu-Glu-tagged Bcl-X_L was produced from a pAcoG-human-Bcl-X_L construct in baculovirus-infected Sf9 cells (a gift of M. J. Fernandez Sarabia, Onyx Pharmaceuticals, Richmond, CA) and purified by affinity chromatography as described (23). The $(His)_6$-tagged recombinant Bad protein was produced and purified from *E. coli* BL21(DE3) carrying pET30a(+)-Bad plasmid as described (24).

***In Vitro* Caspase-9 Assay.** S-100 extracts from 293T cells were prepared essentially as described by Liu *et al.* (25) and frozen at −80°C. Caspase-9 was translated *in vitro* from a pcDNA-3-caspase-9 plasmid in the presence of [^{35}S]methionine (Amersham) by using a Promega TNT transcription/translation kit. Fifty or twenty micrograms of S-100 cellular extract was incubated with or without dATP (1 mM) or bovine cytochrome *c* (0.4 μg, Sigma) in the presence of 1 μl *in vitro* translated caspase-9 in a final volume of 25 μl. The mixtures were incubated for 30 min at 37°C and stopped by adding 5× SDS loading buffer and boiled for 5 min. To determine Apaf-1-dependence of the activation of caspase-9, 0.5 μl of normal rabbit serum or rabbit anti-Apaf-1 serum (a gift of X. Wang) was added to the S-100 extract. Recombinant Bcl-X_L or Bad was preincubated with the S-100 extract for 30 min prior to addition of dATP and cytochrome *c*.

RESULTS

Apaf-1 Interacts with Multiple Caspases Containing Long Prodomains but not with Caspase-3. To determine if Apaf-1 interacts with caspases, we performed *in vivo* interaction analysis using full-length Apaf-1 or two deletion mutants of Apaf-1, N-Apaf-1 (residues 1–559), and C-Apaf-1 (residues 468-1194) comprising the CED-4-like and C-terminal regions of Apaf-1 respectively (Fig. 1*A*). We transiently cotransfected 293T cells with expression plasmids producing caspase-3, -4, -9, *C. elegans* CED-3, or control empty vector and Myc-tagged Apaf-1. Western blot analysis of protein complexes immunoprecipitated with anti-Myc antibody revealed that caspase-4, -9, and CED-3 were coimmunoprecipitated with Apaf-1 but caspase-3 was not (Fig. 1 *B–D*). The interaction of Apaf-1 with caspase-9 confirmed a recent study published while this manu-

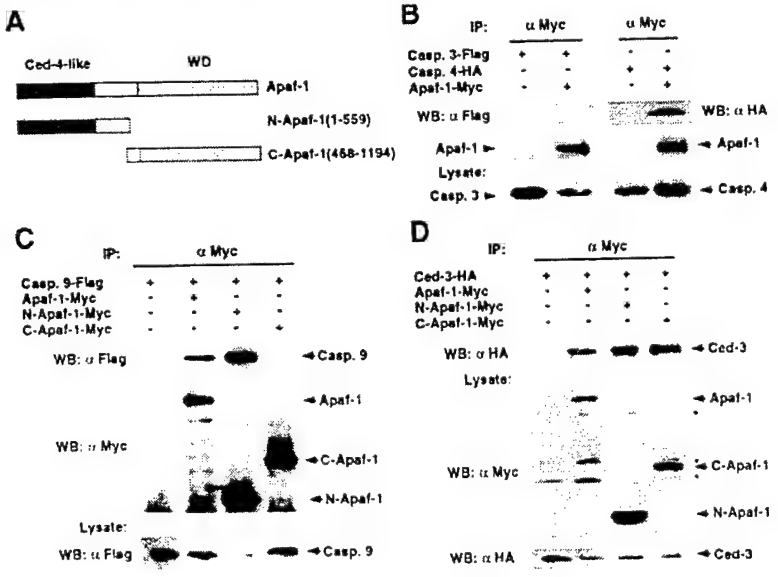

FIG. 1. Apaf-1 interacts with several caspases with long prodomains in mammalian cells. (*A*) Schematic drawing of the Apaf-1 constructs used in this study. (*B–D*) Interaction of Apaf-1 with caspase-4, caspase-9, and CED-3. 293T cells were cotransfected with the indicated tagged caspases and control vector, or tagged Apaf-1, N-terminal, or C-terminal Apaf-1 constructs (Apaf-1-Myc, N-Apaf-1-Myc, and C-Apaf-1-Myc, respectively). (*Upper*) Western blot analysis of immunoprecipitated protein complexes with indicated antibodies. (*Lower*) The expression of caspase-3 and -4 (*B*), caspase-9 (*C*), and CED-3 and Apaf-1 proteins (*D*). Reduced level of pro-caspase-9 in lane 3 of *C* is due to efficient N-Apaf-1-mediated processing of pro-caspase-9. IP: immunoprecipitation. WB: Western blot analysis. Asterisks indicate nonspecific bands.

script was in preparation (20). Analysis of Apaf-1 mutants revealed that Apaf-1 interacted with caspase-9 through its N-terminal CED-4-like domain (Fig. 1*C*). However, both the CED-4-like and C-terminal regions of Apaf-1 interacted with the *C. elegans* CED-3 protease (Fig. 1*D*).

Apaf-1 Interacts with the Death Effector Domain of Caspase-8. As caspase-8 contains a long prodomain with two death effector domains structurally related to the prodomain of CED-3 (19), we determined next if Apaf-1 also interacts with caspase-8. Western blot analysis of complexes immunoprecipitated with anti-Myc antibody revealed that caspase-8 was coimmunoprecipitated with Apaf-1 in 293T cells (Fig. 2*A*). Analysis of Apaf-1 mutants showed that caspase-8 associates with both the CED-4-like and C-terminal regions of Apaf-1 (Fig. 2*A*). To further dissect the Apaf-1-caspase-8 interaction, we engineered two deletion mutants to express either the N-terminal prodomain (residues 1–215) or the C-terminal catalytic domain (residues 216–479) of caspase-8. Immunoprecipitation analysis revealed that Apaf-1 interacts with the prodomain containing the death effector domains but not with the catalytic domain of caspase-8 (Fig. 2*B*).

Apaf-1 Promotes Both Activation of Caspase-9 and Caspase-9-Mediated Apoptosis in Mammalian Cells. The interaction of Apaf-1 with caspase-9 prompted further experiments to assess whether Apaf-1 could regulate the activation of caspase-9. In these experiments, 293T cells were transiently transfected with constructs producing Myc-tagged full-length or truncated mutant Apaf-1 and caspase-9. Expression of

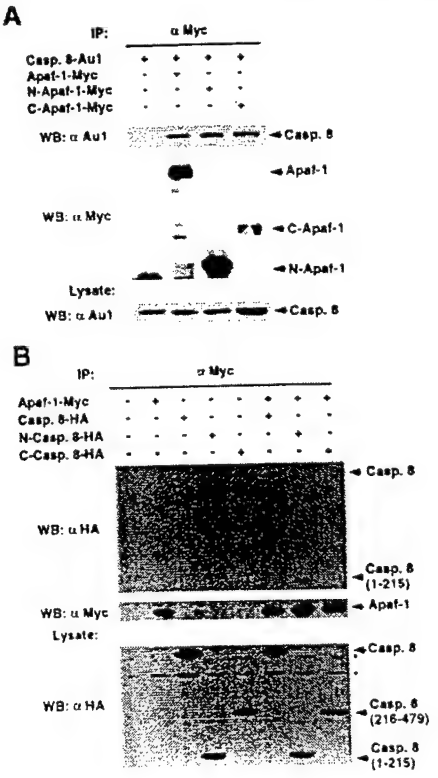

FIG. 2. Apaf-1 interacts with the prodomain of caspase-8. (*A*) Interaction of Apaf-1 with caspase-8. (*B*) Apaf-1 interacts with the prodomain of caspase-8. Immunoprecipitation analysis was performed as described in Fig. 1. (*Upper*) Western blot analysis of immunoprecipitated protein complexes with indicated antibodies. (*A* and *B*, *Lower*) show the expression of caspase-8 (*A*) or Apaf-1 (*B*) in total lysates by Western blot analysis. IP: immunoprecipitation, WB: Western blot analysis. Asterisks indicate nonspecific bands.

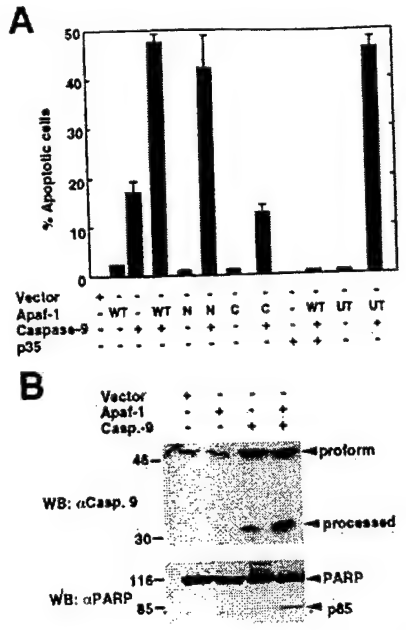

FIG. 3. Regulation of caspase-9 by full-length and N-terminal Apaf-1. (*A*) Apaf-1 enhances caspase-9-induced apoptosis. 293T cells were transiently transfected with a reporter pcDNA3-β-galactosidase plus the indicated plasmids. WT, full-length Apaf-1-Myc; N, N-terminal Apaf-1-Myc; C, C-terminal Apaf-1-Myc; UT, Untagged full-length Apaf-1. The results represent the percentage of blue cells that exhibit morphologic features of apoptosis and are given as the mean +/− SD of triplicate cultures. (*B*) Apaf-1 promotes caspase-9 activation *in vivo*. Lysates from cells transfected with the indicated plasmids were immunoblotted with anti-caspase-9 (*Upper*) or anti-PARP antibodies (*Lower*). Arrows indicate full-length and processed caspase-9 and PARP fragments. Asterisk indicates nonspecific band.

wild-type Apaf-1 or the N-terminal mutant (CED-4-like) but not the C-terminal mutant of Apaf-1 enhanced the killing activity of caspase-9 (Fig. 3*A*). Apoptosis induced by Apaf-1 and caspase-9 was inhibited by baculovirus p35, an inhibitor of caspases (Fig. 3*A*). Untagged Apaf-1 also enhanced the killing activity of caspase-9, ruling out any artifact due to the Myc tag (Fig. 3*A*). We performed further analysis to determine whether the proteolytic processing of caspase-9, a step required for activation of caspases (13), was regulated by Apaf-1 *in vivo*. Expression of Apaf-1 enhanced the formation of a major cleavage product of caspase-9 (p35), that is formed during its proteolytic activation (Fig. 3*B*). To assess the activation of caspase-9, the same cellular lysates were immunoblotted with an antibody against PARP, a protein that is cleaved after caspase-9 activation (20, 25). Western blot analysis revealed that Apaf-1 promotes caspase-9 activation as determined by the detection of p85, a proteolytic fragment of PARP that results from its cleavage by caspases (Fig. 3*B*).

Bcl-X_L Associates with Caspase-9 and Apaf-1 in Mammalian Cells. We examined next whether Bcl-X_L could associate with caspase-9. The analysis showed that Bcl-X_L and caspase-9 coimmunoprecipitated *in vivo* (Fig. 4*A*). As the nematode CED-9 protein, a homolog of mammalian Bcl-X_L, interacts with CED-3 through CED-4 (8, 10), we determined if Bcl-X_L could associate with Apaf-1. Western blot analysis of Bcl-X_L complexes with anti-Myc antibody revealed that Apaf-1 coimmunoprecipitated with Bcl-X_L (Fig. 4*B*). To verify these results, we performed reciprocal experiments in which wild-type Apaf-1 and Apaf-1 deletion mutants were immunoprecipitated with anti-Myc antibody. Western blot analysis with anti-Flag confirmed that Apaf-1 coimmunoprecipitated with

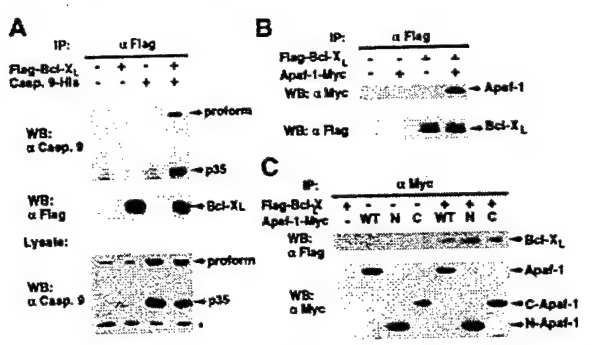

FIG. 4. Bcl-X_L interacts with caspase-9 and Apaf-1. (*A*) Bcl-X_L interacts with caspase-9. (*Upper*) Western blot analysis of immunoprecipitated Bcl-X_L and coimmunoprecipitated pro-caspase-9 and processed form (p35). (*Lower*) The expression of caspase-9 in total lysate. (*B* and *C*) Bcl-X_L interacts with Apaf-1. 293T cells were transfected with indicated plasmids and the lysates immunoprecipitated with anti-Flag (*B*) or anti-Myc (*C*) antibody. WT, full-length Apaf-1-Myc; N, N-terminal Apaf-1-Myc; C, C-terminal Apaf-1-Myc. Panels show Western blot analysis of coimmunoprecipitated Apaf-1 and Bcl-X_L proteins. Asterisk indicates nonspecific band.

Bcl-X_L and revealed that Bcl-X_L associates with both the CED-4-like domain and the C-terminal region that contains the WD repeats of Apaf-1 (Fig. 4*C*).

Bcl-X_L Inhibits the Association of Apaf-1 with Caspase-9. Because Bcl-X_L associated with both Apaf-1 and caspase-9 in mammalian cells, we tested whether Bcl-X_L could affect the Apaf-1-caspase-9 interaction. 293T cells were cotransfected with plasmids producing Apaf-1 and caspase-9 (C287S) in the presence or absence of Bcl-X_L and caspase-9 complexes were immunoprecipitated with anti-HA antibody. Western blot analysis revealed that Bcl-X_L inhibited the association of Apaf-1 with caspase-9 (Fig. 5). Western blot analysis of the same immunocomplexes and lysates showed comparable levels of caspase-9 and Apaf-1 (Fig. 5), indicating that the results were not due to differential expression of these proteins.

Purified Bcl-X_L Inhibits Apaf-1-Mediated Maturation of Caspase-9. To determine if Bcl-X_L could regulate the activity of caspase-9, we performed biochemical experiments by using a cell-free system in which exogenously added dATP and cytochrome *c* induce the activation of caspase-9 (20). Processing of caspase-9 into p37, p35, and p10–12 forms in cellular extracts was dependent on dATP and cytochrome *c* as reported (20). However, we observed a partial cytochrome *c* dependence in our system presumably due to leakage of cytochrome *c* during extract preparation (Fig. 6*A*). The activation of caspase-9 was inhibited by rabbit anti-Apaf-1, but not control

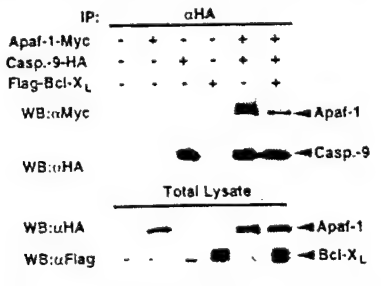

FIG. 5. Bcl-X_L inhibits the association of Apaf-1 with caspase-9. 293T cells were transfected with indicated plasmids and the lysates immunoprecipitated with anti-HA antibody. (*Upper*) Western blot analysis of immunoprecipitated caspase-9 and coimmunoprecipitated Apaf-1. (*Lower*) Western blot analysis of total lysates with anti-Myc and anti-Flag antibody.

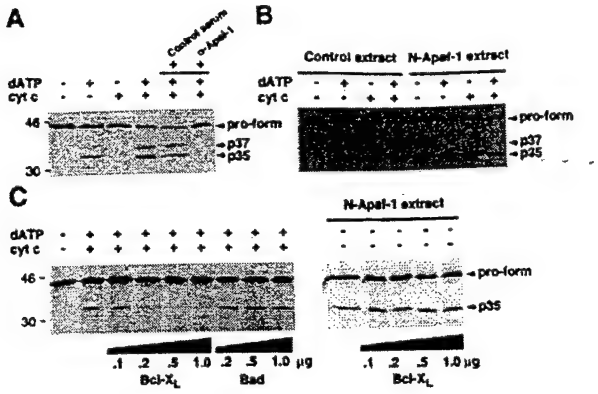

FIG. 6. Purified Bcl-X_L inhibits Apaf-1-dependent maturation of caspase-9 *in vitro*. (*A*) Apaf-1-dependent processing of caspase-9 by Apaf-1 *in vitro*. In the last two lanes normal rabbit serum (control) or anti-Apaf-1 serum were added 30 min prior to the reaction. (*B*) N-terminal Apaf-1 mutant (residues 1–559) activates caspase-9 independently of cytochrome *c* and dATP. Extracts from 293T cells transfected with pcDNA3 (control extract) or pcDNA3-N-Apaf-1 (N-Apaf-1 extract) were used in the analysis. (*C*) Regulation of caspase-9 maturation by recombinant Bcl-X_L. Cellular extracts were incubated with indicated amounts of recombinant Bcl-X_L or Bad and then cytochrome *c* and dATP were added to the reaction. (*Right*) Extracts from cells expressing a N-terminal Apaf-1 mutant (residues 1–559) were incubated with indicated amounts of recombinant Bcl-X_L. Proform and processed caspase-9 are indicated by arrows.

serum, confirming that activation of caspase-9 by cytosolic extracts was dependent on Apaf-1 (Fig. 6*A*). In contrast to caspase-9, we did not observe any enhancement of caspase-4 or caspase-8 processing using this *in vitro* system (data not shown). Significantly, an N-terminal mutant of Apaf-1 (residues 1–559) promoted the activation of caspase-9 independently of dATP and cytochrome *c* (Fig. 6*B*).

We purified Bcl-X_L from *E. coli* to test the ability of Bcl-X_L to regulate Apaf-1-dependent activation of caspase-9. Recombinant Bcl-X_L purified from *E. coli* inhibited the maturation of caspase-9 in a dose-dependent manner (Fig. 6*C*). In control experiments, recombinant Bad purified from *E. coli* did not inhibit the processing of caspase-9 (Fig. 6*C*). In addition, recombinant Bcl-X_L purified from SF9 insect cells also inhibited the maturation of caspase-9 in this cell-free system (data not shown). Because Bcl-X_L associates with both caspase-9 and Apaf-1, we used the constitutively active Apaf-1 mutant (residues 1–559) to assess the possibility that caspase-9 activation is regulated directly by its interaction with Bcl-X_L. Fig. 6*C* shows that Bcl-X_L could not inhibit caspase-9 activation mediated by the N-Apaf-1 mutant. These results indicate that Bcl-X_L requires wild-type Apaf-1 to inhibit caspase-9 activation. Therefore it is unlikely that Bcl-X_L inhibits caspase-9 solely through a direct interaction with caspase-9.

DISCUSSION

In the present studies, we have shown that Apaf-1, a mammalian homolog of *C. elegans* CED-4 interacts with several caspases including caspase-4, -8, -9, and the nematode CED-3 protease in mammalian cells. These results indicate that the association of Apaf-1 with caspases is not restricted to caspase-9 (20). All of these interacting caspases contain long prodomains and are thought to function upstream in a caspase cascade (14). The prodomains of caspase-9 and CED-3 contain a caspase recruitment domain that is conserved in several apoptosis regulatory molecules including Apaf-1, Rip-associated ICHi/CED-3 homologous protein with a death domain (RAIDD), and cellular inhibitors of apoptosis (IAPs)

(19, 20, 26). Caspase-8 is a proximal caspase that is involved in apoptosis mediated through the tumor necrosis factor family of death receptor pathways (27, 28). Caspase-8 contains two death effector domains in its prodomain (27, 28). We have shown here that caspase-8 interacts with Apaf-1 through its prodomain region that contains the death effector domains. In contrast, caspase-3, a death protease that functions downstream of caspase-9 and lacks a long prodomain (20), failed to interact with Apaf-1. These results indicate that Apaf-1 can interact with several other upstream caspases in addition to caspase-9. However, the relevance of the interaction between Apaf-1 and caspase-4 or caspase-8 is unclear. In contrast to caspase-9, Apaf-1 did not promote processing of these other caspases in our *in vitro* system. It is possible that Apaf-1 still plays a role in the activation of caspase-4 and/or caspase-8, but the regulation may require different factors that those required for caspase-9.

Previous studies have demonstrated that Bcl-X_L can associate with caspase-1 and caspase-8 in mammalian cells (8). Here we have shown that Bcl-X_L associates with caspase-9. We further demonstrate that Apaf-1 interacts with Bcl-X_L. This result is consistent with previous observations with the *C. elegans* regulators CED-9 and CED-4 in which CED-4 associated with CED-9 as well as human Bcl-X_L (7, 10). It is unclear, however, if the interaction of Bcl-X_L with caspase-9 is direct or rather through endogenous Apaf-1 or another CED-4 homolog because caspase-9 and Apaf-1 can form a dimeric complex in mammalian cells (Fig. 1). Because Apaf-1 is expressed in 293T cells (Y.H. and G.N., unpublished observation), it is conceivable that Apaf-1 or another Apaf-1-like molecule could mediate the interaction of caspase-9 with Bcl-X_L.

Several models have been proposed to explain the apoptosis inhibitory effect of Bcl-2 family members. It has been hypothesized that these proteins exert their antiapoptotic function by preventing the release of cytochrome *c* from the mitochondria to the cytosol (29, 30). In support of this model, Bcl-X_L and Bcl-2, which reside in the outer mitochondria and other intracellular membranes, have been reported to prevent the release of cytochrome *c*, a molecule that binds to Apaf-1 and participates in the activation of caspase-9 (29–33). This mechanism could be mediated by the ability of Bcl-X_L to maintain the integrity of the mitochondria membrane through the formation of ion channels or other mechanisms (33). However, several observations are not consistent with the hypothesis that antiapoptotic Bcl-2 family members function primarily to regulate cytochrome *c* release. First, in some systems cytochrome *c* release into the cytosol is not induced by apoptotic stimuli known to be inhibited by Bcl-X_L (34). Second, Bcl-X_L inhibits apoptosis in cells that are resistant to apoptosis induced by microinjection of cytochrome *c*, suggesting that the ability of Bcl-X_L to inhibit cell death cannot be due solely to inhibition of cytochrome *c* release from mitochondria (35). Finally, both mutant Bcl-2 that targets to the endoplasmic reticulum, as well as the adenovirus Bcl-2-related E1B-19K protein that is largely excluded from mitochondria, can inhibit apoptosis (36, 37), suggesting that antiapoptotic Bcl-2 family members are active even if they do not reside in the mitochondria.

Our results suggest another model by which Bcl-X_L could inhibit apoptotic cell death. This mechanism involves binding of Bcl-X_L to Apaf-1 and caspase-9 and perhaps other death proteases such as caspase-4 and caspase-8. Recombinant Bcl-X_L purified from *E. coli* or insect cells can inhibit the activation of caspase-9 that is dependent on Apaf-1. These results suggest that like its nematode homolog CED-9, Bcl-X_L can regulate apoptosis by controlling the activation of caspase-9 through Apaf-1. Because recombinant Bcl-X_L inhibited the maturation of caspase-9 mediated by Apaf-1, these results indicate that Bcl-X_L can regulate caspase-9 activation independently of its association with intracellular membranes. In intact cells, the ability of Bcl-X_L to inhibit caspase-9 activation could be enhanced or further regulated by its insertion into intracellular membranes. Our observation that Bcl-X_L inhibited the interaction of Apaf-1 with caspase-9 suggests a mechanism by which Bcl-X_L could inhibit caspase-9 activation. This could be the result of direct competition between Bcl-X_L and caspase-9 for Apaf-1 and/or intracellular sequestration of Apaf-1 by Bcl-X_L. These results do not rule out additional mechanisms of Bcl-X_L function such as alteration of the interaction of Apaf-1 with cytochrome *c* and/or inhibition of conformational changes in the Apaf-1/caspase-9 complex by Bcl-X_L (20). Further studies are clearly needed to fully understand the role of Apaf-1 in caspase activation and its regulation by Bcl-2 family members.

The authors thank L. del Peso for providing recombinant Bad protein; S. Chen, L. Ding, and T. Hlaing for technical help; and L. del Peso, D. Ekhterae, M. Gonzalez-Garcia, and T. Koseki for critical review of the manuscript. We also thank Drs. E. Alnemri, C. Distelhorst, V. Dixit, and particularly X. Wang for generously supplying reagents. This work was supported by National Institutes of Health Grants CA64556 and CA64421 and a grant from the U.S. Army Medical Research and Material Command. Y.H. was supported by a Postdoctoral Immunopathology Training Grant T32A107413-03 from the National Institutes of Health. M.A.B. was supported by a predoctoral fellowship from the U.S. Army Medical Research and Material Command. G.N. was supported by a Research Career Development Award K04 CA64421-01 from the National Institutes of Health.

1. Thompson, C. B. (1995) *Science* **267**, 1456–1462.
2. White, E. (1996) *Genes Dev.* **10**, 1–15.
3. Hengartner, M. O. & Horvitz, H. R. (1994) *Curr. Opin. Genet. Dev.* **4**, 581–586.
4. Yuan, J., Shaham, S., Ledoux, S., Ellis, H. M. & Horvitz, H. R. (1993) *Cell* **75**, 641–652.
5. Hengartner, M. O., Ellis, R. E. & Horvitz, H. R. (1992) *Nature (London)* **356**, 494–499.
6. Shaham, S. & Horvitz, H. R. (1996) *Genes Dev.* **10**, 578–591.
7. Wu, D., Wallen, H. D. & Núñez, G. (1997) *Science* **275**, 1126–1129.
8. Chinnaiyan, A. M., O'Rourke, K., Lane, B. R. & Dixit, V. M. (1997) *Science* **275**, 1122–1126.
9. Spector, M. S., Desnoyers, S., Hoeppner, D. J. & Hengartner, M. O. (1997) *Nature (London)* **385**, 653–656.
10. Wu, D., Wallen, H. D., Inohara, N. & Núñez, G. (1997) *J. Biol. Chem.* **272**, 21449–21454.
11. Seshagiri, S. & Miller, L. K. (1997) *Curr. Biol.* **7**, 455–460.
12. Chinnaiyan, A. M., Chaudhary, D., O'Rourke, K., Koonin, E. V. & Dixit, V. M. (1997) *Nature (London)* **388**, 728–729.
13. Cohen, G. M. (1997) *Biochem J.* **326** (Pt. 1), 1–16.
14. Golstein P. (1997) *Science* **275**, 1081–1082.
15. Hengartner M. O. & Horvitz H. R. (1994) *Cell* **76**, 665–676.
16. Chinnaiyan, A., Orth, K., O'Rourke, K., Duan, H., Poirier, G. G. & Dixit, V. M. (1996) *J. Biol. Chem.* **27**, 4573–4576.
17. Armstrong, R. C., Aja, T., Xiang, J., Gaur, S., Krebs, J. F., Hoang, K., Bai, X., Korsmeyer, S. J., Karanewsky, D. S., Fritz, L. C. *et al.* (1996) *J. Biol. Chem.* **271**, 16850–16855.
18. Zou, H., Henzel, W. J., Liu, X., Lutschg, A. & Wang, X. (1997) *Cell* **90**, 405–413.
19. Hofmann, K., Bucher, P. & Tschopp, J. (1997) *Trends Biochem. Sci* **22**, 155–156.
20. Li, P., Nijhawanl, D., Budihardjol, I., Srinivasula, S., Ahmad, M., Alnemri, E. S. & Wang, X. (1997) *Cell* **91**, 479–489.
21. Boise, L. H., Gonzalez-Garcia, M., Postema, C. E., Ding, L., Lindsten, T., Turka, L. A., Mao, X., Núñez, G. & Thompson, C. B. (1993) *Cell* **74**, 597–608.
22. Inohara, N., Koseki, T., Hu, Y., Chen, S. & Núñez, G. (1997) *Proc. Natl. Acad. Sci. USA* **94**, 10717–10722.
23. Rubinfeld, B., Crosier, W. J., Albert, I., Conroy, L., Clark, R., McCormick, F. & Polakis, P. (1992) *Mol. Cell. Biol.* **12**, 4634–4642.
24. del Peso, L., Gonzalez-Garcia, M., Page, C., Herrera, R. & Núñez, G. (1997) *Science* **278**, 687–689.
25. Liu, X., Kim, C. N., Yang, J., Jemmerson, R. & Wang, X. (1996) *Cell* **86**, 147–157.
26. Duan, H. & Dixit, V. M. (1997) *Nature (London)* **385**, 86–89.

27. Boldin, M. P., Goncharov, T. M., Goltsev, Y. V. & Wallach, D. (1996) *Cell* **85**, 803–815.
28. Muzio, M., Chinnaiyan, A. M., Kischkel, F. C., O'Rourke, K., Shevchenko, A., Ni, J., Scaffidi, C., Bretz, J. D., Zhang, M., Gentz, R., *et al.* (1996) *Cell* **85**, 817–827.
29. Yang, J., Liu, X., Bhalla, K., Kim, C. N., Ibrado, A. M., Cai, J., Peng, T.-I., Jones, D. P. & Wang, X. (1997) *Science* **275**, 1129–1132.
30. Kluck, R. M., Bossy-Wetzel, E., Green, D. R. & Newmeyer, D. D. (1997) *Science* **275**, 1132–1136.
31. Kharbanda, S., Pandey, P., Schofield, L., Israels, S., Roncinske, R., Yoshida, K., Bharti, A., Yuan, Z. M., Saxena, S., Weichselbaum, R., *et al.* (1997) *Proc. Natl. Acad. Sci. USA* **94**, 6939–6942.
32. Kim, C. N., Wang, X., Huang, Y., Ibrado, A. M., Liu, L., Fang, G. & Bhalla, K. (1997) *Cancer Res.* **57**, 3115–3120.
33. Vander Heiden, M. G., Chandel, N. S., Williamson, E. K., Schumacker, P. T. & Thompson, C. B. (1997) *Cell* **91**, 627–637.
34. Chauhan, D., Pandey, P., Ogata, A., Teoh, G., Krett, N., Halgren, R., Rosen, S., Kufe, D., Kharbanda, S. & Anderson, K. (1997) *J. Biol. Chem.* **272**, 29995–29997.
35. Li, F, Srinivasan, A., Wang, Y., Armstrong, R. C., Tomaselli, K. J. & Fritz, L. C. (1997) *J. Biol. Chem.* **272**, 30299–30305.
36. Zhu, W., Cowie, A., Wasfy, G. W., Penn, L. Z., Leber, B. & Andrews, D. W. (1996) *EMBO J.* **15**, 4130–4141.
37. White, E. & Cipriani, R. (1989) *Proc. Natl. Acad Sci. USA* **86**, 9886–9890.

The EMBO Journal Vol.18 No.13 pp.3586–3595, 1999

Role of cytochrome *c* and dATP/ATP hydrolysis in Apaf-1-mediated caspase-9 activation and apoptosis

Yuanming Hu, Mary A.Benedict, Liyun Ding and Gabriel Núñez[1]

Department of Pathology and Comprehensive Cancer Center, University of Michigan Medical School, 1500 East Medical Center Drive, 4219 CCGC, Ann Arbor, MI 48109, USA

[1]Corresponding author
e-mail: gabriel.nunez@umich.edu

Apaf-1 plays a critical role in apoptosis by binding to and activating procaspase-9. We have identified a novel Apaf-1 cDNA encoding a protein of 1248 amino acids containing an insertion of 11 residues between the CARD and ATPase domains, and another 43 amino acid insertion creating an additional WD-40 repeat. The product of this Apaf-1 cDNA activated procaspase-9 in a cytochrome *c* and dATP/ATP-dependent manner. We used this Apaf-1 to show that Apaf-1 requires dATP/ATP hydrolysis to interact with cytochrome *c*, self-associate and bind to procaspase-9. A P-loop mutant (Apaf-1K160R) was unable to associate with Apaf-1 or bind to procaspase-9. Mutation of Met368 to Leu enabled Apaf-1 to self-associate and bind procaspase-9 independent of cytochrome *c*, though still requiring dATP/ATP for these activities. The Apaf-1M368L mutant exhibited greater ability to induce apoptosis compared with the wild-type Apaf-1. We also show that procaspase-9 can recruit procaspase-3 to the Apaf-1–procaspase-9 complex. Apaf-1(1–570), a mutant lacking the WD-40 repeats, associated with and activated procaspase-9, but failed to recruit procaspase-3 and induce apoptosis. These results suggest that the WD-40 repeats may be involved in procaspase-9-mediated procaspase-3 recruitment. These studies elucidate biochemical steps required for Apaf-1 to activate procaspase-9 and induce apoptosis.
Keywords: Apaf-1/apoptosis/caspase-3/caspase-9

Introduction

Programmed cell death, or apoptosis, an evolutionarily conserved and genetically regulated biological process, plays a critical role in the development and the regulation of tissue homeostasis of multicellular organisms (Thompson, 1995; Yuan, 1996). Genetic analyses of the nematode *Caenorhabditis elegans* have identified two genes, *ced-3* and *ced-4*, required for the execution of cell death in the worm (Hengartner and Horvitz, 1994). The product of *ced-3* is homologous to mammalian interleukin-1β-converting enzyme, a finding that provided the first indication that cysteine proteases are critical components of the cell death machinery (Miura *et al.*, 1993). These observations led to the identification of a growing family of cysteine proteases (designated as caspases) related to CED-3 that represent the executionary arm of the apoptotic program in mammals, flies and nematodes (Núñez *et al.*, 1998; Thornberry and Labzenik, 1998). Caspases are synthesized in cells as inactive precursors which upon stimulation with apoptotic signals are processed into mature forms composed of a tetramer of two large and two small subunits (Thornberry *et al.*, 1992; Walker *et al.*, 1994; Rotonda *et al.*, 1996). The apoptotic process is characterized by the proteolytic cascade in which upstream (initiator) caspases mediate the activation of downstrean (effector) caspases (Alnemri, 1997; Núñez *et al.*, 1998). Initiator caspases contain death effector domains (DEDs) or caspase recruitment domains (CARDs) that physically link these proteases to regulatory molecules via homophilic interactions (Li *et al.*, 1997; Pan *et al.*, 1998). Caspase-9 is an upstream caspase that contains a CARD in its N-terminus; a protein module that is also present in the prodomain of several death proteases, including CED-3 and its regulator CED-4 (Hofmann *et al.*, 1997). Activation of caspase-9 initiates a protease cascade that subsequently activates downstream caspase-3 and caspase-7, leading to the cleavage of target proteins and the orderly demise of the cell (Li *et al.*, 1997; Sun *et al.*, 1999).

Our understanding of how caspases are activated in mammalian cells has been greatly enhanced by biochemical studies of the nematode proteins CED-3, CED-4 and CED-9. CED-4 physically interacts with both CED-3 and CED-9, forming a multimeric protein complex (Chinnaiyan *et al.*, 1997; Irmler *et al.*, 1997; James *et al.*, 1997; Spector *et al.*, 1997; Wu *et al.*, 1997a,b). CED-4 promotes the activation of CED-3 and this activation process is inhibited by CED-9 (Seshagiri and Miller, 1997; Wu *et al.*, 1997b). Biochemical experiments have suggested that a mechanism exists whereby CED-3 is activated through oligomerization of CED-4 (Yang *et al.*, 1998). Activation of CED-3 is induced through aggregation of precursor CED-3 molecules, an event leading to CED-3 autoprocessing and enzymatic activation (Yang *et al.*, 1998).

Apaf-1, a mammalian homologue of CED-4, has been identified recently (Zou *et al.*, 1997; Fearnhead *et al.*, 1998). The N-terminal half of Apaf-1 shares extensive homology with CED-4, containing a CARD followed by an ATPase domain with conserved Walker's A and B motifs (Zou *et al.*, 1997). The C-terminal region of Apaf-1 lacks homology with CED-4 and consists of 12 WD-40 repeats. An important role for Apaf-1 in the regulation of apoptosis has been revealed by analysis of mutant mice deficient in Apaf-1. Mice lacking Apaf-1 showed abnormalities in several tissues characterized by the lack of developmental cell death, particularly in brain tissue (Cecconi *et al.*, 1998; Yoshida *et al.*, 1998). Furthermore, cells derived from Apaf-1-deficient mice showed resist-

ance to a wide variety of apoptotic stimuli, including chemotherapy drugs, dexamethasone and γ-irradiation (Yoshida *et al.*, 1998). In the presence of cytochrome *c* and dATP, Apaf-1 adopts a conformation that can bind to procaspase-9, an event that leads to its proteolytic activation (Li *et al.*, 1997). A conserved mechanism similar to that proposed for CED-3 has been suggested for caspase-9 activation (Hu *et al.*, 1998b; Srinivasula *et al.*, 1998). In this model, two or more caspase-9 precursors are brought together via Apaf-1 oligomerization, which is mediated by the ATPase-like domain of Apaf-1 (Hu *et al.*, 1998b; Srinivasula *et al.*, 1998). Mutant analyses of Apaf-1 have suggested that the WD-40 repeat region (WDR) plays an inhibitory role in Apaf-1 function, since mutants lacking the WDR are constitutively active (Hu *et al.*, 1998a,b; Srinivasula *et al.*, 1998). Furthermore, the WDR has been shown to interact with the ATPase-like domain of Apaf-1, inhibiting Apaf-1 self-association. This finding suggests the existence of a mechanism whereby the WDR inhibits Apaf-1 activity (Hu *et al.*, 1998b).

In these studies, we sought to understand further the biochemical mechanism by which Apaf-1 promotes the maturation of procaspase-9 into an active protease. Analysis of wild-type (wt) and mutant Apaf-1 proteins revealed that dATP/ATP hydrolysis is required for cytochrome *c* binding to Apaf-1, Apaf-1 self-association, interaction of Apaf-1 with procaspase-9, and ultimately for caspase-9 activation and caspase-9-mediated apoptosis. We also provide evidence that the Apaf-1–caspase-9 complex recruits procaspase-3, a process that may be regulated by the WDR of Apaf-1.

Results

Identification of Apaf-1XL, an alternatively spliced Apaf-1 cDNA that activates procaspase-9

In our initial studies of Apaf-1-mediated caspase-9 activation, we determined that procaspase-9 could be efficiently activated by endogenous Apaf-1 from several cell lines including HeLa and 293T cells (Hu *et al.*, 1998a; data not shown). We subsequently identified Apaf-1 cDNAs from these two cell lines. An Apaf-1 cDNA cloned from HeLa cells was identical to that previously reported (Zou *et al.*, 1997). However, the Apaf-1 cDNA cloned from 293T cells appeared to represent an alternatively spliced form of the Apaf-1 gene. This form, termed Apaf-1XL, contains an 11 amino acid (aa) insertion, GKDSVSGITSY, after the CARD (inserted between amino acids 98 and 99), and another 43 aa insertion between amino acids 811 and 812 (Figure 1A). This 43 aa region contains the last three amino acids of a WD-40 repeat followed by a large portion of another WD-40 repeat, thus creating an additional WD-40 repeat (Figure 1A). The sequence of these extra 43 aa is identical to that present in a truncated human Apaf-1 cDNA submitted to databases (DDBJ/EMBL/GenBank accession No. AB007873). Moreover, a mouse Apaf-1 cDNA isolated from brain tissue also contained this additional WD-40 repeat (Cecconi *et al.*, 1998). In addition, a recent study has identified an Apaf-1 form in HeLa cells that is identical to Apaf-1XL (Zou *et al.*, 1999). Using reverse transcriptase (RT)–PCR and Western blotting analysis, we have identified both Apaf-1XL mRNA and protein in 16 cell lines tested so far (data not shown). Under our experimental conditions, Apaf-1XL protein expressed in 293T cells activated procaspase-9 in a cytochrome *c*- and dATP-dependent manner (Figure 1D). Under the same conditions, we were unable to demonstrate cytochrome *c*- and dATP-dependent procaspase-9 activation by the product of the original Apaf-1 cDNA (data not shown). Therefore, in the present studies we used the Apaf-1XL cDNA to examine the mechanism by which Apaf-1 activates procaspase-9 and refer to it as Apaf-1 for simplicity.

Mutation of Met368 to Leu enables full-length Apaf-1 to activate procaspase-9 independently of cytochrome c and dATP

We demonstrated previously that the WDR interacts with the N-terminal CED-4 homologous region of Apaf-1 and inhibits procaspase-9 activation when co-expressed with the constitutively active N-terminal Apaf-1 mutants (Hu *et al.*, 1998b). We performed experiments to determine whether the WDR with an extra WD-40 repeat is also capable of binding to N-terminal Apaf-1 with an 11 aa insertion [Apaf-1(1–570)] and inhibiting procaspase-9 activation. The analyses showed that the WDR containing the extra WD-40 repeat associated with Apaf-1(1–570) (Figure 1B) and inhibited procaspase-9 activation promoted by Apaf-1(1–570) (Figure 1C). To understand further how Apaf-1 promotes procaspase-9 activation, we tested several Apaf-1 N-terminal mutants accumulated during PCR mutagenesis for their ability to interact with the WDR. A mutant substituting amino acid Met368 for Leu, Apaf-1(1–570M368L), showed a reduced ability to bind the WDR (Figure 1B), but it retained its ability to promote procaspase-9 activation independent of cytochrome *c* and dATP (Figure 1C). In contrast to Apaf-1(1–570), however, the ability of Apaf-1(1–570M368L) to induce procaspase-9 activation was not inhibited by the WDR (Figure 1C). We next incorporated the M368L point mutation into full-length Apaf-1 and determined the ability of wt and mutant Apaf-1 to activate procaspase-9. In these experiments, we prepared cell extracts from 293T cells transiently transfected with Apaf-1 constructs and diluted the extracts so that endogenous Apaf-1 activity could not be detected in the procaspase-9 activation assay. Full-length Apaf-1 induced activation of procaspase-9 in a dATP- and cytochrome *c*-dependent manner (Figure 1D). In contrast, the point mutant Apaf-1M368L activated procaspase-9 independent of cytochrome *c* and dATP (Figure 1D). Apaf-1K160R, a mutant substituting Lys160 [an essential amino acid residue in the phosphate-binding loop (P-loop)] for Arg, failed to activate procaspase-9 in the presence or absence of dATP and cytochrome *c* (Figure 1D). This result confirmed previous observations that dATP/ATP hydrolysis is required for Apaf-1 to induce procaspase-9 activation (Li *et al.*, 1997).

The cytochrome c–Apaf-1 interaction requires ATP hydrolysis

To determine the role for cytochrome *c* in procaspase-9 activation, we immunoprecipitated wt and mutant Apaf-1 from cytosolic extracts in the presence or absence of dATP and assessed the binding of cytochrome *c* to Apaf-1 proteins by immunoblotting. Cytochrome *c* bound to

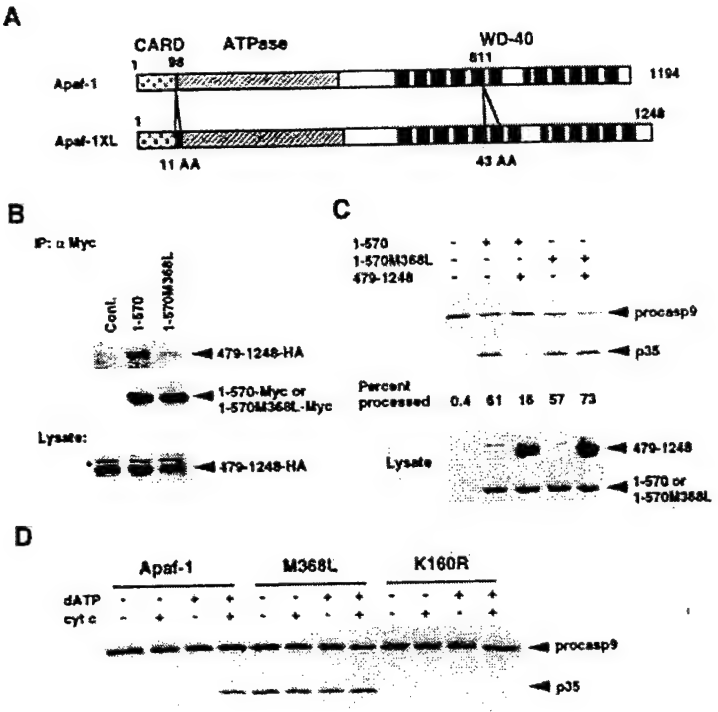

Fig. 1. Mutation of Met368 to Leu renders Apaf-1 capable of activating procaspase-9 independent of cytochrome *c* and dATP. (A) Schematic representation of the original Apaf-1 and Apaf-1XL. The 11 amino acids inserted after aa 98 are GKDSVSGITSY. The sequence of the extra 43 aa was identical to that identified in an Apaf-1 cDNA that is deposited in the DDBJ/EMBL/GenBank database (accession No. AB007873). (B) Mutation of Met368 to Leu decreases binding of Apaf-1(1–570) to WDR (WD-40 repeat region). pcDNA3 or plasmids encoding Myc-tagged Apaf-1(1–570) or Apaf-1(1–570M368L) were transfected into 293T cells with a construct producing HA-tagged WDR (aa 479–1248). Total cell lysates were immunoprecipitated with rabbit anti-c-Myc antibody and immune complexes were immunoblotted with anti-HA to detect the WDR. The asterisk indicates a non-specific band. (C) WDR fails to inhibit Apaf-1(1–570M368L)-mediated procaspase-9 activation. Twenty micrograms of cytosolic extracts containing indicated Apaf-1 mutants were incubated with *in vitro* translated [^{35}S]methionine-labeled procaspase-9 at 30°C for 30 min and separated by SDS–PAGE. Immature and cleaved caspase-9 fragments were scanned and quantitated with a phosphoimager and normalized according to the numbers of methionine residues in each form. Percentage of procaspase-9 converted into p35 is shown below each lane. Lower panel shows equal amounts of Apaf-1 mutant proteins in extracts. (D) Mutation of Met368 to Leu renders full-length Apaf-1 capable of activating procaspase-9 independent of cytochrome *c* and dATP. Two micrograms of extracts containing Apaf-1, Apaf-1M368L, or Apaf-1K160R were incubated with or without 1 mM dATP and 0.2 μg of cytochrome *c* at 30°C for 30 min.

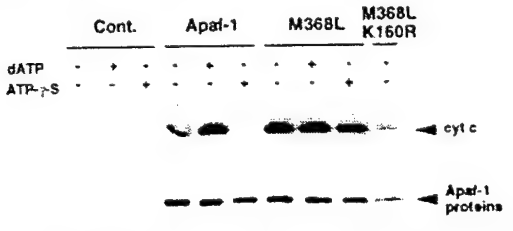

Fig. 2. Binding of cytochrome *c* to Apaf-1 requires dATP hydrolysis. Cytosolic extracts containing Myc-tagged Apaf-1, Apaf-1M368L or Apaf-1M368L/K160R were incubated with 10 μg/ml cytochrome *c* with or without 1 mM dATP or ATP-γS in the presence of monoclonal anti-Myc and protein A/G–agarose beads. After incubation at 4°C for 2 h, immunoprecipitation was performed as described in Materials and methods and cytochrome *c* associated with Apaf-1 proteins detected by immunoblotting. Wt and mutant Apaf-1 proteins precipitated from cytosolic extracts are shown in the lower panel.

Apaf-1, and this binding was greatly enhanced by the presence of dATP in the extract. Incubation of the extracts with the non-hydrolyzable ATP-γS completely abolished cytochrome *c* binding to wt Apaf-1, indicating that dATP/ATP hydrolysis is essential for Apaf-1 to interact with cytochrome *c* (Figure 2). The weak binding of cytochrome *c* to Apaf-1 detected in the absence of dATP is presumably due to low levels of endogenous dATP/ATP in the cell extract. In contrast, cytochrome *c* interacted with Apaf-1M368L in the presence or absence of dATP (Figure 2). Addition of ATP-γS failed to inhibit cytochrome *c* binding to mutant Apaf-1M368L (Figure 2). Mutation of Lys160 (the critical P-loop residue required for ATP binding/hydrolysis) to Arg did not abolish the binding of Apaf-1M368L to cytochrome *c* (Figure 2), providing further evidence that cytochrome *c* can bind to Apaf-1M368L independent of dATP binding and hydrolysis. The diminished binding of cytochrome *c* to the double mutant Apaf-1M368L/K160R, when compared with wt Apaf-1 or Apaf-1M368L, could be explained by reduced expression of the double mutant Apaf-1 protein in the extract (Figure 2).

Apaf-1 self-association requires dATP/ATP hydrolysis

It was previously reported that Apaf-1 requires dATP/ATP to activate procaspase-9 (Li *et al.*, 1997). dATP/ATP hydrolysis could be required for Apaf-1 self-association and/or the Apaf-1–procaspase-9 interaction, since a disrup-

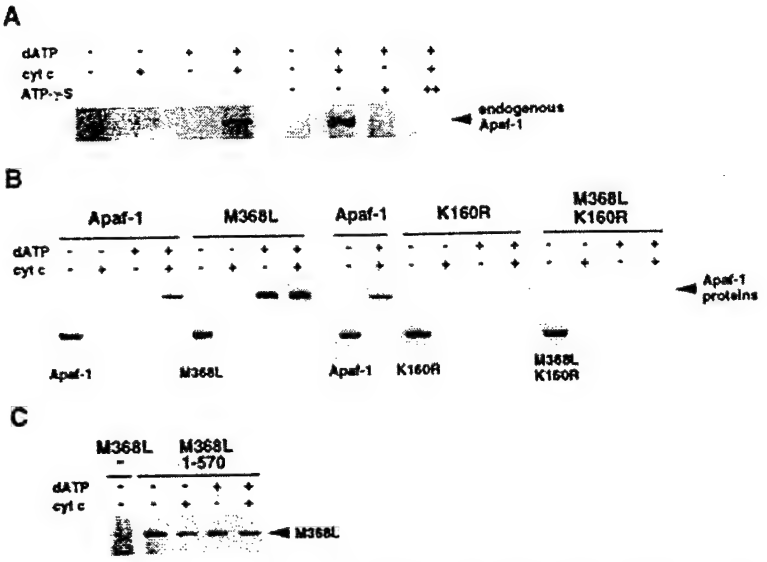

Fig. 3. Apaf-1 self-association requires cytochrome *c* and dATP hydrolysis. (**A**) Endogenous Apaf-1 binds Apaf-1(1–570) in the presence of cytochrome *c* and dATP. Equal amounts of 293T cytosolic extracts containing Myc-tagged Apaf-1(1–570) were incubated with rabbit anti-Myc antibody and protein A/G–agarose beads (1:1) under the indicated conditions at 4°C for 2 h. Then the beads were pelleted and washed four times with 1 ml NP-40 buffer. '++' indicates that 5 mM ATP-γS was included in the extract. (**B**) Interaction of wt Apaf-1, Apaf-1M368L, Apaf-1K160R, or Apaf-1M368L/K160R with Apaf-1(1–570). The experiments were performed as in (A) except that Apaf-1(1–570)-FLAG-containing extracts were mixed with lysates containing Apaf-1, Apaf-1M368L, Apaf-1K160R, or Apaf-1M368L/K160R. Expression of wt and mutant Apaf-1 proteins in total lysates is shown in lower panels. (**C**) Apaf-1M368L can associate with Apaf-1(1–570) independent of cytochrome *c* and dATP. Constructs producing Apaf-1(1–570) and Apaf-1M368L were cotransfected into 293T cells and prepared total lysates were used for immunoprecipitation as described in (A).

tion of either step might be sufficient to inhibit procaspase-9 activation (Hu *et al.*, 1998b; Srinivasula *et al.*, 1998). We first determined whether dATP/ATP hydrolysis is required for Apaf-1 self-association in cytosolic extracts. We transiently transfected 293T cells with a Myc-tagged Apaf-1(1–570) construct and assessed its interaction with endogenous Apaf-1 in the absence of detergent. Immunoprecipitation experiments showed that endogenous Apaf-1 associated with Apaf-1(1–570) in the presence of cytochrome *c* and dATP, but not in the absence of these factors (Figure 3A). The non-hydrolyzable ATP analogue, ATP-γS, failed to substitute for dATP (Figure 3A), indicating that ATP hydrolysis rather than simple ATP binding is required for Apaf-1 to self-associate. We next prepared extracts from cells transfected with wt and mutant Apaf-1 constructs to analyze further the requirement of dATP and/or cytochrome *c* for Apaf-1 self-association. Immunoprecipitation analysis showed that Apaf-1 self-association required both cytochrome *c* and dATP (Figure 3B), in agreement with the results obtained with endogenous Apaf-1. The constitutively active Apaf-1M368L mutant associated with Apaf-1 in the absence of cytochrome *c*, but required dATP for association with Apaf-1(1–570) (Figure 3B). Mutation of the critical P-loop Lys160 to Arg (M368L/K160R) abolished the ability of Apaf-1M368L to associate with Apaf-1 (Figure 3B). When co-expressed with Apaf-1(1–570), Apaf-1M368L interacted with Apaf-1(1–570) without the addition of exogenous dATP (Figure 3C), suggesting that intracellular dATP/ATP can promote their association.

Procaspase-9 binding to Apaf-1 requires dATP/ATP hydrolysis

To examine the role of dATP/ATP hydrolysis in procaspase-9 binding, we first determined whether dATP/ATP binding/hydrolysis is required for endogenous Apaf-1 to bind procaspase-9 in cytosolic extracts. We began by transiently transfecting 293T cells with hemagglutinin (HA)-tagged procaspase-9 (C287S) and assessing the interaction of procaspase-9 with endogenous Apaf-1 in the absence of detergent. Immunoprecipitation of procaspase-9 showed that endogenous Apaf-1 binds to procaspase-9 in the presence of cytochrome *c* and dATP, but not in the absence of these factors (Figure 4A). In addition, the non-hydrolyzable ATP analogue, ATP-γS, inhibited procaspase-9 binding to endogenous Apaf-1 (Figure 4A), indicating that ATP hydrolysis is required for Apaf-1 to bind procaspase-9. We next performed immunoprecipitations with cytosolic extracts from cells transfected with wt and mutant Apaf-1 constructs to further dissect the requirement of dATP and/or cytochrome *c* for the binding of procaspase-9 to Apaf-1. To avoid the formation of Apaf-1 protein complexes in living cells, we prepared cellular extracts expressing wt or mutant Apaf-1 and incubated them with separately prepared extracts containing procaspase-9 (C287S). As we showed with endogenous Apaf-1, exogenous Apaf-1 required both cytochrome *c* and dATP to interact with procaspase-9 (Figure 4B). Mutation of Lys160 to Arg abolished procaspase-9 binding to Apaf-1, confirming that dATP/ATP hydrolysis is needed for the Apaf-1–procaspase-9 interaction. The constitutively active Apaf-1M368L mutant interacted with procaspase-9 in the absence of dATP and cytochrome *c* (Figure 4B), which is consistent with the observation that this mutant does not require these factors for activation of procaspase-9. Furthermore, in contrast to endogenous Apaf-1, incubation with ATP-γS did not inhibit the binding of mutant Apaf-1M368L to procaspase-9 (data not shown). Surprisingly, mutation of

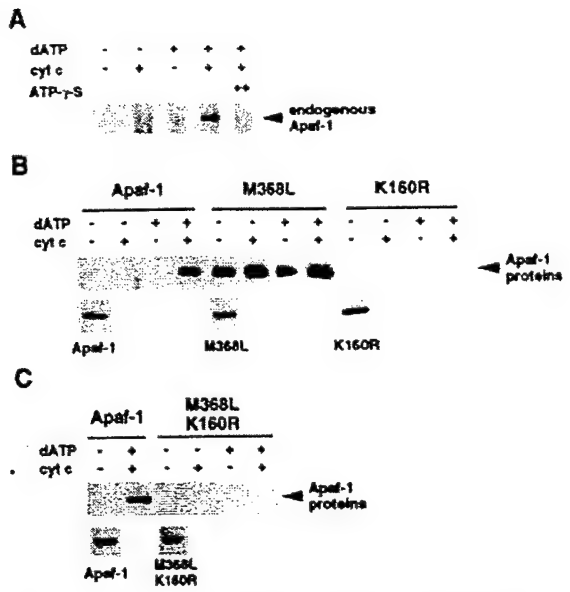

Fig. 4. Cytochrome *c* and ATP hydrolysis are required for Apaf-1 to interact with procaspase-9. (A) Procaspase-9 interacts with endogenous Apaf-1 in a cytochrome *c* and dATP-dependent manner. Equal amounts of 293T cytosolic extracts containing procaspase-9 (C287S)-HA were incubated with rabbit anti-HA antibody and protein A/G–agarose beads (1:1) under the indicated conditions at 4°C for 2 h. Then the beads were pelleted and washed four times with 1 ml NP-40 buffer. '++' indicates that 5 mM ATP-γS was included in the extract. (B) Procaspase-9 interacts with Apaf-1M368L in the absence of cytochrome *c* and dATP. The experiments were performed as in (A) except that procaspase-9(C287S)-HA-containing extracts were mixed with lysates containing Apaf-1, Apaf-1M368L or Apaf-1K160R. (C) A double-point mutant, Apaf-1M368L/K160R fails to interact with procaspase-9. Expression of wt and mutant Apaf-1 proteins in total lysates is shown in the lower panels in (B) and (C).

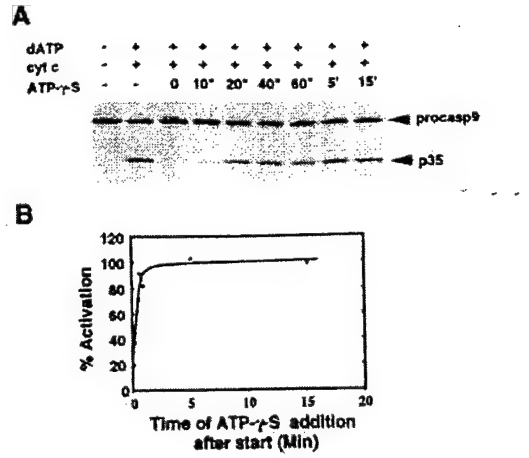

Fig. 5. dATP hydrolysis is only required for a short time in Apaf-1-mediated procaspase-9 activation. Two micrograms of Apaf-1-containing extract was mixed with 1 μl [^{35}S]methionine-labeled procaspase-9 on ice in the presence of 0.1 mM dATP and 0.2 μg of cytochrome *c*. One millimolar ATP-γS was added to the reaction mixture at different time intervals after the tubes containing reaction mixtures were transferred into 30°C waterbath. The reaction was incubated for a total of 30 min at 30°C. (A) Procaspase-9 activation profile in the presence of ATP-γS when added at different times after the beginning of the reactions. (B) Time course of inhibition of procaspase-9 processing by ATP-γS. The amount of unprocessed and processed caspase-9 (p35) forms were scanned and quantitated using a phosphoimager. First, the amount of p35 processed forms was normalized to full-length procaspase-9 and added to the corresponding unprocessed procaspase-9 to obtain the total amount of procaspase-9 used in each lane. Then, p35 bands were normalized relative to total procaspase-9 in each lane. Finally, normalized p35 fragments were divided by the p35 fragment without ATP-γS (positive control).

Lys160 to Arg abolished the ability of Apaf-1M368L to interact with procaspase-9 (Figure 4C), suggesting that dATP/ATP binding/hydrolysis is indeed required for this point mutant to associate with procaspase-9. These apparently conflicting data for the dATP/ATP requirement are probably explained by the pre-formation of Apaf-1M368L oligomeric complex within the cell after exposure to endogenous dATP/ATP.

ATP hydrolysis is only required for a brief period of time for Apaf-1 to activate procaspase-9

Next we performed experiments to determine whether dATP/ATP hydrolysis is continuously required for Apaf-1-mediated activation of procaspase-9. To do this, we added the non-hydrolyzable ATP analog, ATP-γS, to the procaspase-9 activation assay at various times, incubating the reaction for a total of 30 min. As depicted in Figure 5, procaspase-9 activation was greatly inhibited by ATP-γS when added at the beginning of the reaction. ATP-γS inhibited procaspase-9 activation by ~70% when added after 10 s and by ~30% after 20 s (Figure 5). ATP-γS minimally inhibited or could no longer inhibit procaspase-9 activation when it was added after 40 s (Figures 5). These experiments suggest that dATP/ATP hydrolysis is required for a brief period of time to activate procaspase-9.

Apaf-1M368L exhibits enhanced ability to induce apoptosis

The experiments shown in Figure 1D indicate that the Apaf-1M368L mutant can activate procaspase-9 independently of cytochrome *c*. To determine the significance of these findings for induction of apoptosis, we transiently transfected wt and mutant Apaf-1 constructs into 293T cells and assessed their ability to induce apoptosis 19 h after transfection. Wt Apaf-1 failed to induce cell death at low concentrations, but induced low-level apoptosis at higher concentrations of plasmid DNA (Figure 6). In contrast, Apaf-1M368L induced significant apoptosis even at low levels of plasmid DNA and exhibited greater proapoptotic activity than wt Apaf-1 at higher levels of plasmid (Figure 6B). The P-loop mutant of Apaf-1 (K160R) deficient in Apaf-1 self-association and procaspase-9 binding failed to induce apoptosis at all concentrations of plasmid tested (Figure 6B). Apaf-1M368L-induced apoptosis was effectively inhibited by a catalytically inactive caspase-9 mutant (C287S) that acts as a dominant-negative inhibitor (Figure 6B) (Li *et al.*, 1997; Pan *et al.*, 1998), indicating that apoptosis induced by Apaf-1M368L is caspase-9 dependent. Significantly, the Apaf-1 double mutant, M368L/K160R, did not induce apoptosis consistent with a requirement of dATP/ATP hydrolysis for Apaf-1M168L to self-associate and binding to procaspase-9 (Figure 6C).

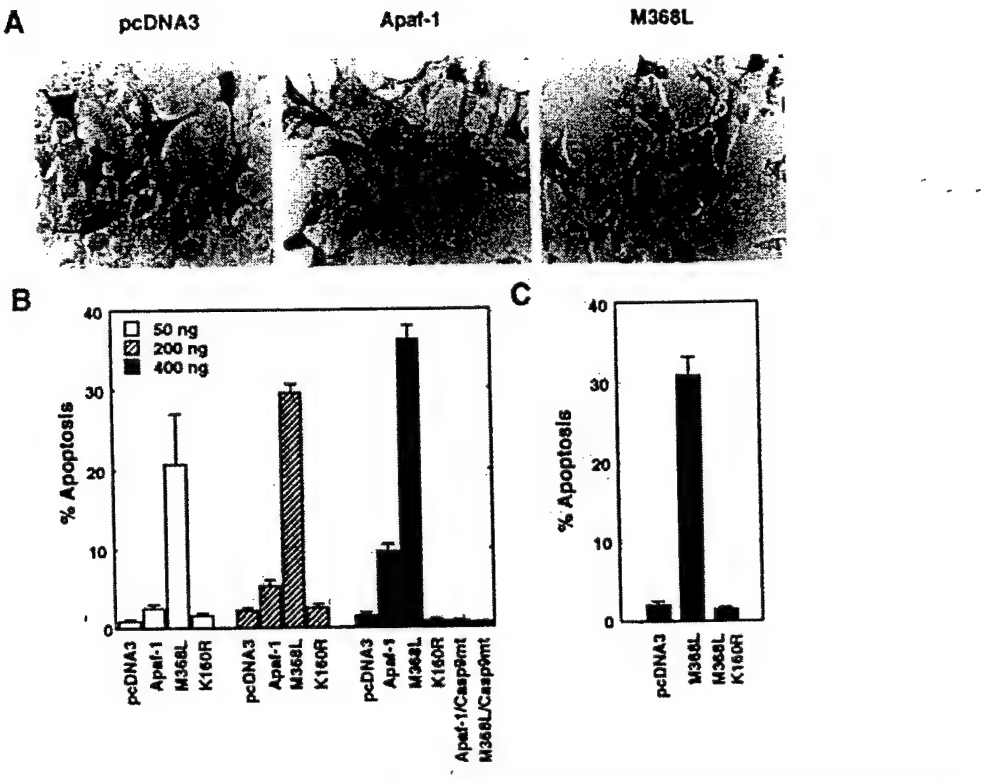

Fig. 6. Induction of apoptosis by wt and Apaf-1 mutants. (A) Representative field of 293T cells transfected with 400 ng of indicated control and Apaf-1 constructs and stained for β-galactosidase activity. Darker cells represent transfected and β-galactosidase-positive cells. The arrowheads indicate round-up apoptotic cells with membrane blebbing. (B) Apaf-1M368L induces apoptosis in 293T cells. 293T cells were transiently transfected with a reporter pcDNA3-galactosidase plus the indicated plasmids. The results represent the percentage of blue cells that exhibit morphological features of apoptosis and are given as the mean ±SD of triplicate cultures. Casp9mt represents a catalytically inactive mutant of procaspase-9 (C287S). (C) Apaf-1M368L/K160R failed to induce apoptosis. Four-hundred nanograms of indicated plasmids were used to transiently transfect 293T cells as in (B).

Apaf-1(1–570) fails to induce apoptosis and activate procaspase-3

Like the Apaf-1M368L mutant, Apaf-1 mutants lacking the WDR can activate procaspase-9 independent of cytochrome *c* and dATP (Figure 1C) (Hu *et al.*, 1998a,b; Srinivasula *et al.*, 1998). Therefore, we compared the ability of Apaf-1M368L and Apaf-1(1–570) to induce apoptosis. Significantly, Apaf-1(1–570) did not kill 293T cells while Apaf-1M368L induced significant apoptosis in transfected cells (Figure 7A). Immunoblotting analysis with anti-caspase-9 antibody showed that both Apaf-1M368L and Apaf-1(1–570) induced processing of endogenous procaspase-9 into its signature p35 fragment (Figure 7B, upper panel), indicating that the differential activity of these Apaf-1 mutants cannot be explained by lack of procaspase-9 activation. To assess the activation of procaspase-3, a downstream caspase activated by caspase-9, we immunoblotted the same extracts with anti-caspase-3 antibody. Expression of Apaf-1M368L induced processing of procaspase-3, as determined by the appearance of the p18 subunit and reduction of procaspase-3 levels (Figure 7B, lower panel, reduced levels of procaspase-3 could be observed in a shorter exposure; data not shown). Significantly, procaspase-3 from cells transfected with Apaf-1(1–570) remained unprocessed even though procaspase-9 was cleaved (Figure 7B). Thus, the differential proapoptotic activity exhibited by the constitutively active Apaf-1 mutants, Apaf-1(1–570) and Apaf-1M368L, might be explained by the differential processing of procaspase-3. To gain more insight into this mechanism, we further assessed the activation of procaspase-3 and procaspase-9 in cytosolic extracts prepared from Apaf-1M368L and Apaf-1(1–570)-transfected cells. In Apaf-1M368L extracts, procaspase-9 could be effectively processed into the signature p35 proteolytic fragment resulting from autoactivation of procaspase-9 and p37, a fragment resulting from cleavage of procaspase-9 by active caspase-3 (Figure 7C, upper panel) (Srinivasula *et al.*, 1998). In contrast, procaspase-9 was only cleaved into p35 but not p37 in the Apaf-1(1–570) extract (Figure 7C), providing additional evidence that caspase-3 was not activated in extracts expressing Apaf-1(1–570). To verify this result, we assessed the processing of procaspase-3 in the same extracts. The analysis confirmed that Apaf-1M368L but not Apaf-1(1–570) promoted procaspase-3 activation (Figure 7C, lower panel).

Apaf-1M368L but not Apaf-1(1–570) can recruit procaspase-3 to the Apaf-1–procaspase-9 complex through procaspase-9

Next we wanted to determine the mechanism by which procaspase-3 is activated in extracts from Apaf-1M368L

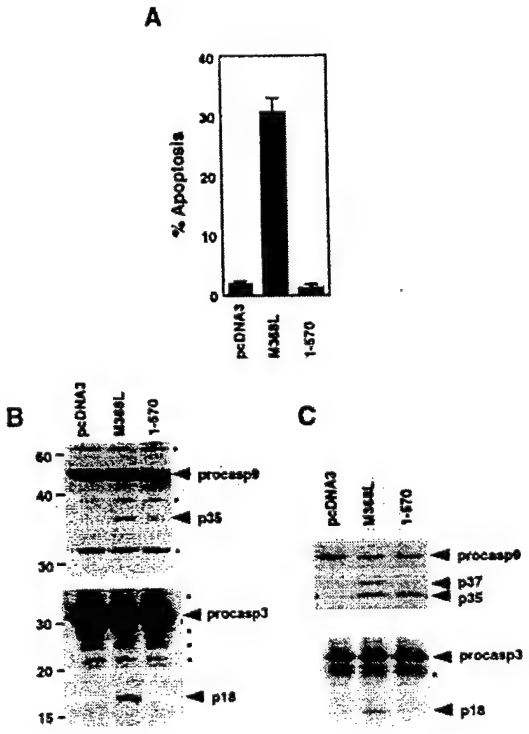

Fig. 7. Apaf-1(1–570) fails to induce apoptosis and activate procaspase-3. (A) Apaf-1(1–570) is unable to induce apoptosis of 293T cells. 293T cells were transiently transfected with a reporter pcDNA3-galactosidase plus 0.4 μg of the indicated plasmids. The results represent the percentage of blue cells that exhibit morphological features of apoptosis and are given as the mean ±SD of triplicate cultures. (B) Procaspase-9 but not procaspase-3 is processed in Apaf-1(1–570)-transfected 293T cells. Total cell lysates from 293T cells as indicated in (A) were separated on SDS–PAGE gel and immunoblotted for caspase-9 (upper panel) and caspase-3 (lower panel). Molecular weight markers are indicated on the left of each blot. (C) Both Apaf-1M368L and Apaf-1(1–570) can activate procaspase-9 but only Apaf-1M368L is able to activate procaspase-3. Forty micrograms of cytosolic extracts containing Apaf-1M368L or Apaf-1(1–570) were incubated with [^{35}S]methionine-labeled procaspase-9 (upper panel) or procaspase-3 (lower panel) in the absence of cytochrome *c* and dATP at 30°C for 30 min. Arrows indicate immature and processed forms of caspase-9 (upper panel) and caspase-3 (lower panel). p35 and p18 represent processed forms of procaspase-9 and -3 respectively. Asterisks indicate non-specific bands.

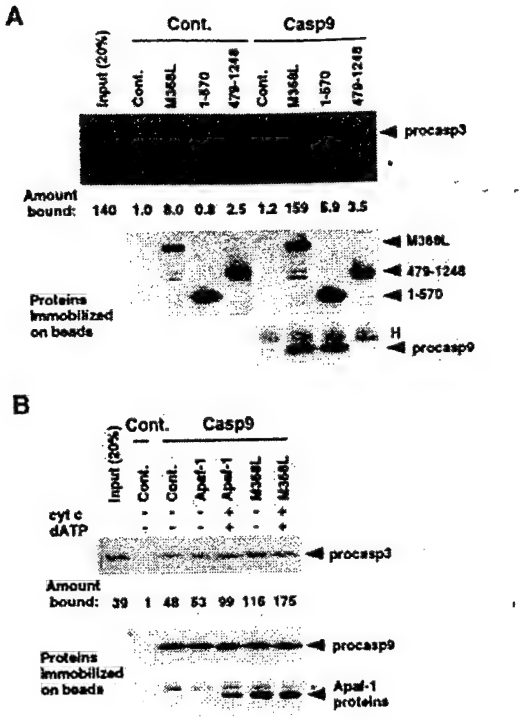

Fig. 8. Procaspase-3 is recruited into the Apaf-1–caspase-9 complex but not into the Apaf-1(1–570)–caspase-9 complex. (A) Procaspase-3 is recruited into Apaf-1M368L–caspase-9 complex. Apaf-1 proteins were immobilized on agarose beads and packed into gel filtration columns as described in Materials and methods. *In vitro*-translated [^{35}S]methionine-labeled procaspase-3 was loaded onto the beads. After extensive washing proteins bound to the beads were eluted, separated by SDS–PAGE and transferred to nitrocellulose membrane. (B) Procaspase-3 binds to procaspase-9 directly. Experiments were performed as in (A) except procaspase-9 (C287S) was immobilized on agarose beads. Procaspase-3 bound was detected by autoradiography and Apaf-1 proteins and procaspase-9 (C287S) were detected by immunoblotting. The upper panels show an autoradiograph of procaspase-3 bound and amounts of bound procaspase-3 as quantitated with a phosphoimager (procaspase-3 bound to control beads was arbitrarily designated as 1). Apaf-1 proteins and procaspase-9 (C287S) bound to beads were shown in lower two panels. Asterisks indicate non-specific bands. H, immunoglobulin heavy chain; Cont., control lysates transfected with pcDNA3.

transfected cells but not from those expressing Apaf-1(1–570). One possibility we considered is that procaspase-3 could be recruited to the Apaf-1M368L–procaspase-9 complex but not to the Apaf-1(1–570)–procaspase-9 complex. To examine this, we immobilized various Apaf-1 mutants on agarose beads in the presence or absence of procaspase-9 and incubated the immobilized Apaf-1 or Apaf-1–procaspase-9 complexes with *in vitro* translated procaspase-3. In the absence of procaspase-9 (C2827S), procaspase-3 interacted weakly with Apaf-1M368L, while procaspase-3 did not associate with Apaf-1(1–570) or Apaf-1(479–1248) (Figure 8A). The presence of procaspase-9 greatly enhanced the binding of procaspase-3 to Apaf-1M368L (Figure 8A). In contrast, procaspase-3 did not bind to Apaf-1(1–570) even in the presence of procaspase-9 (Figure 8A). To determine whether procaspase-3 interacts with procaspase-9 alone or with the Apaf-1M368L–procaspase-9 complex, we performed similar experiments with immobilized procaspase-9 (Figure 8B). As shown in Figure 8B, procaspase-3 did bind to procaspase-9 in the absence of Apaf-1. Addition of Apaf-1M368L or wt Apaf-1 in the presence of cytochrome *c* and dATP enhanced the binding of procaspase-3 to immobilized procaspase-9 by 2- to 4-fold (Figure 8B). This effect is presumably due to increased recruitment of procaspase-9 to the complex by binding to Apaf-1M368L or Apaf-1 in the presence of cytochrome *c* and dATP. A direct interaction between procaspase-3 and procaspase-9 was also confirmed by co-immunoprecipitation analysis (data not shown). Thus, wt Apaf-1 and Apaf-1M368L but not Apaf-1(1–570) can recruit procaspase-3 to the Apaf-1–procaspase-9 complex through procaspase-9.

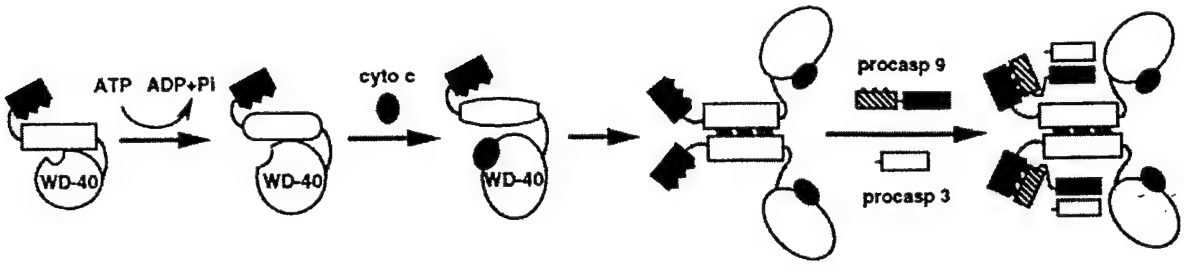

Fig. 9. A model depicting the mechanism of apoptosome formation and procaspase-9 activation. Apaf-1 undergoes sequential conformational changes induced by ATP hydrolysis and cytochrome *c* binding and acquires the ability to oligomerize. Subsequent binding of procaspase-9 to the Apaf-1 oligomer results in recruitment of procaspase-3 and possibly procaspase-7 to this complex to form a functional apoptosome. Apaf-1M368L may bypass the first two steps and adopts a conformation that is competent in oligomerizing and binding to procaspase-9 in the presence of dATP. Alternatively, Apaf-1M368L may assume a conformation that bypasses cytochrome *c* binding but still requires a single dATP/ATP hydrolysis event for oligomerization and procaspase-9 binding. This model is presented in greater detail in the Discussion.

Discussion

In this report we used Apaf-1 and various mutants to elucidate the mechanism by which Apaf-1 mediates procaspase-9 activation and induces apoptosis. Our studies revealed that the binding of cytochrome *c* to Apaf-1 requires dATP/ATP hydrolysis. We also demonstrated that two essential steps involved in procaspase-9 activation, Apaf-1 self-association and procaspase-9 recruitment to Apaf-1, require dATP/ATP hydrolysis and cytochrome *c* binding to Apaf-1. These steps are important for proapoptotic activity since Apaf-1 mutants deficient in dATP/ATP hydrolysis or cytochrome *c* binding are impaired in their ability to promote procaspase-9 activation and apoptosis. Finally, we provide evidence that procaspase-3 is recruited into the Apaf-1–procaspase-9 complex via interaction with procaspase-9. The WDR may play an important role in the recruitment of procaspase-3 to the Apaf-1–procaspase-9 complex, since mutant Apaf-1(1–570) lacking the WDR can bind to procaspase-9 but cannot recruit procaspase-3 and is deficient in apoptosis.

Our observations that the WDR with an extra WD-40 repeat can interact with Apaf-1(1–570) and inhibit activation of procaspase-9 mediated by Apaf-1(1–570) (Figure 1B and C) support conclusions of our previous paper obtained with the original Apaf-1 cDNA clone (Hu *et al.*, 1998b). Based on the results of our present study and previous studies (Hu *et al.*, 1998b; Srinivasula *et al.*, 1998), we provide a model depicting the events that lead to the formation of a functional apoptosome (Figure 9). In this model, dATP/ATP hydrolysis induces a conformational change so that Apaf-1 acquires the ability to bind cytochrome *c*. Upon cytochrome *c* binding, Apaf-1 undergoes further conformational changes to allow Apaf-1 oligomerization and CARD exposure. Procaspase-9 is then recruited into Apaf-1 oligomers via CARD–CARD homophilic interactions, and procaspase-3 is recruited into the complex via interaction with procaspase-9. Once recruited to the apoptosome, procaspase-9 is activated via autocatalysis by Apaf-1 oligomerization-induced proximity of multiple procaspase-9 molecules (Hu *et al.*, 1998b; Srinivasula *et al.*, 1998). Procaspase-9 might be cleaved and activated by adjacent procaspase-9 molecules (intermolecular catalysis). Alternatively, procaspase-9, forming part of the apoptosome, might adopt a conformation that results in intramolecular cleavage. Activated caspase-9 then cleaves and activates procaspase-3 recruited to the apoptosome. Once the functional apoptosome is formed, dATP/ATP hydrolysis would not longer be required for procaspase-9 recruitment, activation or release of active caspase-9, as suggested by our finding that dATP/ATP hydrolysis is only required for a brief period of time in order for Apaf-1 to activate procaspase-9. A model of Apaf-1 function that is consistent with our findings has been proposed recently based on studies with purified Apaf-1 and procaspase-9 proteins (Zou *et al.*, 1999).

In this study, we generated and characterized an Apaf-1 mutant that activates procaspase-9 independent of cytochrome *c*. Apaf-1M368L constitutively self-associates when synthesized in living cells. However, additional mutation of Lys160 to Arg abrogated its ability to self-associate and bind procaspase-9, as well as its capacity to promote procaspase-9 activation and apoptosis. Although the precise mechanism that accounts for its constitutional activation remains to be determined, these results suggest that Apaf-1M368L may bind and hydrolyze dATP/ATP *in vivo*, and induce Apaf-1 oligomerization and procaspase-binding and activation as intracellular dATP or ATP levels are available in cells at concentrations of 10 μM and 10 mM, respectively (Skoog and Bjursell, 1974). The ability of Apaf-1 to bind and hydrolyze dATP/ATP was demonstrated by a recent paper that was published while this paper was under review (Zou *et al.*, 1999). In the absence of dATP/ATP hydrolysis, the ability of wt Apaf-1 to oligomerize and to bind procaspase-9 might be repressed by an interaction between its N-terminal region and the WDR (Figure 1B and C) (Hu *et al.*, 1998b). One role of dATP/ATP hydrolysis might be to induce a conformational change that enables cytochrome *c* to bind Apaf-1. This hypothesis is supported by our finding that cytochrome *c* binding to Apaf-1 requires dATP/ATP hydrolysis. Binding of cytochrome *c* to the WDR may disrupt or alter the negative interaction between the N-terminal region and the WDR, allowing Apaf-1 to oligomerize and to bind procaspase-9. This model is supported by the analysis of the Apaf-1M368L mutant. This mutant exhibited reduced interaction between the N-terminal region and the WDR, bypassing the requirement of cytochrome *c* to disrupt the negative interaction. The lack of requirement for cytochrome *c* suggests that Apaf-

1M368L spontaneously adopts a conformation that is competent for oligomerization and procaspase-9 binding in the presence of dATP/ATP. Mutation of Met368 to Leu, therefore, might mimic conformational changes induced by dATP hydrolysis and cytochrome *c* binding. Thus, our findings that Apaf-1M368L still requires dATP/ATP binding or hydrolysis suggest that a second dATP/ATP binding or hydrolysis event may be required. Alternatively, Apaf-1M368L may assume a conformation that bypasses cytochrome *c* binding but still requires a single dATP/ATP hydrolysis event for oligomerization and procaspase-9 binding. CED-4, the *C.elegans* homologue of Apaf-1, lacks the WDR implying that CED-4 could constitutively activate CED-3, unless repressed by its physical association with CED-9. This model is supported by genetic analysis of *C.elegans* that showed that loss-of-function mutants of *ced-9* are lethal due to increased developmental cell deaths, but can be rescued by loss-of-function mutations in *ced-4* (Hengartner *et al.*, 1992). Furthermore, biochemical experiments in mammalian cells have revealed that the ability of CED-4 to activate CED-3 is inhibited by the association of CED-9 with CED-4 (Seshagiri and Miller, 1997; Wu *et al.*, 1997b). Interestingly, the equivalent position of Met368 is conserved in mouse Apaf-1 but is a leucine residue in CED-4. These observations suggest that cytochrome *c* is probably not a factor required for CED-4-mediated CED-3 activation. However, additional studies to test this hypothesis need to be performed in *C.elegans*.

Apaf-1M368L acts as a gain-of-function mutation in that, unlike wt Apaf-1, it activates procaspase-9 independent of cytochrome *c* and dATP *in vitro* and exhibits enhanced ability to induce apoptosis *in vivo*. In contrast, another mutant, Apaf-1(1–570), activates procaspase-9 independent of cytochrome *c* and dATP *in vitro*, but fails to induce apoptosis. Our results indicate that procaspase-9 complexed with Apaf-1M368L, but not procaspase-9 complexed with Apaf-1(1–570), can recruit and activate procaspase-3, providing an explanation for the differential phenotypes. Our studies support a model whereby procaspase-3 is recruited into the apoptosome formed by the Apaf-1–procaspase-9 complex via its interaction with procaspase-9. Apaf-1(1–570) lacking the WDR binds and activates procaspase-9 suggesting that its inability to recruit procaspase-3 is independent of these activities. Several possibilities could be envisioned to explain these results. First, conformational changes in the procaspase-9 bound to wt Apaf-1 and Apaf-1M368L could be critical for the recruitment of procaspase-3. Procaspase-9 bound to Apaf-1(1–570) might assume a conformation that is unsuitable for procaspase-3 recruitment. Another possibility is that the WDR, which is lacking in Apaf-1 (1–570), might be involved in the recruitment of procaspase-3 to the Apaf-1–procaspase-9 complex. In the absence of the WDR, Apaf-1(1–570) may be unable to induce the conformational changes of procaspase-9 required for recruitment of procaspase-3.

The cytochrome *c*/Apaf-1/caspase-9/caspase-3 pathway is now known to contribute to apoptosis induced by various stresses, including UV and γ-irradiation and chemotherapeutic drugs (Hakem *et al.*, 1998; Yoshida *et al.*, 1998). In addition, inactivation of either Apaf-1 or caspase-9 in this pathway contributes to cellular transformation and tumorigenesis (Soengas *et al.*, 1999). Under normal conditions, cytochrome *c* is unavailable to induce procaspase-9 activation since it resides in the intermembrane space of the mitochondria. After apoptotic stimuli lead to mitochondrial damage, cytochrome *c* is released and can activate procaspase-9 in an Apaf-1-dependent manner (Zou *et al.*, 1997; Fearnhead *et al.*, 1998). Prosurvival Bcl-2 family members are overexpressed in many tumors and inhibit caspase-9-mediated apoptosis by binding and inhibiting procaspase-9 activation directly and/or preventing the release of cytochrome *c* from mitochondria (Kharbanda *et al.*, 1997; Kim *et al.*, 1997; Kluck *et al.*, 1997; Yang *et al.*, 1997; Hu *et al.*, 1998a). Therefore, it will be interesting to examine whether prosurvival Bcl-2 family members like Bcl-X_L can directly inhibit Apaf-1M368L-mediated procaspase-9 activation. If Bcl-X_L can no longer exert its inhibitory effect on Apaf-1M368L-mediated activation of procaspase-9, the ability of Apaf-1M368L to activate procaspase-9 in the absence of cytochrome *c* could provide a potential method of inducing apoptosis in cancer cells in which cytochrome *c* release is blocked by overexpression of anti-apoptotic members of the Bcl-2 family.

Materials and methods

Plasmids and reagents

The Apaf-1XL cDNA was isolated by RT–PCR amplification from RNA template isolated from 293T cells and cloned into the pcDNA3 plasmid. The nucleotide sequence of the Apaf-1XL cDNA has been submitted to the DDBJ/EMBL/GenBank database (accession No. AF149794). pcDNA3-Apaf-1XL-M368L and pcDNA3-Apaf-1XL-K160R were generated by replacing the *Bst*EII–*Eco*RV fragment of pcDNA3-Apaf-1XL with the corresponding fragments from pcDNA3-Apaf-1(1–559M357L) and pcDNA3-Apaf-1(1–559K149R), respectively (Hu *et al.*, 1998b). pcDNA3-Apaf-1XL-M368L/K160R was constructed by ligation of a *Bst*EII–*Xba*I fragment from pcDNA3-Apaf-1(1–559K149R) and a *Xba*I–*Eco*RV fragment from pcDNA3-Apaf-1(1–559M357L) into *Bst*EII–*Eco*RV-digested pcDNA3-Apaf-1XL. All the constructs were verified by nucleotide sequencing. Polyclonal anti-Apaf-1 antibody was kindly provided by Xiaodong Wang, Southwestern Medical School, Dallas, TX. Polyclonal anti-caspase-9 and anti-caspase-3 antibodies were gifts from Donald Nicholson (Merck).

Transfection, immunoprecipitation and Western blot analysis

Human embryonic kidney 293T cells ($2–5\times10^6$) were transfected with 5 μg of the indicated plasmid DNA by the calcium phosphate method as reported (Inohara *et al.*, 1997). Cytosolic extracts were made essentially as described previously (Hu *et al.*, 1998a). Protein immunoprecipitation and Western blot analysis with relevant antibodies were performed as described previously (Inohara *et al.*, 1997). The proteins were detected by an enhanced chemiluminescence system (ECL; Amersham).

In vitro caspase-9 and caspase-3 assay

Cytosolic extracts were prepared and stored frozen at –80°C. Procaspase-9 was translated *in vitro* from a pcDNA3-caspase-9 plasmid in the presence of [^{35}S]methionine (Amersham) with a Promega TNT transcription/translation kit and purified through a desalting column free of radioactive methionine and ATP (Pharmacia). Procaspase-3 was translated *in vitro* using the same kit. To avoid contaminating dATP/ATP from cytosolic extracts in testing cytochrome *c* and dATP-dependent activation of procaspase-9 by Apaf-1 proteins, the cytosolic extracts were passed through a desalting column (Pharmacia). We incubated 2 μg (Figures 1D and 5A) or 40 μg (Figure 7C) of cellular extracts with or without dATP (1 mM) or bovine cytochrome *c* (0.2 μg, Sigma) in the presence of 1 μl *in vitro* translated procaspase-9 in a final volume of 25 μl. The mixtures were incubated for 30 min at 30°C and the reactions stopped by adding 5× SDS loading buffer and boiling for 5 min.

Apoptosis assay

293T cells (1×10^5) were seeded in each well of 12-well plates. After 18 h, cells were transiently transfected with 0.2 μg of the reporter pcDNA3-galactosidase plasmid plus indicated amount of test plasmids, as reported (Hu *et al.*, 1998a). pcDNA3 was used to adjust total plasmid DNA to an equal amount. The percentage of apoptotic cells was determined 19 h after transfection in triplicate cultures as described previously (Hu *et al.*, 1998a).

Procaspase-3 recruitment assay

Cytosolic extracts containing Myc-tagged Apaf-1 proteins and control or caspase-9 extracts were incubated with either anti-c-Myc (to immobilize Apaf-1 protein) or anti-HA (to immobilize procaspase-9) antibodies and protein A/G–agarose beads (1:1) for 2 h. The beads were washed three times with 1 ml NP-40 buffer (Inohara *et al.*, 1997) and once with 1 ml buffer A (Hu *et al.*, 1998a). Apaf-1- or procaspase-9-coated beads were packed into disposable gel filtration columns. Then *in vitro* translated caspase-3 was loaded onto the beads and washed four times with 1 ml buffer A. Bound proteins were eluted with 50 μl of hot 1× SDS loading buffer. We quantitated bound caspase-3 using a PhosphorImager from Molecular Dynamics.

Acknowledgements

We would like to thank Xiaodong Wang, Donald Nicholson, Nancy Thornberry and Margarita Garcia-Calvo for generous gifts of reagents. We thank Naohiro Inohara and Luis del Peso for thoughtful discussions and critical review of the manuscript. This work was supported by grant CA-64556 from the National Institutes of Health and by grant DAMD17-96-609 from US Army Medical Research Command. Y.H. was supported by the National Institutes of Health Postdoctoral Training Grant 2T32HL07517. M.A.B. was supported by a predoctoral fellowship from the US Army Medical Research Command. G.N. is the recipient of Research Career Development Award CA-64421 from the National Institutes of Health.

References

Alnemri,E.S. (1997) Mammalian cell death proteases: a family of highly conserved aspartate specific cysteine proteases. *J. Cell. Biochem.*, **64**, 33–42.

Cecconi,F., Alvarez-Bolado,G., Meyer,B.I., Roth,K.A. and Gruss,P. (1998) Apaf1 (CED-4 homolog) regulates programmed cell death in mammalian development. *Cell*, **94**, 727–737.

Chinnaiyan,A.M., O'Rourke,K., Lane,B.R. and Dixit,V.M. (1997) Interaction of CED-4 with CED-3 and CED-9: a molecular framework for cell death. *Science*, **275**, 1122–1126.

Fearnhead,H.O., Rodriguez,J., Govek,E.E., Guo,W., Kobayashi,R., Hannon,G. and Lazebnik,Y.A. (1998) Oncogene-dependent apoptosis is mediated by caspase-9. *Proc. Natl Acad. Sci. USA*, **95**, 13664–13669.

Hakem,R. *et al.* (1998) Differential requirement for caspase 9 in apoptotic pathways *in vivo*. *Cell*, **94**, 339–352.

Hengartner,M.O. and Horvitz,H.R. (1994) Programmed cell death in *Caenorhabditis elegans*. *Curr. Opin. Genet. Dev.*, **4**, 581–586.

Hengartner,M.O., Ellis,R.E. and Horvitz,H.R. (1992) *Caenorhabditis elegans* gene *ced-9* protects cells from programmed cell death. *Nature*, **356**, 494–499.

Hofmann,K., Bucher,P. and Tschopp,J. (1997) The CARD domain: a new apoptotic signaling motif. *Trends Biochem. Sci.*, **22**, 155–156.

Hu,Y., Benedict,M.A., Wu,D., Inohara,N. and Núñez,G. (1998a) Bcl-X_L interacts with Apaf-1 and inhibits Apaf-1-dependent caspase-9 activation. *Proc. Natl Acad. Sci. USA*, **95**, 4386–4391.

Hu,Y., Ding,L., Spencer,D.M. and Núñez,G. (1998b) WD-40 repeat region regulates Apaf-1 self-association and procaspase-9 activation. *J. Biol. Chem.*, **273**, 33489–33494.

Inohara,N., Koseki,T., Hu,Y., Chen,S. and Núñez,G. (1997) CLARP, a death effector domain-containing protein interacts with caspase-8 and regulates apoptosis. *Proc. Natl Acad. Sci. USA*, **94**, 10717–10722.

Irmler,M., Hofmann,K., Vanx,D. and Tschopp,J. (1997) Direct physical interaction between *Caenorhabditis elegans* 'death proteins' CED-3 and CED-4. *FEBS Lett.*, **406**, 189–190.

James,C., Gschmeissner,S., Fraser,A. and Evan,G.I. (1997) CED-4 induces chromatin condensation in *Schizosaccharomyces pombe* and is inhibited by direct physical association with CED-9. *Curr. Biol.*, **7**, 246–252.

Kharbanda,S. *et al.* (1997) Role for Bcl-X_L as an inhibitor of cytosolic cytochrome *c* accumulation in DNA damage-induced apoptosis. *Proc. Natl Acad. Sci. USA*, **94**, 6939–6942.

Kim,C.N., Wang,X., Huang,Y., Ibrado,A.M., Liu,L., Fang,G. and Bhalla,K. (1997) Overexpression of Bcl-X_L inhibits Ara-C-induced mitochondrial loss of cytochrome *c* and other perturbations that activate the molecular cascade of apoptosis. *Cancer Res.*, **57**, 3115–3120.

Kluck,R.M., Bossy-Wetzel,E., Green,D.R. and Newmeyer,D.D. (1997) The release of cytochrome *c* from mitochondria: a primary site for Bcl-2 regulation of apoptosis. *Science*, **275**, 1132–1136.

Li,P., Nijhawan,D., Budihardjo,I., Srinivasula,S.M., Ahmad,M., Alnemri,E.S. and Wang,X. (1997) Cytochrome *c* and dATP-dependent formation of Apaf-1/caspase-9 complex initiates an apoptotic protease cascade. *Cell*, **91**, 479–489.

Miura,M., Zhu,H., Rotello,R., Hartwieg,E.A. and Yuan,J. (1993) Induction of apoptosis in fibroblasts by IL-1β-converting enzyme, a mammalian homolog of the *C. elegans* cell death gene *ced-3*. *Cell*, **75**, 653–660.

Núñez,G., Benedict,M.A., Hu,Y. and Inohara,N. (1998) Caspases: the proteases of the apoptotic pathway. *Oncogene*, **17**, 3237–3245.

Pan,G., O'Rourke,K. and Dixit,V.M. (1998) Caspase-9, Bcl-x_L and Apaf-1 form a ternary complex. *J. Biol. Chem.*, **273**, 5841–5845.

Rotonda,J. *et al.* (1996) The three-dimensional structure of apopain/CPP32, a key mediator ofapoptosis. *Nature Struct. Biol.*, **3**, 619–625.

Seshagiri,S. and Miller,L.K. (1997) *Caenorhabditis elegans* CED-4 stimulates CED-3 processing and CED-3-induced apoptosis. *Curr. Biol.*, **7**, 455–460.

Skoog,L. and Bjursell,G. (1974) Nuclear and cytoplasmic pools of deoxyribonucleoside triphosphates in Chinese hamster ovary cells. *J. Biol. Chem.*, **249**, 6434–6438.

Soengas,M.S., Alarcon,R.M., Yoshida,H., Giaccia,A.J., Hakem,R., Mak,T.W. and Lowe,S.W. (1999) Apaf-1 and caspase-9 in p53-dependent apoptosis and tumor inhibition. *Science*, **284**, 156–159.

Spector,M.S., Desnoyers,S., Hoeppner,D.J. and Hengartner,M.O. (1997) Interaction between the *C. elegans* cell-death regulators CED-9 and CED-4. *Nature*, **385**, 653–656.

Srinivasula,S.M., Ahmad,M., Fernandes-Alnemri,T. and Alnemri,E.S. (1998) Autoactivation of procaspase-9 by Apaf-1-mediated oligomerization. *Mol. Cell*, **1**, 949–957.

Sun,X.M., MacFarlane,M., Zhuang,J., Wolf,B.B., Green,D.R. and Cohen,G.M. (1999) Distinct caspase cascades are initiated in receptor-mediated and chemical induced apoptosis. *J. Biol. Chem.*, **274**, 5053–5060.

Thompson,C.B. (1995) Apoptosis in the pathogenesis and treatment of disease. *Science*, **267**, 1456–1462.

Thornberry,N.A. *et al.* (1992) A novel heterodimeric cysteine protease is required for interleukin-1β processing in monocytes. *Nature*, **356**, 768–774.

Thornberry,N.A. and Lazebnik,Y. (1998) Caspases: enemies within. *Science*, **281**, 1312–1316.

Walker,N.P. *et al.* (1994) Crystal structure of the cysteine protease interleukin-1β-converting enzyme: a (p20/p10)2 homodimer. *Cell*, **78**, 343–352.

Wu,D., Wallen,H.D., Inohara,N. and Núñez,G. (1997a) Interaction and regulation of the *Caenorhabditis elegans* death protease CED-3 by CED-4 and CED-9. *J. Biol. Chem.*, **272**, 21449–21454.

Wu,D., Wallen,H.D. and Núñez,G. (1997b) Interaction and regulation of subcellular localization of CED-4 by CED-9. *Science*, **275**, 1126–1129.

Yang,J., Liu,X., Bhalla,K., Kim,C.N., Ibrado,A.M., Cai,J., Peng,T.I., Jones,D.P. and Wang,X. (1997) Prevention of apoptosis by Bcl-2: release of cytochrome *c* from mitochondria blocked. *Science*, **275**, 1129–1132.

Yang,X., Chang,H.Y. and Baltimore,D. (1998) Essential role of CED-4 oligomerization in CED-3 activation and apoptosis. *Science*, **281**, 1355–1357.

Yoshida,H., Kong,Y.Y., Yoshida,R., Elia,A.J., Hakem,A., Hakem,R., Penninger,J.M. and Mak,T.W. (1998) Apaf1 is required for mitochondrial pathways of apoptosis and brain development. *Cell*, **94**, 739–750.

Yuan,J. (1996) Evolutionary conservation of a genetic pathway of programmed cell death. *J. Cell. Biochem.*, **60**, 4–11.

Zou,H., Henzel,W.J., Liu,X., Lutschg,A. and Wang,X. (1997) Apaf-1, a human protein homologous to *C. elegans* CED-4, participates in cytochrome *c*-dependent activation of caspase-3. *Cell*, **90**, 405–413.

Zou,H., Li,Y., Liu,X. and Wang,X. (1999) An APAF-1–cytochrome *c* multimeric complex is a functional apoptosome that activates procaspase-9. *J. Biol. Chem.*, **274**, 11549–11556.

Received April 26, 1999; revised and accepted May 18, 1999

THE JOURNAL OF BIOLOGICAL CHEMISTRY
Vol. 275, No. 12, Issue of March 24, pp. 8461–8468, 2000
Printed in U.S.A.

Expression and Functional Analysis of Apaf-1 Isoforms

EXTRA WD-40 REPEAT IS REQUIRED FOR CYTOCHROME *c* BINDING AND REGULATED ACTIVATION OF PROCASPASE-9*

(Received for publication, August 5, 1999, and in revised form, December 29, 1999)

Mary A. Benedict‡, Yuanming Hu§, Naohiro Inohara, and Gabriel Núñez¶

From the Department of Pathology, Comprehensive Cancer Center and Cellular and Molecular Biology Program, University of Michigan Medical School, Ann Arbor, Michigan 48109

Apaf-1 is an important apoptotic signaling molecule that can activate procaspase-9 in a cytochrome *c*/dATP-dependent fashion. Alternative splicing can create an NH_2-terminal 11-amino acid insert between the caspase recruitment domain and ATPase domains or an additional COOH-terminal WD-40 repeat. Recently, several Apaf-1 isoforms have been identified in tumor cell lines, but their expression in tissues and ability to activate procaspase-9 remain poorly characterized. We performed analysis of normal tissue mRNAs to examine the relative expression of the Apaf-1 forms and identified Apaf-1XL, containing both the NH_2-terminal and COOH-terminal inserts, as the major RNA form expressed in all tissues tested. We also identified another expressed isoform, Apaf-1LN, containing the NH_2-terminal insert, but lacking the additional WD-40 repeat. Functional analysis of all identified Apaf-1 isoforms demonstrated that only those with the additional WD-40 repeat activated procaspase 9 *in vitro* in response to cytochrome *c* and dATP, while the NH_2-terminal insert was not required for this activity. Consistent with this result, *in vitro* binding assays demonstrated that the additional WD-40 repeat was also required for binding of cytochrome *c*, subsequent Apaf-1 self-association, binding to procaspase-9, and formation of active Apaf-1 oligomers. These experiments demonstrate the expression of multiple Apaf-1 isoforms and show that only those containing the additional WD-40 repeat bind and activate procaspase-9 in response to cytochrome *c* and dATP.

Programmed cell death, or apoptosis is an evolutionarily conserved mechanism of cellular demise that is critical for embryonic development and homeostasis in adult tissues (1, 2). Genetic studies in *Caenorhabditis elegans* have identified two genes, *ced-3* and *ced-4*, that are required for programmed cell death (3). Once the protein product of *ced-3* was determined to be a cysteine protease (4), a family of multiple related cysteine proteases (designated caspases) was identified and found to function as the executionary arm of the apoptotic program (5, 6). This executionary arm consists of a proteolytic cascade in which upstream regulatory caspases, such as caspase-9, activate downstream effector caspases, such as caspases-3 and -7 (7). *In vivo*, this process ultimately results in the cleavage of target proteins and the orderly demise and removal of the cell (5, 8).

Apaf-1 was identified as a mammalian homologue of CED-4 involved in the cytochrome *c*-dependent activation of caspase-3 through capase-9 (9), and also as an activity that activates caspases in non-transformed cell extracts (10). The NH_2 terminus of Apaf-1 is highly homologous to CED-4 and contains a caspase recruitment domain (CARD)[1] followed by an ATPase domain (9). This structural similarity is consistent with their roles as activators of apoptosis. A critical role for Apaf-1 in the regulation of apoptosis was confirmed by the analysis of Apaf-1-deficient mice in which abnormalities were observed in several tissues, particularly the brain, and characterized by the lack of developmental cell death (11, 12). Cells derived from these mice were also resistant to a wide variety of apoptotic stimuli, including chemotherapy, dexamethasone, and γ-irradiation, but not Fas or tumor necrosis factor (12). In contrast to the NH_2 terminus of Apaf-1, the COOH terminus lacks homology with CED-4 and is comprised of either 12 or 13 WD-40 repeats (WDRs) (9, 13–15).

In the presence of both cytochrome *c* and dATP, Apaf-1 is thought to undergo a conformational change such that it binds procaspase-9 (7). The activation of caspase-9 is thought to be due to the induced proximity of procaspase-9 molecules, which leads to autoprocessing and enzymatic activation (16, 17). It has been proposed that this assembly of procaspase-9 molecules is mediated by the oligomerization of multiple Apaf-1 molecules (13–17), and that this oligomerization can be inhibited by the WDR region (16–18). Cytochrome *c* binds partially purified Apaf-1 and is clearly required for Apaf-1 mediated activation of procaspase-9 (9). However, the mechanism by which cytochrome *c* functions and its binding site remain unknown.

Recently, several investigators have described the existence of multiple Apaf-1 splice variants (13–15). In tumor cell lines, alternative splicing can create an NH_2-terminal 11-amino acid insert between the CARD and ATPase domains or an additional COOH-terminal WDR between the fifth and sixth WDRs. However, the relative expression of these forms and their ability to activate procaspase-9 remain unknown. In the present studies, we used RT-PCR to demonstrate that the

* This work was supported in part by National Institutes of Health Grant CA-64556 (to G. N.) and U. S. Army Medical Research Command Grant DAMD196-609. The costs of publication of this article were defrayed in part by the payment of page charges. This article must therefore be hereby marked "*advertisement*" in accordance with 18 U.S.C. Section 1734 solely to indicate this fact.

‡ Supported by a pre-doctoral fellowship from the U. S. Army Medical Research Command.

§ Supported by National Institutes of Health Postdoctoral Training Grant 2T32HL07517.

¶ Recipient of Research Career and Development Award CA-64421 from the National Institutes of Health. To whom correspondence should be addressed. Tel.: 734-764-8514; Fax: 734-647-9654; E-mail: Gabriel.Nunez@umich.edu.

[1] The abbreviations used are: CARD, caspase recruitment domain; ATPγS, adenosine 5′-*O*-(thiotriphosphate); HA, hemagglutinin; PCR, polymerase chain reaction; RT, reverse transcriptase; WDR, WD-40 repeat region; Pipes, 1,4-piperazinediethanesulfonic acid; Chaps, 3-[(3-cholamidopropyl)dimethylammonio]-1-propanesulfonic acid; DEVD-AMC, Asp-Glu-Val-Asp-7-amino-4-methylcoumarin.

Apaf-1 isoform containing both the NH_2-terminal and COOH-terminal inserts (termed here Apaf-1XL) is the major form expressed in all human tissues examined. A form containing the NH_2-terminal insert but lacking the extra WDR was also expressed. Comparative analysis of all the Apaf-1 isoforms isolated to date demonstrated that the NH_2-terminal 11-amino acid insert of Apaf-1XL was not required for cytochrome *c* binding or cytochrome *c*/dATP promotion of procaspase-9 activation. However, only Apaf-1 isoforms containing the additional WDR were able to bind cytochrome *c*, self-associate, and bind and activate procaspase-9 in a cytochrome *c*/dATP-dependent fashion.

EXPERIMENTAL PROCEDURES

RT-PCR Analysis of Cell Lines, and Normal Human Tissues—Five μg of RNA from HeLa cells, human embryonic kidney 293T cells, or a panel of normal human tissues (CLONTECH, Palo Alto, CA) were used to generate first strand cDNA using a commercially available kit (Life Technologies, Inc., Gaithersburg, MD). Full-length Apaf-1 cDNAs were obtained by PCR from 293T cDNA, a HeLa cDNA library, or normal human tissue cDNAs using the specific primers: (5′-GATGGATCCAC-CCTAGGACCATGGATGCAAAAGCTCGAAATTG-3′ and 5′-CTAGCT-AGCTTACTCGAGTTCTAAAGTCTGTAAAATATATAAAATAC-3′). PCR conditions were as follows: 30 cycles of 30 s denaturation at 94 °C, 30 s annealing at 62 °C, and 5 min extension at 72 °C, followed by a 10-min extension at 72 °C. The relative amounts of Apaf-1 cDNAs with or without the NH_2-terminal 11-amino acid insert were determined using the specific primers: N1, 5′-AAGAGGAAAAAGTAAG-3′ and N2, 5′-TACTCCACCTTCACACAG-3′ (see Fig. 1), and the following PCR conditions: 25 cycles of 30 s denaturation at 94 °C, 30 s annealing at 52 °C, and 3-min extension at 72 °C, followed by a 10-min extension at 72 °C. The relative amounts of Apaf-1 cDNAs with or without the additional COOH-terminal WDR were determined using the specific primers: C1, 5′-CAGCTGATGGAACCTTAAAGC-3′ and C2, 5′-GTCTGGT-CATCAGAAGATGTC-3′ (see Fig. 1) and the following PCR conditions: 25 cycles of 30 s denaturation at 94 °C, 30 s annealing at 62 °C, and 3 min extension at 72 °C, followed by a 10-min extension at 72 °C. Positive controls for these PCR reactions included as templates, 10-pg samples containing the indicated ratios of gel purified insert DNA from the two Apaf-1 plasmids, Apaf-1XL and Apaf-1S. Specific amplification of Apaf-1 fragments was confirmed using the following negative controls: PCR reactions with no template and PCR reactions performed with first strand cDNA control reactions were made without reverse transcriptase. PCR products were run on 0.8, 1, or 2.5% agarose gels and analyzed by staining with ethidium bromide.

Plasmid Constructions—Full-length Apaf-1 PCR products were digested with *Bam*HI and *Xho*I and cloned in-frame into a pcDNA3 vector engineered to encode a COOH-terminal Myc epitope tag (19). Plasmids were prepared in *Escherichia coli* strains XL-10 (Stratagene, La Jolla, CA) or STBL2 (Life Technologies, Inc.) grown at 30 °C to avoid spontaneous mutations. Inserts were sequenced in their entirety. The HeLa Apaf-1 cDNA cloned (termed here Apaf-1S) was identical to that previously described (9) (Fig. 1). The Apaf-1 cDNAs cloned from 293T cells, however, contained an additional 11-amino acid NH_2-terminal insert and an extra WD repeat (termed here Apaf-1XL; see Fig. 1). Two other full-length Apaf-1 isoforms identified by us (Figs. 1, *B*, *C*, and *D*) and others (13, 14), with either the NH_2-terminal insert (termed here as Apaf-1LN) or the COOH-terminal WD-40 insert (termed here as Apaf-1LC; see Fig. 1), were constructed by exchanging the *Bam*HI/*Eco*RV fragments of Apaf-1S and Apaf-1XL. The Myc epitope-tagged Apaf-1 NH_2-terminal deletion mutant (Apaf-1S 1–559) referred to herein as "N−," has been previously described (16). The Myc epitope-tagged "N+" deletion mutant (Apaf-1XL 1–570) containing the 11-amino acid insert was constructed from the N− construct by replacing the *Bam*HI/*Eco*RV fragment with that from Apaf-1XL (Fig. 1). The Myc epitope-tagged Apaf-1S deletion mutant (468–1194), referred to herein as "C−," has been previously described (16). The "C+" deletion mutant (Apaf-1XL 479–1248) containing the additional WDR was generated from the C− construct, by replacing the *Eco*RI fragment with that from pcDNA3 Apaf-1XL (Fig. 1). All hemagglutinin (HA) epitope-tagged Apaf-1 constructs were generated by transferring the sequenced *Bam*HI/*Xho*I cDNA inserts from the pcDNA3-Myc vector to the pcDNA3-HA vector (19). An expression plasmid containing the untagged Apaf-1S cDNA first described in Ref. 9 was obtained from Dr. X. Wang (University of Texas Southwestern Medical Center, Dallas, TX). Both the pcDNA3 HA-procaspase-9 (C287S) mutant and the pcDNA3 procaspase-9 used for the *in vitro* caspase-9 assay have been previously described (20)

Transfection, Immunoprecipitation, and Immunoblotting—2.5×10^6 human embryonic kidney 293T cells were transfected by the calcium phosphate method with 1–5 μg each of the indicated plasmids, as reported (19). 24 h after transfection, cells were lysed in hypotonic Buffer A (7) containing 250 mM sucrose and disrupted using a 30-gauge needle. Following centrifugation at 17,000 × *g* at 4 °C, cytosolic extracts were collected and used for either *in vitro* binding assays or *in vitro* caspase-9 assays. In some experiments, transfected cells were lysed with 0.2% Nonidet P-40 buffer, as described previously (19) prior to immunoprecipitation. Protein immunoprecipitation and immunoblotting with relevent antibodies were performed as described (20). Rabbit anti-Myc, mouse anti-Myc, and rabbit anti-HA antibodies were obtained from Santa Cruz Biotech (Santa Cruz, CA). Mouse anti-HA antibody was obtained from Roche Molecular Biochemicals (Indianapolis, IN) and mouse anti-cytochrome *c* antibody was obtained from Pharmingen (San Diego, CA). Proteins were detected using the enhanced chemiluminescence (ECL) system (Amersham Pharmacia Biotech). For anti-Apaf-1 immunoblotting, Nonidet P-40 lysates were made as described above, using the following human cell lines: embryonic kidney 293T, breast cancer T47D, cervical cancer C33A, erythroleukemia K562, and monocytic leukemia U937. Apaf-1 protein was detected with two different polyclonal anti-Apaf-1 antibodies obtained from Dr. X. Wang (University of Texas Southwestern Medical School) and Cayman Chemical Co. (Ann Arbor, MI).

In Vitro Caspase-9 Assay—Cytosolic extracts were prepared as described above. The *in vitro* caspase-9 assay was performed as described previously (15). Reactions were stopped with 5 × SDS loading buffer, boiled, and loaded onto a 15% polyacrylamide/SDS gel. Gels were dried and exposed for autoradiography.

In Vitro Binding Assay—293T cells were transiently transfected with the indicated Myc- or HA-tagged Apaf-1 plasmid. Cytosolic extracts (see above) of the indicated plasmids were combined with or without 8 μg/ml cytochrome *c* (Sigma), 1 mM dATP (Roche Molecular Biochemicals), and 5 mM ATPγS (Sigma) for 2 h at 4 or 23 °C, in the presence of polyclonal anti-Myc antibody and protein A/G-agarose beads. Immunoprecipitation and anti-Myc or -HA immunoblotting was performed as described above.

Fractionation of Apaf-1 Isoforms by Gel Filtration—4×10^7 293T cells were transfected with Myc-tagged pcDNA3, pcDNA3-Apaf-1XL, or pcDNA3-Apaf-1LN. 24 h post-transfection, S-100 cytosolic extracts were prepared as described (20) and incubated at 30 °C for 30 min in the presence or absence of 10 μg/ml cytochrome *c* and 1 mM dATP. Then 300 μl of lysates were loaded on a Superdex-200 HR gel filtration column (Amersham Pharmacia Biotech) pre-equilibrated with buffer A (20 mM Hepes-KOH, pH 7.5, 10 mM KCl, 1.5 mM $MgCl_2$, 1 mM EDTA, 1 mM EGTA, 1 mM dithiothreitol and 0.1 mM phenylmethylsulfonyl fluoride) at a flow rate of 0.5 ml/min using a Bio-Rad BioLogic HR Workstation. The column was calibrated with an Amersham Pharmacia Biotech HMW gel filtration protein standards kit plus carbonic anhydrase and cytochrome *c* (thyroglobulin, M_r = 669,000; ferritin, M_r = 440,000; catalase, M_r = 232,000; bovine serum albumin, M_r = 66,000; carbonic anhydrase, M_r = 29,000; cytochrome *c*, M_r = 12,400). After discarding the majority of the void volume, fractions of 400 μl were collected. Aliquots of 50 μl from each fraction were run on a SDS-polyacrylamide electrophoresis gel followed by immunoblotting with anti-Myc polyclonal antibody. Aliquots of 50 μl from each fraction were also incubated with 100 μM DEVD-AMC to measure DEVDase activity.

Fluorimetric Assay of Caspase Activity—Assays of DEVD-AMC cleaving activity were carried out as described (22) using synthetic fluorogenic substrate Ac-Asp-Glu-Val-Asp-7-amino-4-methylcoumarin (Ac-DEVD-AMC) (Alexis Biochemicals, San Diego, CA). 50 μl from each column fraction were assayed in 100 μl of caspase assay buffer (20 mM Pipes, pH 7.2, 100 mM NaCl, 10 mM dithiothreitol, 1 mM EDTA, 0.1% Chaps, 10% sucrose). The reaction was started with addition of 100 μM DEVD-AMC and AMC released was measured at various times following the start of the reaction. The DEVD-AMC cleaving activity was expressed as normalized fluorescence produced after 3 h incubation at 37 °C.

RESULTS AND DISCUSSION

Identification of Apaf-1 Splice Variants—Previous studies in our laboratory analyzed the mechanism by which the carboxyl terminus of Apaf-1 binds and inhibits the NH_2 terminus, preventing oligomerization and caspase-9 activation (16). Cytochrome *c* was reported to bind to purified Apaf-1 and be re-

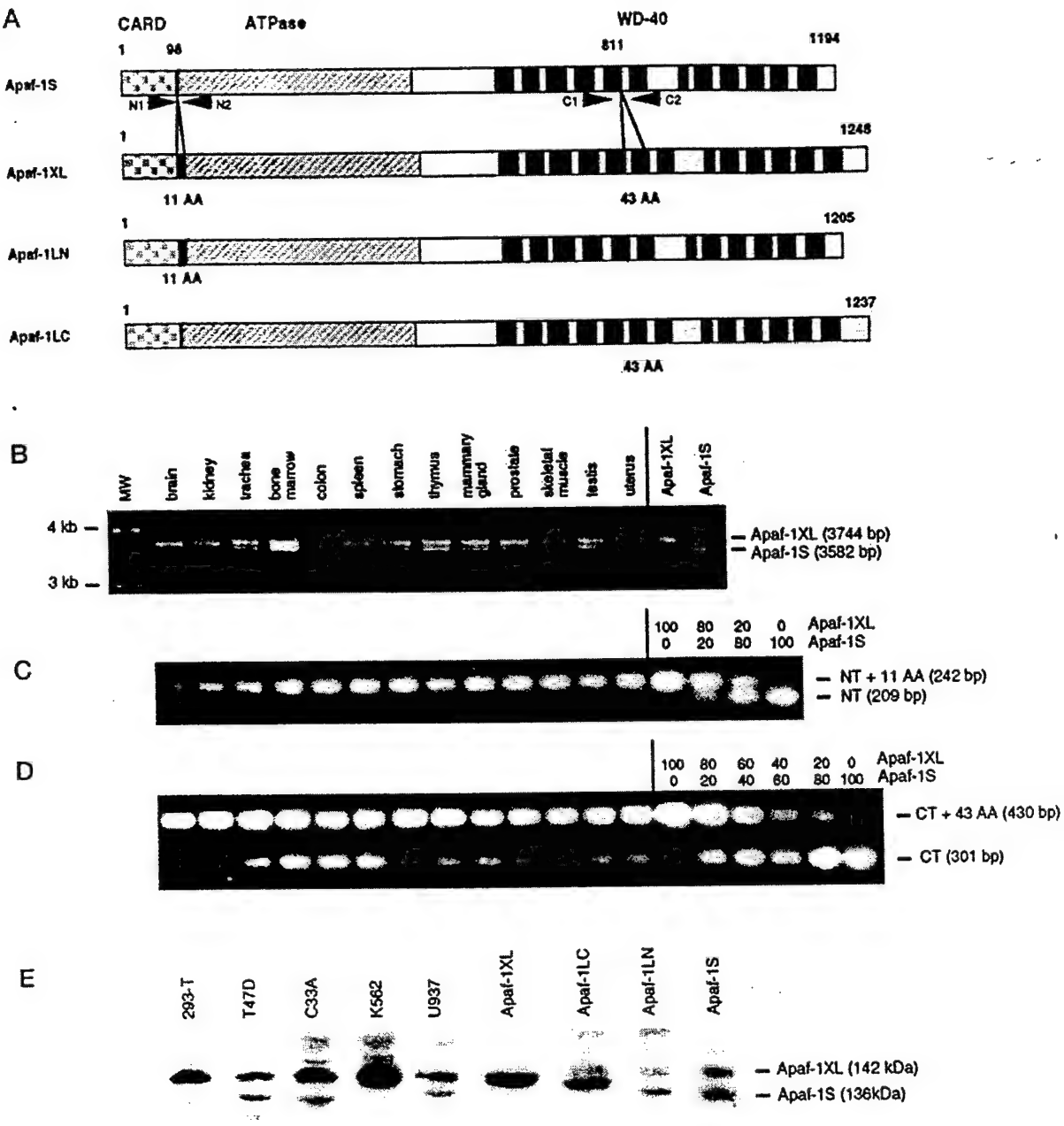

FIG. 1. **Expression of Apaf-1 isoforms.** *A*, schematic representation of Apaf-1 isoforms examined in this study. The CARD, ATPase domain, and WDRs are shown, as are the presence or absence of the 11-amino acid NH_2-terminal insert following the CARD and the 43-amino acid COOH-terminal insert between the fifth and sixth WDRs. N1/N2 and C1/C2 represent the primers used to amplify the regions flanking the NH_2-terminal and COOH-terminal inserts, respectively. The deletion mutant Apaf-1S (1–559) has been termed N−, while the deletion mutant Apaf-1XL (1–570) has been termed N+. C− refers to the deletion mutant Apaf-1S (468–1194), while C+ refers to the deletion mutant Apaf-1XL (479–1248). *B*, RT-PCR analysis of the expression of full-length Apaf-1 forms in human tissue RNAs. Primers used were identical to those used to amplify full-length Apaf-1 cDNAs (see "Experimental Procedures"). The last two lanes are positive control reactions using either 10 pg of gel purified Apaf-1XL or Apaf-1S inserts as templates. *C*, RT-PCR analysis of the same human tissue RNAs as above, using primers N1 and N2. The last four lanes are positive control reactions in which the templates were 10 pg of Apf-1 XL and Apaf-1S, mixed at the indicated ratios. *D*, RT-PCR analysis of the human tissue RNAs using primers C1 and C2. The *last six lanes* are positive controls, with Apaf-XL and Apaf-1S mixed at the indicated ratios. *E*, anti-Apaf-1 immunoblot analysis of 200 μg of cell lysate from various tumor cell lines. The *last four lanes* are positive control lysates from 293T cells transiently transfected with the indicated Apaf-1 plasmid. In addition to the transfected Apaf-1 isoforms, an endogenous Apaf-1 protein is observed in 293T cells.

quired as a co-factor for Apaf-1-mediated procaspase-9 activation (7, 9). We hypothesized that the inhibitory effect of the COOH-terminal WDRs might be relieved by binding to cytochrome *c*. However, we were unable to demonstrate cytochrome *c* binding (Fig. 3*A*) to the Apaf-1S isoform originally described by Zou *et al.* (9) and also cloned by us from HeLa cDNA (Fig. 1). We also noticed that endogenous 293T Apaf-1 protein appeared to migrate somewhat slower than transfected

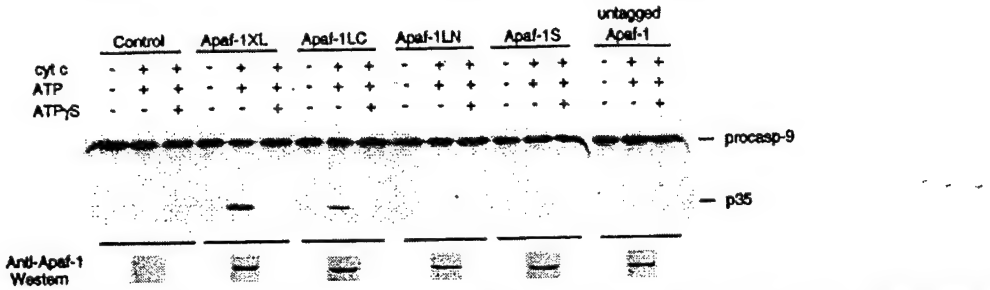

FIG. 2. **Cytochrome *c*-dependent *in vitro* activation of procaspase-9 requires the additional WD-40 repeat.** Ten μg cytosolic extracts of 293T cells transiently transfected with either the vector control or the indicated Myc-tagged or untagged Apaf-1 isoforms were incubated with *in vitro* translated [^{35}S]methionine-labeled procaspase-9, with or without 1 mM dATP, 8 μg/ml cytochrome *c*, or 5 mM ATPγS at 30 °C for 30 min. Anti-Apaf-1 (X. Wang) immunoblot analysis of the cytosolic extracts used to measure *in vitro* procaspase-9 activation, is shown in the *lower panel*. Endogenous Apaf-1 protein, although present, is not detected in this exposure.

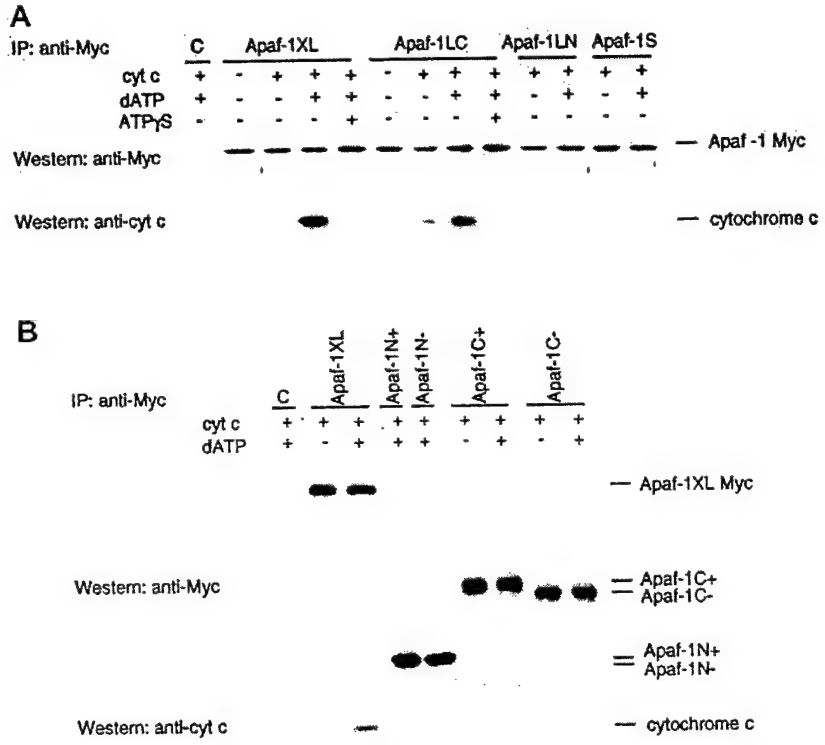

FIG. 3. **The additional WD-40 repeat of Apaf-1 is necessary but not sufficient for the binding of cytochrome *c*.** Cytosolic extracts from 293T cells transiently transfected with either vector control or the indicated Myc-tagged Apaf-1 plasmids were incubated with or without 8 μg/ml cytochrome *c*, 1 mM dATP, and 5 mM ATPγS in the presence of monoclonal anti-Myc antibody and protein A/G-agarose beads. After incubation for 2 h at 4 °C, immunoprecipitation was performed as described under "Experimental Procedures." Cytochrome *c* associated with Apaf-1 proteins was detected by immunoblotting. Similar results were obtained when cell extracts were incubated with cytochrome *c* and dATP for 2 h at 25 °C or for 20 h at 4 °C. *A*, immunoprecipitated full-length Myc-tagged Apaf-1 proteins are shown in the *upper panel*. Cytochrome *c* bound to Apaf-1 proteins is shown in the *lower panel*. *B*, immunoprecipitated Myc-Apaf-1XL and Myc-tagged Apaf-1 deletion mutants are shown in the *upper panel*. Bound cytochrome *c* is shown in the *lower panel*.

Apaf-1S (Fig. 1*E*), and in our hands we were unable to demonstrate cytochrome *c*/dATP-dependent *in vitro* activation of procaspase-9 by the Apaf-1S isoform (Fig. 2). We, therefore, used RT-PCR to clone other potential full-length Apaf-1 cDNAs from 293T cells. Two full-length Apaf-1 cDNAs were cloned from 293T cells and were identical to the Apaf-1S isoform, except that they contained an 11-amino acid insert (GKDSVSGITSY) at position 98 between the CARD and ATPase domain and a 43-amino acid WDR inserted between the fifth and sixth existing WDRs of Apaf-1S (Fig. 1*A*) (15). The presence of the NH_2-terminal insert is consistent with the utilization of an alternative exon donor site in exon 3 and a single acceptor site in exon 4 (GenBank accession numbers AF098871 and AF098873, respectively). The presence of the additional COOH-terminal WDR is consistent with the utilization of an additional exon 17a (GenBank accession numbers AF117658 and AF117659). Recently, Zou *et al.* (13) have also reported the cloning of this Apaf-1 cDNA from HeLa cells. For consistency and clarity in this paper, we have termed this isoform Apaf-1XL (15). This was done to distinguish it from two other alternative human Apaf-1 cDNA splice variants (13, 14) (and identified in Fig. 1, *B*, *C*, and *D*) that are also longer than the originally identified Apaf-1S (Fig. 1*A*). We constructed these two alternative Apaf-1 cDNAs using the Apaf-1S and Apaf-1XL cDNAs as described under "Experimental Procedures." For clarity in this paper, we have termed them Apaf-1LC (long COOH terminus: containing the additional WDR, but lacking the NH_2-terminal insert) and Apaf-1LN (long NH_2 terminus: containing the NH_2-terminal insert, but lacking the additional WDR) (Fig. 1*A*).

Expression Apaf-1 Isoforms in Tissues and Cell Lines—All of the human Apaf-1 cDNAs described have been isolated from tumor cell lines (9, 13–15). To determine if multiple Apaf-1 cDNAs are present in normal human tissues, we performed full-length Apaf-1 PCR analysis on cDNAs generated from normal human tissue RNAs (Fig. 1*B*). This analysis demonstrated the existence of at least two Apaf-1 cDNA forms. The larger form co-migrated with the cloned Apaf-1XL fragment, while the smaller form migrated slightly above that of Apaf-1S (Fig. 1*B*).

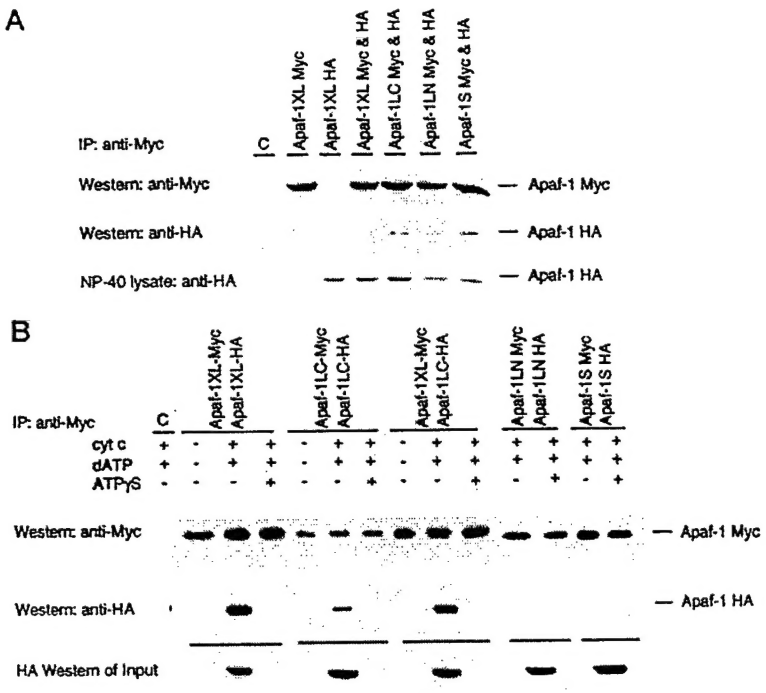

FIG. 4. **Cytochrome *c*/dATP-dependent Apaf-1 self-association requires the additional WD-40 repeat.** *A*, in Nonidet P-40 extracts, all Apaf-1 isoforms can self-associate. Nonidet P-40 extracts of 293T cells transiently transfected with the indicated Myc- or HA-tagged Apaf-1 plasmids were immunoprecipitated with rabbit anti-Myc antibody and immune complexes were immunoblotted with either mouse anti-Myc or mouse anti-HA. Immunoprecipitated Myc-Apaf-1 proteins are shown in the *upper panel*, and self-associated HA-Apaf-1 proteins are shown in the *middle panel*. The *lower panel* depicts an anti-HA immunoblot of the Nonidet P-40 extracts to confirm equivalent expression of the HA-Apaf-1 isoforms used. *B*, in cytosolic extracts, cytochrome *c*/dATP-dependent Apaf-1 self-association requires the additional WD-40 repeat. 293T cells were transiently transfected with the indicated Myc- or HA-tagged Apaf-1 plasmid. Cytosolic extracts of the indicated plasmids were combined with or without 8 μg/ml cytochrome *c*, 1 mM dATP, and 5 mM ATPγS, in the presence of polyclonal anti-Myc antibody and protein A/G-agarose beads. Immunoprecipitation and anti-Myc or -HA immunoblotting was performed as described above. Immunoprecipitated Myc-Apaf-1 isoforms are shown in the *upper panel*, and associated HA-Apaf-1 isoforms are shown in the *middle panel*. The *lower panel* depicts an anti-HA immunoblot of the cytosolic extracts to confirm equivalent expression of the HA-Apaf-1 isoforms used.

Restriction mapping of each of these gel purified full-length Apaf-1 PCR products confirmed their identities as Apaf-1 cDNAs.[2] Because of limited gel resolution, minor amounts of other Apaf-1 cDNAs may have been present but not detectable. To better examine the relative amounts of the different Apaf-1 forms, we performed PCR analysis of the human tissue cDNAs using two sets of primers that flank the two different insertions. Primers N1 and N2 flank the NH_2-terminal 11-amino acid insertion, while primers C1 and C2 flank the additional WDR (Fig. 1*A*). PCR analysis using primers N1 and N2 showed that in all tissues the great majority of the products (>80%) contained the 11-amino acid NH_2-terminal insertion, as determined by comparison with control reactions containing various ratios of Apaf-1XL and Apaf-1S DNAs (Fig. 1*C*). PCR analysis using primers C1 and C2 showed that in all tissues both types of products are represented, although the relative amounts of the two types varied among the tissues (Fig. 1*D*). A compilation of the PCR results from Fig. 1, *C* and *D*, suggests that the major full-length Apaf-1 cDNAs observed in most of these tissues appears to be Apaf-1XL (containing both NH_2-terminal and COOH-terminal insertions). At the level of mRNA expression, tissues such as bone marrow, colon, and spleen appear to have roughly equal amounts of Apaf-1XL and Apaf-1LN (containing just the NH_2-terminal insertion), while tissues such as brain, kidney, stomach, and skeletal muscle express more Apaf-1XL.

To determine whether multiple Apaf-1 isoforms are also expressed at the protein level, we examined multiple cell lines by immunoblotting using a polyclonal anti-Apaf-1 antibody. Lysates of 293T cells transiently transfected with the different Apaf-1 forms (described in Fig. 1*A*) were run as controls. The major immunoreactive band in each of the cell lines co-migrated with the Apaf-1XL form (Fig. 1*E*), which is consistent with the data from the mRNA analysis of human tissues identifying Apaf-1XL as the major form expressed (Fig. 1, *B-D*). As in the tissue mRNAs, multiple Apaf-1 protein isoforms were also expressed in these cell lines (Fig. 1*E*). These other bands appear to co-migrate with the Apaf-1LN and Apaf-1S forms, however, exact identification would require either protein sequencing or isoform-specific antibodies. Immunoblotting of these lysates with another polyclonal anti-Apaf-1 antibody (Cayman Chemical Co.) confirmed these results.[2]

Cytochrome c/dATP-dependent in Vitro Activation of Procaspase-9 requires the additional WD-40 repeat—Purified Apaf-1 has been reported to activate procaspase-9 in a cytochrome *c* and dATP-dependent fashion (7). To determine if the newly identified Apaf-1 cDNAs also share this activity, and to determine the role of the NH_2-terminal and COOH-terminal insertions, the four full-length Myc-tagged Apaf-1 constructs (Fig. 1) and the originally described untagged Apaf-1S were expressed in 293T cells. Cytosolic extracts of these cells were prepared and anti-Apaf-1 immunoblotting confirmed comparable expression of each of the transfected Apaf-1 forms (Fig. 2). Ten μg of the fresh cytosolic extracts were also analyzed for their ability to activate procaspase-9 *in vitro*. Extracts were diluted so that endogenous Apaf-1 activity could not be detected. As shown in Fig. 2, only Apaf-1XL and Apaf-1LC con-

[2] M. Benedict and G. Núñez, unpublished results.

taining the extra WDR, but not those isoforms lacking it, were able to activate procaspase-9 in a cytochrome *c* and dATP-dependent fashion as indicated by the appearance of the intermediate p35 proteolytic fragments. These same results were obtained using 1, 3, and 30 μg of cytosolic extracts or when the extracts were incubated for 30, 60, or 90 min at 30 °C with cytochrome *c* and dATP.[2] Due to the presence of low levels of dATP or ATP in the cytosolic extracts, we confirmed the requirement for ATP by the addition of the non-hydrolyzable ATP analogue, ATPγS, which almost completely inhibited the cytochrome *c*/dATP-dependent activation of procaspase-9 (Fig. 2). Although the original untagged Apaf-1S was previously reported to activate procaspase-9 in a cytochrome *c*/dATP-dependent fashion (9), we were unable to detect such activity under our assay conditions (Fig. 2).

The additional WD-40 Repeat of Apaf-1 Is Necessary but Not Sufficient for the Binding of Cytochrome c—The apparent requirement of the extra WDR for cytochrome *c*/dATP-dependent activation of procaspase-9 prompted us to examine the ability of the different Apaf-1 forms to bind cytochrome *c*. As shown in Fig. 3*A*, following anti-Myc antibody immunoprecipitation in the presence or absence of cytochrome *c*, dATP, or ATPγS and immunoblotting with mouse anti-cytochrome *c* antibody, only the Apaf-1 constructs Apaf-1XL and Apaf-1LC, containing the extra WDR, bound to cytochrome *c*. This cytochrome *c* binding also required ATP/dATP, as binding was greatly inhibited by the addition of the non-hydrolyzable ATP analogue, ATPγS (Fig. 3*A*). The NH_2-terminal 11-amino acid insert was not required for cytochrome *c* binding, as the form Apaf-1LC, lacking the NH_2-terminal insert, bound cytochrome *c* (Fig. 3*A*). Cytochrome *c* binding to the COOH-terminal deletion mutant, C+ (Apaf-1XL 479–1248), containing the extra WDR was not detected, suggesting that this region, although necessary (Fig. 3*A*), is not sufficient to mediate cytochrome *c* binding (Fig. 3*B*). Cytochrome *c* also failed to bind to either the N+ (Apaf-1XL 1–570) or N− (Apaf-1S 1–559) deletion mutants (Fig. 3*B*). This data is consistent with a model in which the COOH-terminal WDR region with the additional WDR contains a binding site for cytochrome *c* that may be unmasked only following a conformational change driven by ATP hydrolysis in the NH_2 terminus.

Cytochrome c/dATP-dependent Apaf-1 Self-association Requires the Additional WD-40 Repeat—We and others have previously shown that Apaf-1 can self-associate to form homo-oligomers (13–18). As our previous studies utilized Apaf-1 protein in Nonidet P-40 cellular extracts, we first used Nonidet P-40 extracts to compare the four different full-length Apaf-1 constructs for their ability to form homo-oligomers. Myc- and HA-tagged isoforms were expressed in 293T cells, lysed in Nonidet P-40 buffer, immunoprecipitated with anti-Myc antibody, and immunoblotted with anti-HA or anti-Myc antibodies. As shown in Fig. 4*A*, all four Apaf-1 isoforms were able to self-associate. Anti-HA immunoblotting confirmed similar expression of the HA-Apaf-1 isoforms in the Nonidet P-40 extracts. Since these studies were performed in the presence of detergent which could affect protein conformation, we repeated these self-association experiments in the absence of detergent. Cytosolic extracts of Myc- and HA-Apaf-1 isoforms made without detergent were mixed in the presence or absence of cytochrome *c*, dATP, or ATPγS. Under these conditions, only Apaf-1XL and Apaf-1LC, both containing the extra WDR, underwent cytochrome *c*/dATP-dependent self-association (Fig. 4*B*). Because Apaf-1LC lacks the NH_2-terminal 11-amino acid insert, this region is clearly not required for cytochrome *c*/dATP-dependent self-association. Anti-HA immunoblotting confirmed similar expression of the HA-Apaf-1 isoforms. This data is

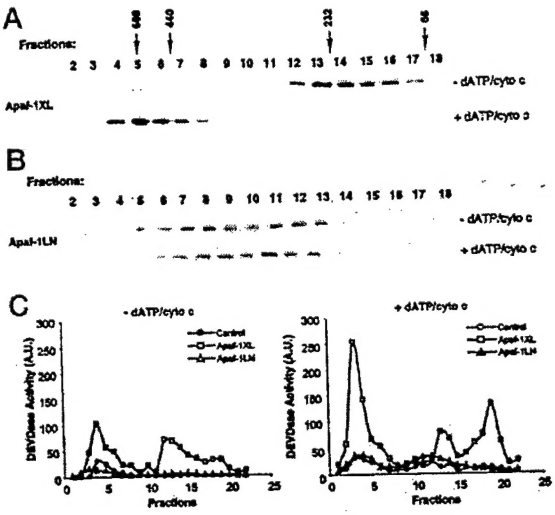

FIG. 5. **The extra WD-40 repeat is required for cytochrome *c* and dATP-dependent oligomerization of Apaf-1.** *A* and *B*, 293T lysates containing Myc-tagged Apaf-1XL (*A*) or Apaf-1LN (*B*) were incubated with or without dATP and cytochrome *c* and fractionated on a Superdex 200 HR column. Equal amounts (50 μl) of each fraction were separated on a SDS-polyacrylamide electrophoresis gel, and Apaf-1XL (*A*) or Apaf-1LN (*B*) were detected by immunoblotting with anti-Myc polyclonal antibody. The elution profiles of selected size exclusion standards are indicated by *arrowheads* on top in kilodaltons. *C*, the elution profile of DEVD-AMC cleaving activity of control (*circles*), Apaf-1XL (*squares*), or Apaf-1LN (*triangles*) lysates incubated without (*left panel*) or with (*right panel*) dATP and cytochrome *c*. Equal amounts (300 μl) of lysates were incubated with or without cytochrome *c* and dATP and fractionated on a Superdex 200 HR column as in *A* and *B*. The DEVD-AMC cleaving activity was measured as described under "Experimental Procedures," and expressed as arbitrary units (normalized fluorescence at 460 nM).

consistent with a model in which cytochrome *c* binds the Apaf-1 COOH terminus with the extra WDR, thus relieving the inhibition of the NH_2 terminus, and allowing Apaf-1 self-association (16). The requirement of the extra WDR for Apaf-1 self-association is also consistent with our observation that it is required for procaspase-9 activation (Fig. 2). Not surprisingly, the two constructs, Apaf-1XL and Apaf-1LC, with the extra WDRs, were capable of forming cytochrome *c*/dATP-dependent hetero-oligomers (Fig. 4*B*). However, hetero-oligomers between the two major cDNAs detected in human tissues, Apaf-1XL (with the extra WDR) and Apaf-1LN (lacking the extra WDR), were not observed.[2]

Cytochrome c/dATP-dependent Formation of Active Apaf-1 Oligomers Requires the Extra WD-40 Repeat—To further characterize the role of the extra WD-40 repeat in Apaf-1 oligomerization, we used size exclusion chromatography to fractionate extracts from 293T cells transiently transfected with plasmids producing Myc-tagged Apaf-1XL and Apaf-1LN which only differ in the presence of an extra WD-40 repeat (Fig. 1). Cell extracts were prepared and incubated *in vitro* with cytochrome *c* and dATP to induce Apaf-1 oligomerization or similarly treated in the absence of cytochrome *c* and dATP as a control. Fractions separated by gel filtration chromatography were evaluated for Apaf-1 by immunoblotting with anti-Myc antibody. In the absence of cytochrome *c* and dATP, Apaf-1XL eluted predominantly as a ~200-kDa protein which is consistent with a monomeric form of this protein (Fig. 5*A*). Preincubation of Apaf-1XL extracts with cytochrome *c* and dATP resulted in a significant shift in the Apaf-1 elution profile such that the majority of the Apaf-1XL eluted around fraction 5 which corresponds to ~700 kDa (Fig. 5*A*). These results agree

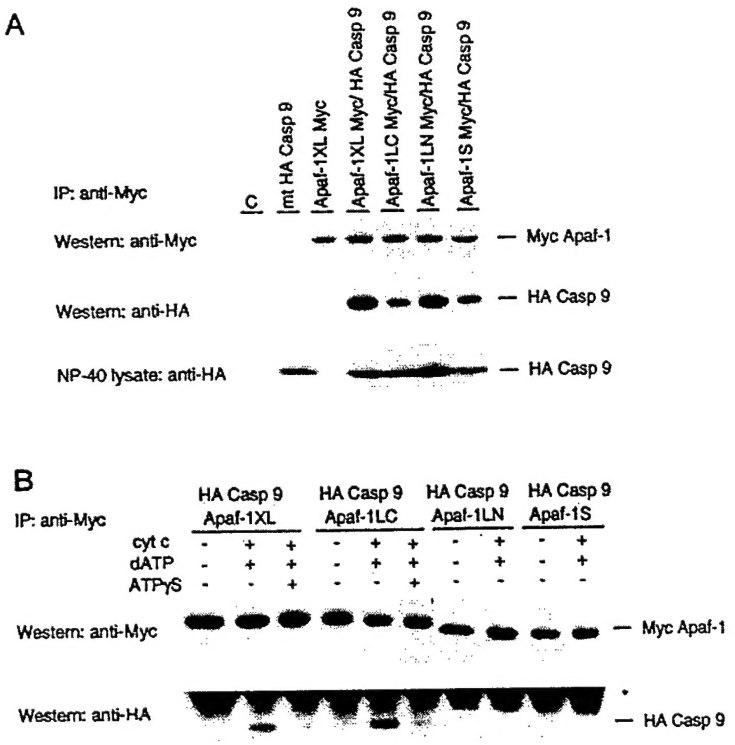

FIG. 6. **Cytochrome *c*-dependent binding of Apaf-1 to procaspase-9 requires the extra WD-40 repeat.** *A*, in Nonidet P-40 extracts, all Apaf-1 isoforms can bind to procaspase-9. Nonidet P-40 extracts of 293T cells transiently co-transfected with the indicated Myc-Apaf-1 plasmids and HA-mt procaspase-9(C287S) were immunoprecipitated with rabbit anti-Myc antibody and immune complexes were immunoblotted with either mouse anti-Myc or mouse anti-HA. Immunoprecipitated Myc Apaf-1 isoforms are shown in the *upper panel*, and associated HA-mt procaspase-9 is shown in the *middle panel*. The *lower panel* depicts an anti-HA immunoblot of the Nonidet P-40 extracts to confirm similar expression of HA-mt procaspase-9 in each extract. *B*, in cytosolic extracts, cytochrome *c*/dATP-dependent binding of Apaf-1 to procaspase-9 requires the additional WDR. 293T cells were transiently transfected with the indicated Myc-Apaf-1 plasmid or HA-mt procaspase-9. Cytosolic extracts of the indicated plasmids were combined with or without 8 μg/ml cytochrome *c*, 1 mM dATP, and 5 mM ATPγS, in the presence of polyclonal anti-Myc antibody and protein A/G-agarose beads. Immunoprecipitation and anti-Myc or -HA immunoblotting was performed as described above. Immunoprecipitated Myc-Apaf-1 isoforms are shown in the *upper panel* and associated HA-mt procaspase-9 is shown in the *bottom panel*. The *asterisk* denotes nonspecific IgG heavy chain bands.

with recent work by several laboratories that showed that endogenous Apaf-1 in cells or purified Apaf-1 forms containing the extra WD-40 repeat form a large multimeric complex upon addition of cytochrome *c* and dATP (13, 14, 23). The elution profile of Apaf-1LN was different from that of Apaf-1XL in that Apaf-1LN eluted in multiple consecutive fractions, corresponding to 200 to 700 kDa (Fig. 5*B*). This elution profile could potentially be the result of specific association of Apaf-1LN with another protein(s), altered protein folding, and/or formation of Apaf-1LN complexes. However, in contrast to Apaf-1XL, preincubation of Apaf-1LN extracts with cytochrome *c* and dATP did not change its elution profile (Fig. 5*B*). The multimeric Apaf-1 complex that is formed upon incubation with cytochrome *c* and dATP has been shown to include the processed forms of caspase-9 and caspase-3 (23). To determine the caspase activity associated with Apaf-1 protein complexes, the different protein fractions prepared from Apaf-1XL, Apaf-1LN, or control extracts were evaluated for DEVDase activity. We detected DEVDase activity in Apaf-1XL extracts in the absence and presence of cytochrome *c* and dATP, although the activity was clearly increased after addition of cytochrome *c* and dATP (Fig. 5*C*). The major peak of DEVDase activity in Apaf-1XL extracts was found around fraction 5 which corresponds to oligomeric Apaf-1XL (Fig. 5*C*). The DEVDase activity detected in the absence of cytochrome *c* and dATP may be explained by low level Apaf-1XL oligomerization that is detected in extracts from cells transiently transfected with the Apaf-1XL construct (Fig. 5*A*). Other peaks of DEVDase activity were found around fractions 13 and 18 (Fig. 5*C*). The latter was most prominent in Apaf-1XL extracts preincubated with cytochrome *c* and dATP and corresponds to a size of ~60 kDa. The DEVDase activity associated with fraction 18 most likely corresponds to a dimeric form of active caspase-3, as we found that purified processed caspase-3 also eluted in fraction 18.[3] Active caspase-3 not bound to the Apaf-1 complex appears to represent caspase-3 that is processed by the oligomeric Apaf-1-caspase-9 complex and subsequently released from the complex (14, 23). Significantly, extracts from cells transfected with Apaf-1LN were devoid of DEVDase activity even after preincubation of the extracts with cytochrome *c* and dATP, when compared with extracts prepared from cells transfected with control plasmid (Fig. 5*C*).

Cytochrome c/dATP-dependent Binding of Apaf-1 to Procaspase-9 Requires the Extra WD-40 Repeat—We and others have previously demonstrated the binding between the originally described Apaf-1S and procaspase-9 (20, 21). We, therefore, compared the four full-length Apaf-1 isoforms for their ability to associate with procaspase-9 in the presence of Nonidet P-40. Each Myc-tagged Apaf-1 construct and HA-procaspase-9 (C287S) were expressed in 293T cells, lysed in Nonidet P-40 buffer, immunoprecipitated with anti-Myc antibody,

[3] Y. Hu and G. Núñez, unpublished results.

and immunoblotted with anti-HA or anti-Myc antibodies. As shown in Fig. 6*A*, all Apaf-1 isoforms tested bound to procaspase-9. Anti-HA immunoblotting confirmed similar expression of procaspase-9 in each extract. However, when binding was analyzed in cytosolic extracts lacking detergent, in the presence or absence of cytochrome *c*, dATP or ATPγS, only Apaf-1XL and Apaf-1LC containing the extra WDR bound to procaspase-9 in a cytochrome *c* and dATP-dependent fashion (Fig. 6*B*). Because Apaf-1LC lacks the NH_2-terminal 11-amino acid insert, this region is clearly not required for cytochrome *c*/dATP-dependent procaspase-9 binding. The requirement of the extra WDR for procaspase-9 binding is in complete agreement with our observation that this region is also required for procaspase-9 activation (Fig. 2). Previous data from our laboratory suggests that the COOH-terminal WDRs of Apaf-1 can bind and inhibit the ability of the NH_2 terminus to self-associate and activate procaspase-9 *in vitro* (16). Taken together, the data presented herein suggest a model in which cytochrome *c*, in the presence of ATP/dATP, binds to the COOH termini of only those Apaf-1 isoforms containing the extra WDR, thus relieving the inhibition of the NH_2 terminus, and allowing Apaf-1 self-association, procaspase-9 binding, and the activation of procaspase-9.

The Apaf-1XL form, with both the NH_2-terminal and COOH-terminal inserts, appears to be the major Apaf-1 RNA expressed in most tissues and likely represents the cytochrome *c*/dATP-dependent activator of procaspase-9 originally described (7, 9, 10). It is interesting to note that at the mRNA level, some tissues such as bone marrow, spleen, and colon express significant amounts of Apaf-1LN, (which lacks the extra WDR and fails to bind and activate procaspase-9 in response to cytochrome *c* and dATP). In addition, anti-Apaf-1 immunoblotting of some tumor cell lines revealed bands that co-migrate with Apaf-1LN, suggesting that this Apaf-1 form is expressed at the protein level. It is tempting to speculate as to a possible function for Apaf-1LN. Given that in the presence of detergent the Apaf-1LN can both self-associate and bind procaspase-9, it might function as either an activator or an inhibitor of procaspase-9 activation, depending on whether it formed a functional or non-functional apoptosome complex. In our hands, Apaf-1LN does not inhibit *in vitro* cytochrome *c*/dATP-dependent procaspase-9 activation by the Apaf-1XL form,[2] suggesting that it does not function as a cytochrome *c*/dATP-dependent inhibitor. However, this is not unexpected, because of its inability to bind cytochrome *c*. In order for the Apaf-1LN form to function as an activator or inhibitor of procaspase-9 activation, one might hypothesize the existence of a cellular signal or co-factor other than cytochrome *c* that would bind specifically to the COOH terminus of Apaf-1 forms lacking the additional WDR. This co-factor might function similarly to cytochrome *c* and act to relieve the inhibitory action of the COOH terminus, allowing Apaf-1 self-association and procaspase-9 binding. Such a modification in binding specificity due to a change in the number of structural repeats is not without precedent. In some plants, the specificity of disease-resistance genes can be altered simply by a change in the number of leucine-rich repeats (24). In the case of Apaf-1 isoforms lacking the extra WDR, the specific binding of some unknown co-factor could potentially result in a non-cytochrome *c*-dependent pathway of procaspase-9 activation or inhibition.

Acknowledgment—We are grateful to Dr. Xiaodong Wang for the generous gift of reagents.

REFERENCES

1. Thompson, C. B. (1995) *Science* **267,** 1456–1462
2. Yuan, J. (1996) *J. Cell. Biochem.* **60,** 4–11
3. Hengartner, M. O., and Horvitz, H. R. (1994) *Curr. Opin. Genet. Dev.* **4,** 581–586
4. Miura, M., Zhu, H., Rorello, R., Hartweig, E. A., and Yuan, J. (1993) *Cell* **75,** 653–660
5. Nunez, G., Benedict, M. A., Hu, Y., and Inohara, N. (1998) *Oncogene* **17,** 3237–3245
6. Thornberry, N. A., and Lazebnik, Y. (1998) *Science* **281,** 1312–1316
7. Li, P., Nijhawan, D., Budihardjo, I., Srinivasula, S., Ahmad, M., Alnemri, E. S., and Wang, X. (1997) *Cell* **91,** 479–489
8. Sun, X. M., MacFarlane, M., Zhuang, J., Wolf, B. B., Green, D. R., and Cohen, G. M. (1999) *J. Biol. Chem.* **274,** 5053–5060
9. Zou, H., Henzel, W. J., Liu, X., Lutschg, A., and Wang, X. (1997) *Cell* **90,** 405–413
10. Fearnhead, H. O., Rodriguez, J., Govek, E. E., Guo, W., Kobayashi, R., Hannon, G., and Lazebnik, Y. A. (1998) *Proc. Natl. Acad. Sci. U. S. A.* **95,** 13664–13669
11. Cecconi, F., Alvarez-Bolado, G., Meyer, B. I., Roth, K. A., and Gruss, P. (1998) *Cell* **94,** 727–737
12. Yoshida, H., Kong, Y. Y., Yoshida, R., Elia, A. J., Hakem, A., Hakem, R., Penninger, J. M., and Mak, T. W. (1998) *Cell* **94,** 739–750
13. Zou, H., Li, X., Liu, X., and Wang, X. (1999) *J. Biol. Chem.* **274,** 11549–11556
14. Saleh, A., Srinivasula, S. M., Acharya, S., Fishel, R., and Alnemri, E. S. (1999) *J. Biol. Chem.* **274,** 17941–17945
15. Hu, Y., Benedict, M. A., Ding, L., and Núñez, G. (1999) *EMBO J.* **18,** 3586–3595
16. Hu, Y., Ding, L., Spencer, D. M., and Núñez, G. (1998) *J. Biol. Chem.* **273,** 33489–33494
17. Srinivasula, S. M., Ahmad, M., Fernandes-Alnemri, T., and Alnemri, E. S. (1998) *Mol. Cell* **1,** 949–957
18. Adrain, C., Slee, E. A., Harte, M. T., and Martin, S. J. (1999) *J. Biol. Chem.* **274,** 20855–20860
19. Inohara, N., Koseki, T., Chen, S., Wu, X., and Núñez, G. (1998) *EMBO J.* **17,** 2526–2533
20. Hu, Y., Benedict, M. A., Wu, D., Inohara, N., and Núñez, G. (1998) *Proc. Natl. Acad. Sci. U. S. A.* **95,** 4386–4391
21. Pan, G., O'Rourke, K., and Dixit, V. M. (1998) *J. Biol. Chem.* **273,** 5841–5845
22. Stennicke, H. R., and Salvesen, G. S. (1999) *Methods: Companion Methods Enzymol.* **17,** 313–319
23. Cain, K., Brown, D. G., Langlais, C., and Cohen, G. M. (1999) *J. Biol. Chem.* **274,** 22686–22692
24. Parniske, M., Hammond-Kosack, K. E., Golstein, C., Thomas, C. M., Jones, D. A., Harrison, K., Wulff, B. B., and Jones, J. D. G. (1997) *Cell* **91,** 821–832